Study of Power Supply Configurations for Advanced Nimbus Missions

Final Report

April 30, 1968 thru January 31, 1969

Contract No. NAS5-11549

Prepared by

RCA | Defense Electronic Products
Astro Electronics Division | Princeton, New Jersey

Prepared for

National Aeronautics and Space Administration
Goddard Space Flight Center
Greenbelt, Maryland

R-3431

Study of Power Supply Configurations for Advanced Nimbus Missions

Final Report

April 30, 1968 thru January 31, 1969

Contract No. NAS5-11549

Goddard Space Flight Center

Contracting Officer: S. Provenzano
Technical Officer: R.C. Falwell

Prepared by

RCA Defense Electronic Products
Astro Electronics Division Princeton, New Jersey
Project Manager: R. Packer

Prepared for

National Aeronautics and Space Administration
Goddard Space Flight Center
Greenbelt, Maryland

R-3431

PRECEDING PAGE BLANK NOT FILMED.

PREFACE

This Final Report describes the selection, analysis and comparison of various solar conversion power subsystem configurations for the Nimbus Meteorological Satellite. Because the future Nimbus missions are in a relatively flexible state at this time, it is necessary to project the capabilities of several power system configurations that will accommodate a range of potential mission requirements. The effort on this Study Program was performed by the Astro-Electronics Division of RCA for the National Aeronautics and Space Administration under contract No. NAS-5-11549. The period covered by this report extends from April 30, 1968 to January 31, 1969.

PRECEDING PAGE BLANK NOT FILMED.

TABLE OF CONTENTS

TABLE OF CONTENTS (Continued)

TABLE OF CONTENTS (Continued)

LIST OF ILLUSTRATIONS

LIST OF ILLUSTRATIONS (Continued)

LIST OF ILLUSTRATIONS (Continued)

LIST OF TABLES

PRECEDING PAGE BLANK NOT FILMED.

FOREWORD

The Nimbus B power subsystem has been used as the basis of comparison for evaluating other power subsystem configurations during this study. Except for some differences in solar array energy conversion efficiency or series-parallel solar cell arrangement, the Nimbus B-2 and Nimbus D power subsystems are identical to Nimbus B, providing a practical reference with a wealth of test experience to substantiate performance predictions for the various components comprising the subsystem.

This study has given extensive consideration to the use of the existing Nimbus Storage Module and Control Module in configuring the various systems, as well as other components developed to breadboard stage and several system concepts heretofore not applied to the Nimbus Program.

Technical direction and consultation during this study have been provided by Mr. R.C. Falwell, NASA Technical Officer on this contract, and Mr. C.M. MacKenzie, NASA-GSFC, who has directed equipment development and power systems analysis on previous Nimbus contracts. Technical direction at AED was the responsibility of Mr. R. Rasmussen, Study Director for this contract. The following personnel of the RCA-Astro-Electronics Division provided major contributions to the contract.

Mr. P.S. Abitanto	Mr. E. Holloway
Mr. C.A. Berard	Mr. P.J. Hyland
Mr. F. Gleason	Mr. R.A. Newell
Mr. R.C. Greene	Mr. H.J. Thierfelder

STUDY OF POWER SUPPLY CONFIGURATIONS FOR ADVANCED NIMBUS MISSIONS

SECTION I

INTRODUCTION AND SUMMARY

The purpose of this Study is to analyze and compare various solar conversion power subsystems for possible application in future Nimbus missions. Although the basic Nimbus spacecraft configuration has stabilized to a considerable extent, the future mission power requirements are in a relatively flexible state at this time.

The Nimbus B power system configuration is highly reliable, providing automatic protection against, or recovery from, a large number of conceivable failure modes. Energy transfer efficiency from the solar array to the spacecraft electrical loads is relatively good compared to other power systems that operate on the solar array output characteristics at a voltage slightly greater than battery voltage; this is due to the low-dissipation pulse-width-modulated (PWM) voltage regulator employed in the present Nimbus power systems. The limitation of this system is described by a nominal orbit-average load power capability that decreases from about 225 watts at beginning-of-life to about 175 watts at the end of one year in orbit.

In the event that the load capability of the Nimbus B type power subsystem is insufficient to meet future mission requirements, a change in subsystem hardware is mandatory. This study has considered maximum utilization of existing flight-qualified Nimbus hardware and techniques developed on Nimbus-related contracts to configure alternate power subsystems that will supply more load power. The ground rules for this study stipulate the use of modular sensory-ring-mounted equipment boxes and the optimally-efficient sun-oriented solar platforms in the 600 NM, high noon Nimbus orbit. The addition of the bifold solar array sections to the F-3-type solar array, in conjunction with a subsystem which provides maximum transfer of energy from the solar array to the spacecraft regulated bus, results in a nominal orbit-average load capability which decreases from greater than 500 watts at beginning of life to about 350 watts at the end of a two-year mission. A more modest load power increase can be obtained using the F-3-type solar array in conjunction with a subsystem configuration which has been successfully developed and breadboard-tested at RCA and NASA-GSFC; the parallel maximum power tracker configuration will supply more than a 20 percent load power increase over an optimized Nimbus B-type system for a two-year orbit lifetime, with no additional spacecraft "real estate" required.

At the start of the study, numerous power systems were considered, including the Nimbus B type, variations of series and parallel maximum power tracker configurations and a boost charger direct energy transfer system. A compilation of some of the more readily-apparent advantages and disadvantages of each system was prepared, and three power system configurations were selected jointly by RCA and GSFC to be analyzed in detail for a two-year mission with both the F-3-type and the bifold solar arrays.

Each of the three selected system configurations (Nimbus B type, Series Maximum Power tracker with single tracking unit, and a Parallel Maximum Power Tracker) was investigated in detail at the functional block level. The solar array, battery and electronics were selected and characterized for the range of environmental conditions expected in orbit. Packaging, weight and volume requirements of each system were defined, along with recommended redundancy, electromagnetic interference protection, telemetry and ground command provisions.

A computer program was developed which performs an electrical energy balance analysis of each power system on a per-orbit basis. This program was instrumental in the evaluation of system performance, providing values of maximum load capability, battery voltage and current profiles during an orbit, battery depth of discharge and power dissipation for various load profiles, and other significant solar array and system parameters. The computer program was delivered to GSFC in order to provide NASA with the capability of evaluating the effect of various power system component characteristics, battery temperatures, performance in other than the planned orbit, etc.

SECTION II

SYSTEM CONFIGURATIONS

A. INITIAL POWER SUBSYSTEM CONFIGURATIONS CONSIDERED

Definition at the functional block diagram level of various solar conversion power subsystem configurations as possible candidates for providing an increased load capability for future Nimbus missions was the initial task in this study. Subsequent derivation of approximate energy balance equations, assessment of required storage capacity and number of spacecraft sensory ring bays, power dissipation, development status, voltage operating range, utilization of existing Nimbus hardware, load power capability and other considerations provided the basis for a comparison between the various system configurations. It was then possible to compile a list of the apparent advantages and disadvantages of each system configuration initially considered.

1. Functional Block Description and Operation of Power Systems

a. NIMBUS B (NB)

A functional block diagram of the Nimbus B type power subsystem is shown in Figure 1. A number of solar cell module strings are paralleled at the output side of the isolation diodes, D1, to comprise the solar array. Slip rings provide current paths for both the negative and positive (common) bus to the rest of the subsystem. Each storage module contains a battery and its independently-operated charge controller; storage modules are connected electrically in parallel between the solar array bus and ground. The PWM load bus voltage regulator derives power from the unregulated bus, to supply -24.5V power to the spacecraft loads. System shunt losses are representatively shown at the unregulated bus. The shunt dissipator is a device which limits the maximum voltage on the solar array bus.

During nighttime operation, no current is generated in the solar cells and the voltage at the solar cell strings and the solar array bus is essentially zero, which places a reverse bias on diodes D1 and D3. The charge controllers are internally reverse-biased, so that the batteries can only discharge through diodes D2 to the unregulated bus. Current sharing is determined by the voltage of each battery; a colder temperature and/or a higher state of charge will cause a battery to supply more than average current. However, that battery then loses charge at a greater rate; the result, as demonstrated by simulated orbital

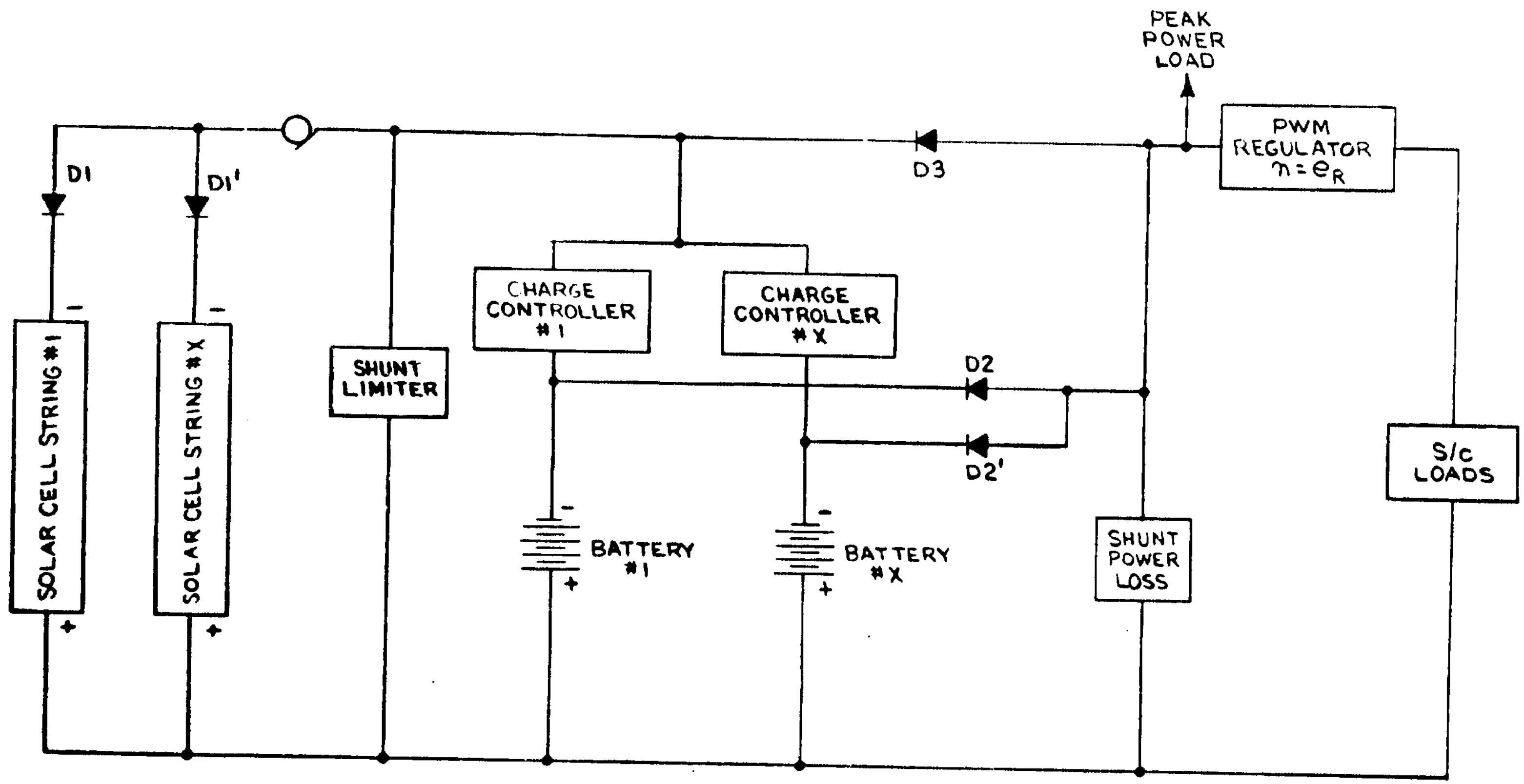

Figure 1. Nimbus B (NB)

cycling, is excellent long-term battery load sharing. The PWM regulator duty cycle is automatically adjusted to maintain regulation; for a given load, the input current to the regulator will decrease as the input (unregulated bus) voltage increases.

When the solar array is illuminated, diodes D1 and D3 and the charge controllers are forward biased; diodes D2 are reverse-biased, preventing uncontrolled charging of the batteries from the unregulated bus. Each charge controller limits the charge current so that the maximum charge current limit is not exceeded, and reduces the charge current to maintain the battery voltage at a safe upper limit, as a function of temperature, as a full state of charge is approached. This control is commonly referred to as voltage-temperature limiting, or tapered charge control. Additionally, if battery temperature exceeds a predetermined value, charge current is automatically reduced to a nominally low trickle charge value. If none of the three limits is exceeded, the charge controller will pass whatever charge current is available from the solar array bus to the battery. The independent action of each charge controller allows different modes of operation simultaneously in different batteries. Normally, the system operating voltage (solar array bus voltage) will be about one volt greater than the battery charge voltage. If the load demand is small, system voltage will rise; when the threshold voltage of the shunt dissipator is reached, it will divert solar array current from the solar array bus so that the system will operate at the safe voltage limit instead of moving towards open-circuit voltage of the solar array in order to obtain the small amount of current needed for the load and batteries.

Peak load power is taken from the unregulated bus, and is conditioned to suit the particular load demand. If this peak load demand plus the PWM regulator demand exceeds the available solar array current, the batteries will discharge through diodes D2, the solar array bus voltage will be approximately equal to the battery discharge voltage, and no charge current will exist. When the peak load demand disappears, normal battery charging operation resumes.

b. Series Tracker, Single Tracking Unit (STS)

A functional block diagram of the series maximum power tracker with a single tracker unit is shown in Figure 2. The Nimbus B type voltage regulator and storage modules are specified with this system, so that system operation on the output side of the tracker unit is identical to Nimbus B, except that no shunt dissipator is required.

During periods of solar array illumination the duty cycle of a constant-frequency solid state switch in the series tracker unit is varied, while an instantaneous

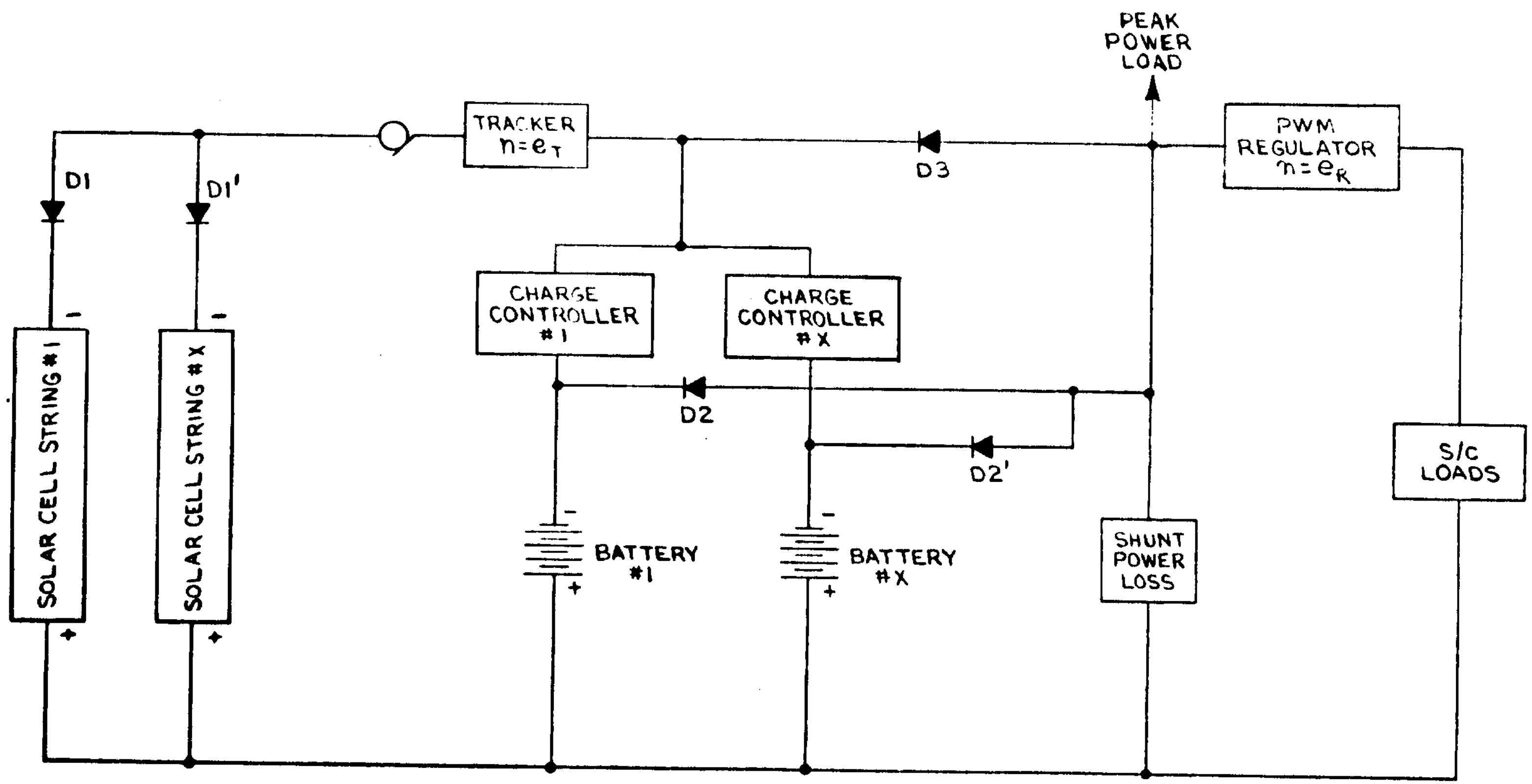

Figure 2. Series Tracker (Single) (STS)

source power sensor observes the value of solar array power. The direction of the duty cycle scanner is reversed when the observed solar array power begins to decrease, resulting in continuous operation at or near the array maximum-power voltage. Output voltage of the tracker unit is typically about one volt greater than battery charge voltage, while the tracker unit input voltage may be as high as -70 or -80 volts during cold solar array operation.

The tracker output voltage is continuously sensed, so that in the event the PWM regulator load decreases and/or the batteries reach a near-fully-charged state and their charge current demand is reduced, normal tracker scanning is inhibited and a low duty cycle value is imposed on the switch, resulting in operation at lower array power, in a direction approaching array open-circuit voltage. In this manner, the input power to the rest of the subsystem never exceeds that amount which is useable, resulting in reduced excess power dissipation.

This configuration is classified as a full-time tracker since the system operating voltage will remain at the array maximum-power voltage even when the batteries have to discharge in order to apply peak load demands. Maximum utilization of available solar array energy is thus achieved.

Note that all input energy to the power subsystem must be processed by the series tracker unit, resulting in considerable power dissipation in that component. Also, power supplied to the spacecraft loads during solar array illumination is subject to a double efficiency penalty: the series tracker unit as well as the load voltage regulator.

c. Series Tracker, Multiple Tracking Units (STM)

Figure 3 presents a functional block diagram of the series maximum power tracker with multiple tracking units. In this configuration, there is a series tracker unit for each battery. The tracker unit functions also as the charge controller, so that a battery is connected directly to the output of each tracker unit. The individual tracker unit outputs are also tied together at the unregulated bus, at the common positive side of diodes D2 which also serve as battery discharge diodes for nighttime operation. Battery charge current is sensed separately from tracker output current, but if battery voltage or current approaches the limit value, the output current from that tracker unit is reduced by decreasing the on-time duty cycle of the solid-state switch in that unit.

All tracker units are synchronized to the same switching frequency and the duty cycle scanning and solar array power sensing functions are performed just as in the STS system, but the battery protection circuitry in any unit can override the "system" duty cycle. It becomes obvious, then, that if the battery voltage

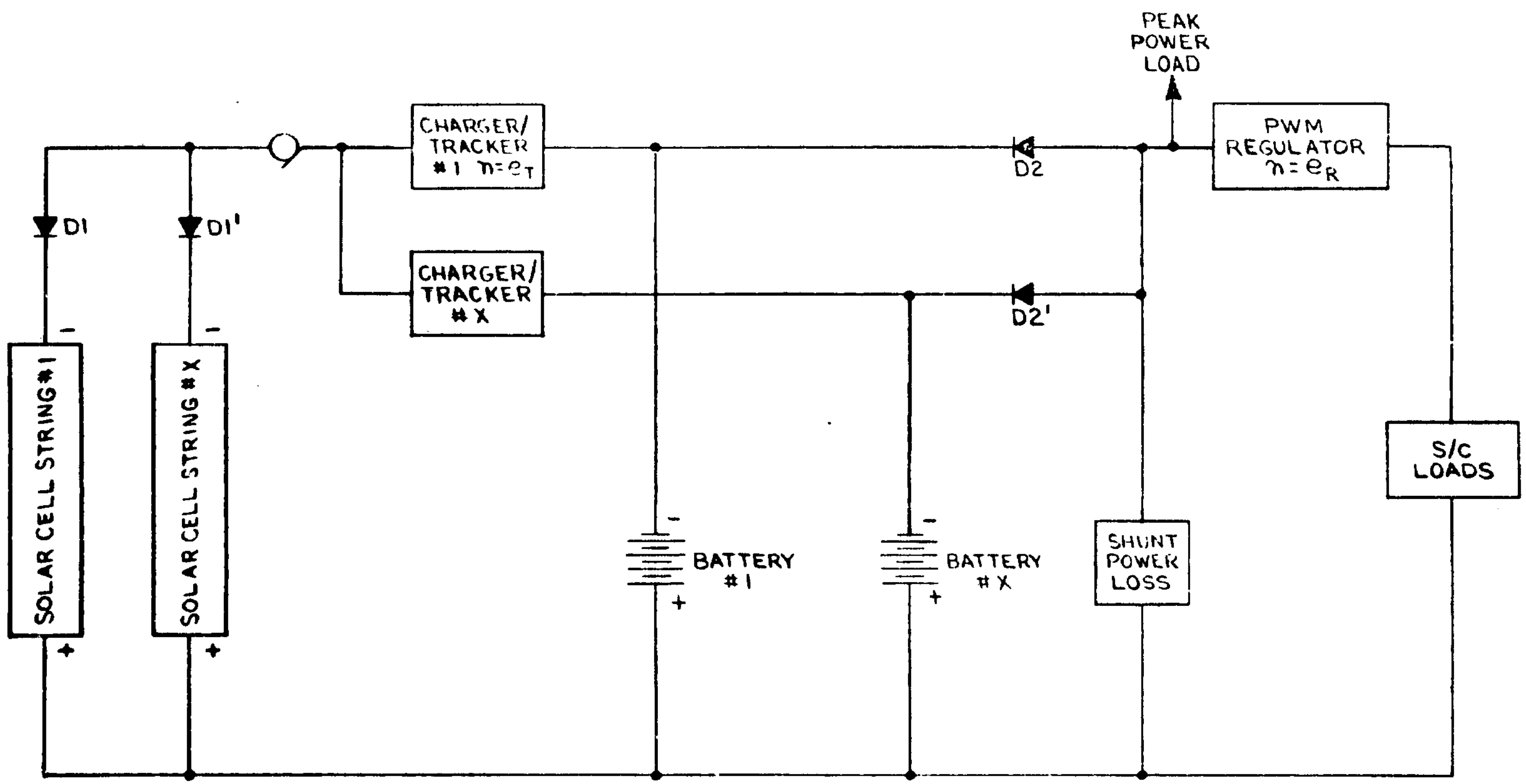

Figure 3. Series Tracker (Multiple) (STM)

in all but one unit is at the individual high limit value, the remaining tracker unit would have to supply the entire PWM regulator load. In other words, each of the multiple tracking units must have the current and power dissipating capability needed to supply the entire spacecraft load, just as the single tracker unit in the STS system does.

The advantage of the multiple series tracker system over the STS system is only the slight system efficiency gain due to eliminating the separate charge controller in series with the tracker unit. The STM configuration is classified as a full-time tracker because it can operate at the solar array maximum-power point while the batteries are discharging to supply a peak load demand.

d. Parallel Part-Time Tracker (PPT)

A functional block diagram of the parallel part-time maximum power tracker is shown in Figure 4. This configuration is similar to the NB system, except that the shunt dissipator has been eliminated, and the components labeled " charger/tracker" have replaced the NB charge controllers. To understand the development of the parallel tracker concept, consider a NB system having PWM charge controllers instead of the series dissipative charge controllers actually used in the Nimbus B system. Figure 5 shows the familiar current-voltage (I-V) relationships of the various components in such a system and Figure 6 presents the power-voltage (P-V) representation of the system. The " PWM voltage regulator and system loss" curve represents a spacecraft load of 220W plus a power system loss of 50W. The " PWM charger load line" curve represents a battery and PWM charger combination starting to accept charge current at 30 volts, and reaching a maximum permissible 8.8A of charge current at 33 volts. At any higher operating voltage, the power demand remains constant at the product of 8.8A × 33V.

The source curve is obtained by superimposing the battery discharge I-V curve on the solar array I-V curve. The composite load curve is obtained by superimposing the regulator and system loss curve on the PWM charger curve, and is shown by the dashed line in Figure 5.

Initially, let it be assumed that the three circled intersections of the composite load line with the source curve are possible system operating points. The left-hand intersection results in only about 5.5A of battery charge current, while the center and right-hand intersections allow battery charging at the maximum allowable 8.8A. The PWM charger pass element is saturated (100% duty cycle) at the left hand intersection. Limiting the maximum duty cycle to some other value, say 90%, would change the slope of the load curve, moving the left-hand intersection to the right along the array I-V curve and thereby increasing battery charge current. If the duty cycle were further decreased, the operating

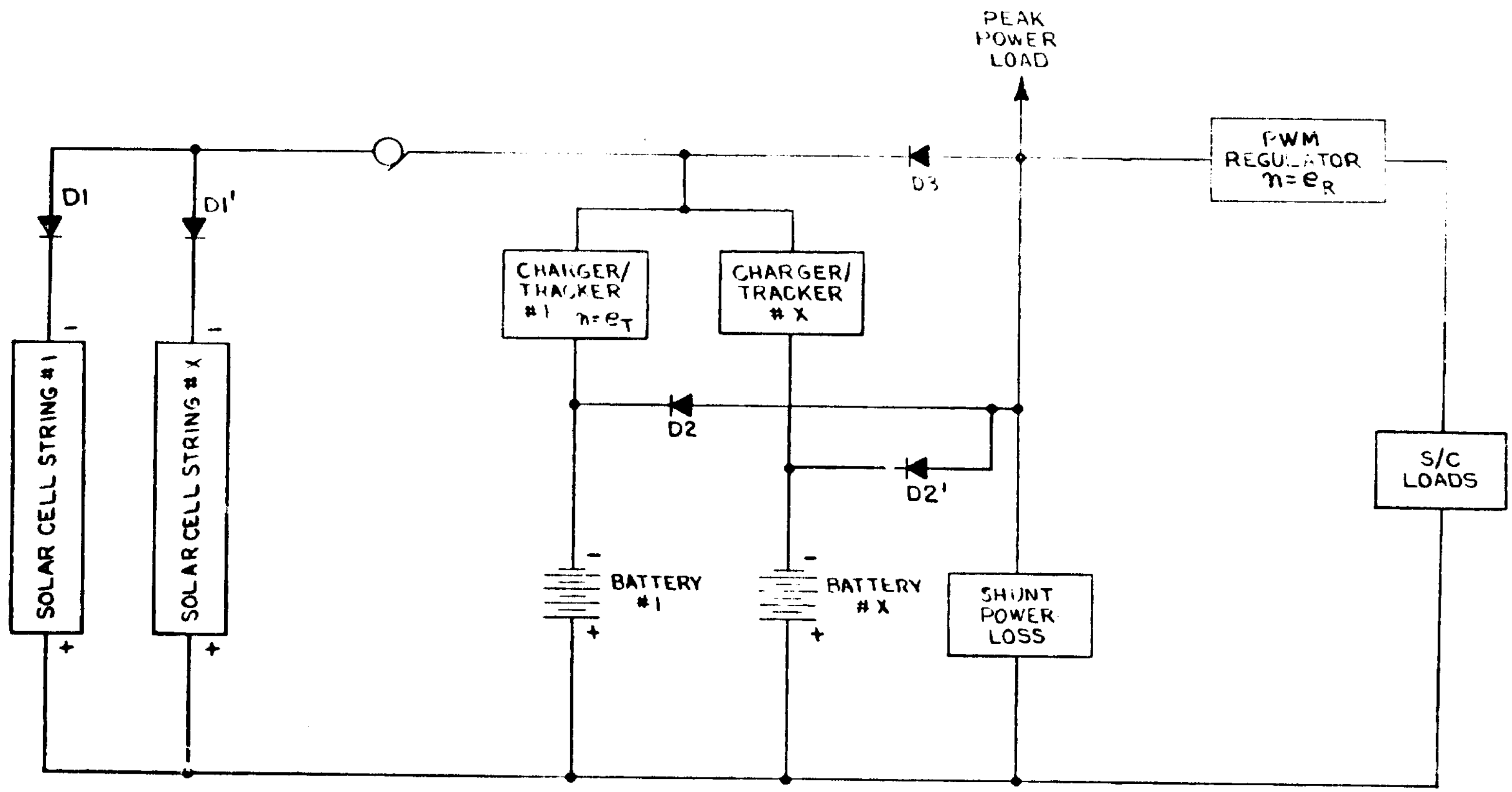

Figure 4. Parallel Part-Time Tracker (PPT)

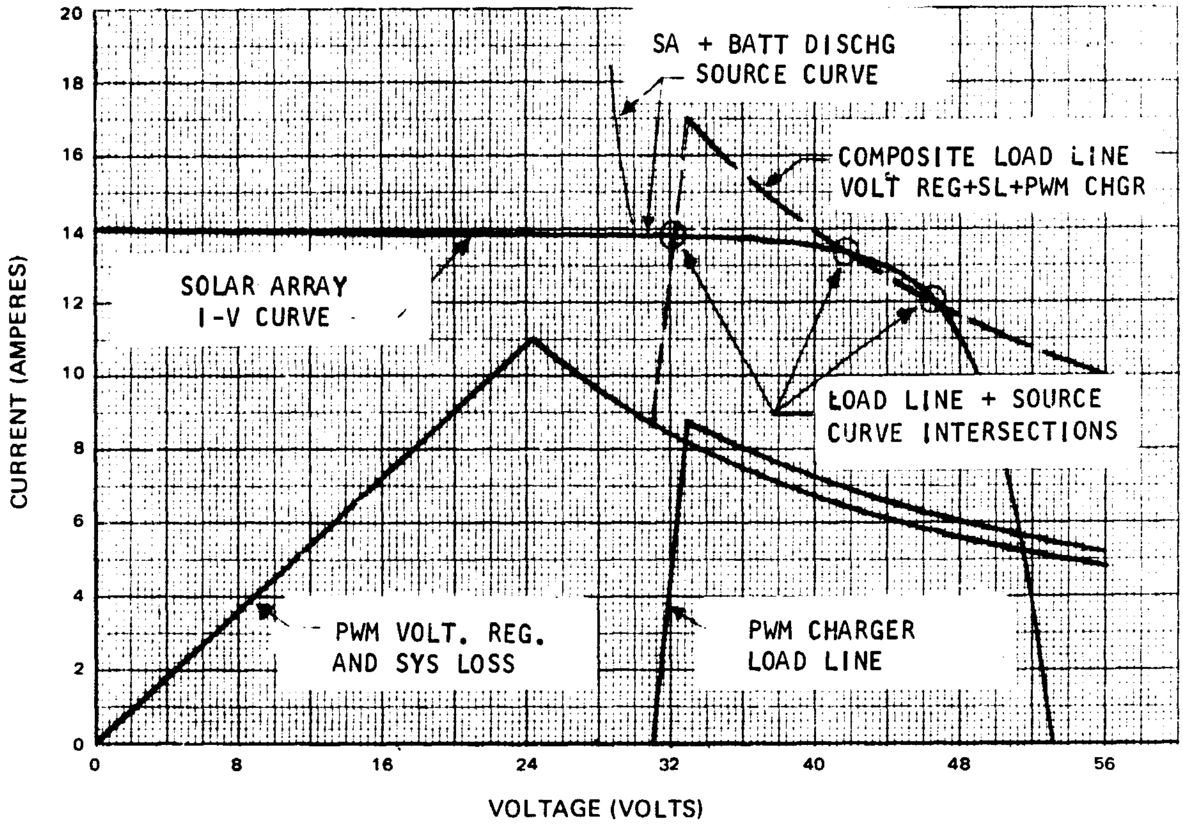

Figure 5. I-V Characteristics of System with PWM Battery Charger

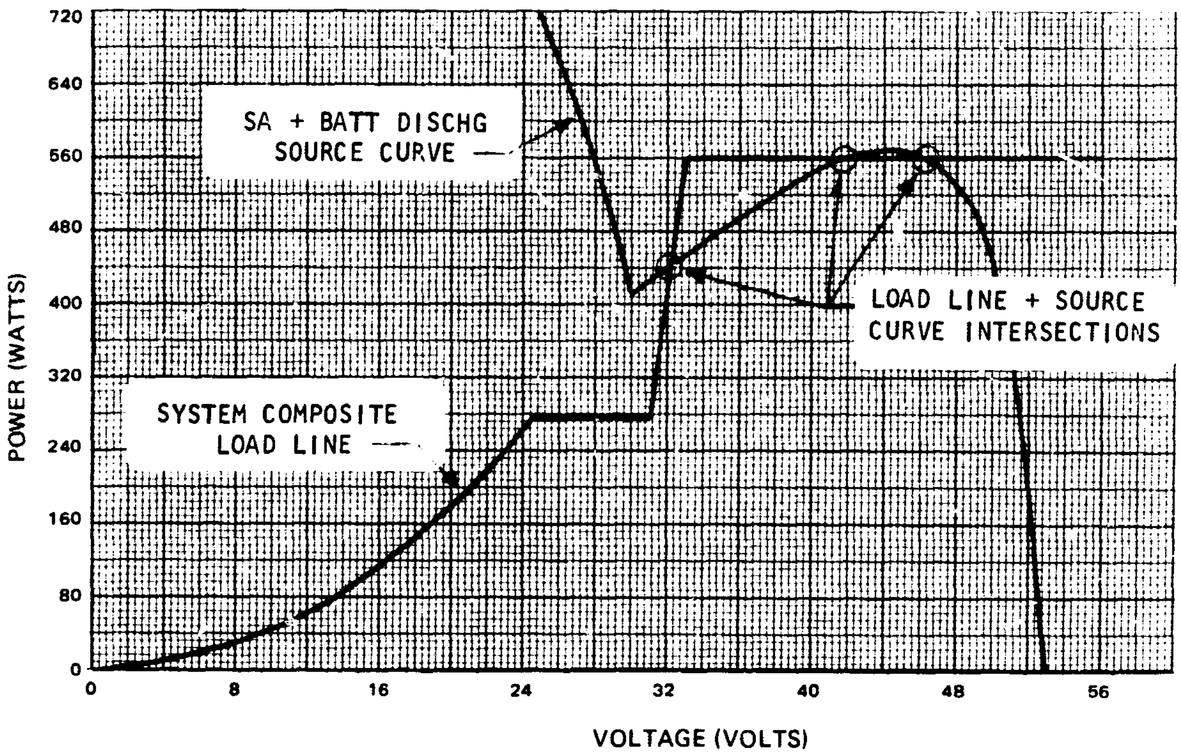

Figure 6. P-V Characteristics of System with PWM Battery Charger

point would continue to the right until the circled intersection in the center is reached. Operation on the solar array I-V curve between the center and right-hand intersections would necessitate a battery charge current greater than the maximum desired value of 8.8A. Therefore we must have, with a PWM charger, a closed loop technique which would very rapidly decrease the pass element duty cycle when the maximum current limit starts to be exceeded. This forced, rapid decrease in duty cycle would move the system operating point to the right-hand intersection, where 8.8A of charge current would exist, but not be exceeded. A further decrease in duty cycle would move system operation along the array curve to the right of the right-hand circled intersection, resulting in lower and lower values of battery charge current.

Consider now a circuit that would sense the source power and change the PWM switch duty cycle in a direction to obtain more source power, and reverse the direction of duty cycle change after the point of maximum source power has been passed. A PWM switch whose duty cycle is scanned and maintained at or near the source point of maximum output power by the action of a solar array power sensor is called a maximum power tracker.

Referring again to the parallel part-time tracker (PPT) configuration shown in Figure 4, it is seen that nighttime operation of this system is identical to that of the NB system. When the solar array is illuminated, the duty cycle of all the charger/tracker units is adjusted to allow system operation at the solar array maximum-power voltage. As an individual battery approaches a fully-charged state (reaches its maximum voltage limit), its current demand is smaller and the duty cycle of the PWM switch in its charger/tracker units is independently decreased. This allows more current for charging the other batteries. If the total available power at the array maximum-power point is greater than what the load regulator and the batteries will accept, the duty cycle of the PWM switches automatically decreases such that the system operating voltage moves toward open-circuit voltage of the array until the available source power is equal to the total power demand of the load and batteries.

The PPT system is classified as a part-time tracker because when the load power (PWM regulator and/or peak load) demand exceeds the power available from the solar array, the batteries discharge, clamping the solar array bus to battery discharge voltage and forcing operation at a voltage considerably less than maximum-power voltage for the ON-time of the peak load.

e. Parallel Full-Time Tracker (PFT)

Figure 7 presents a functional block diagram of the parallel full-time maximum power tracker. The charger/tracker and battery combination is

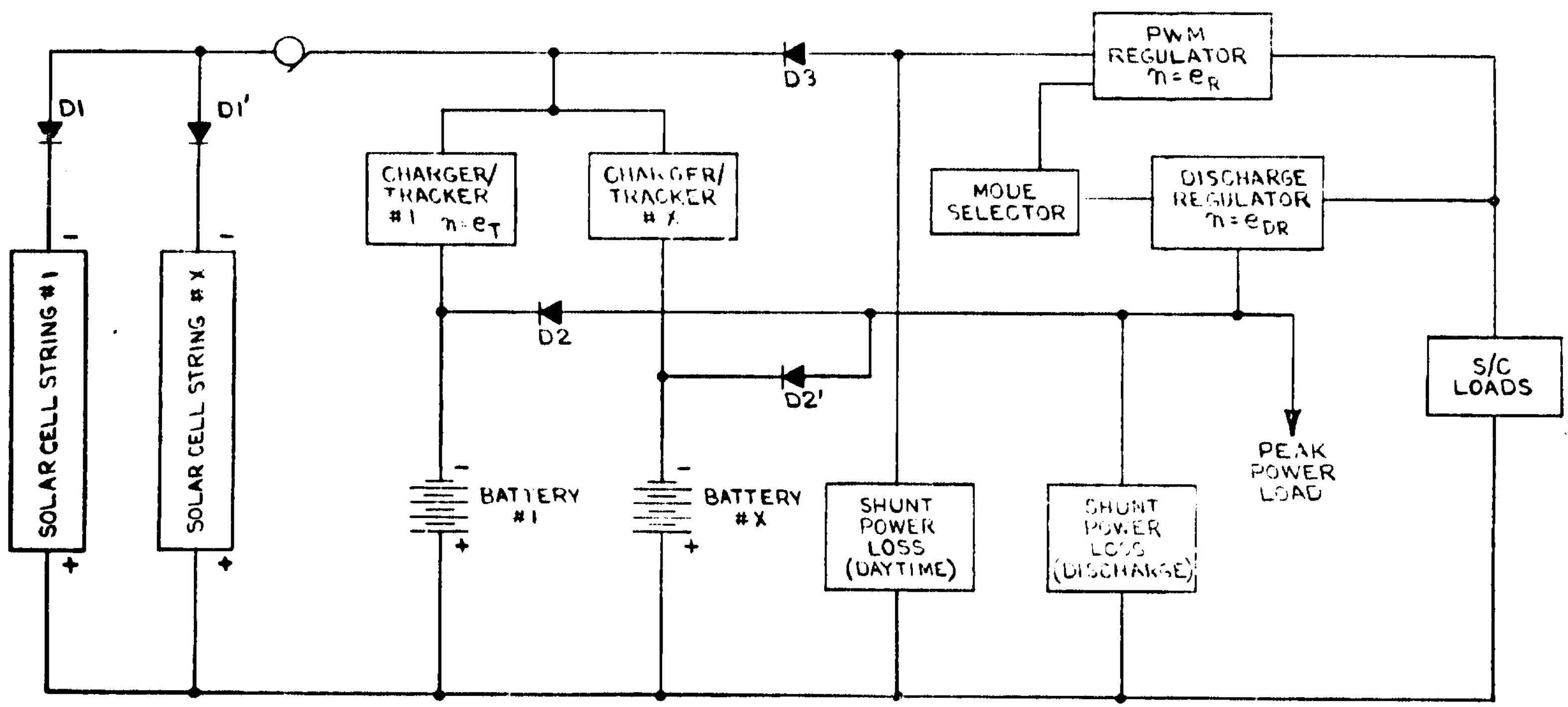

Figure 7. Parallel Full-Time Tracker (PFT)

connected in parallel with the PWM load regulator and spacecraft loads, as in the part-time parallel tracker. During normal daytime operation, the PFT system functions exactly the same as the PPT system; solar array bus voltage is maintained at the array maximum power voltage as long as the loads and batteries can use this much power. The discharge regulator is inhibited by the mode selector; all normal loads are supplied by the "daytime" PWM regulator. However, when the load demand on the main regulated bus exceeds the available power from the solar array bus, the mode selector will turn on the discharge regulator to provide the additional required power from the batteries. During this heavy load duration, the solar array bus is maintained at the array maximum-power voltage, so that maximum utilization is made of the available array energy. Any power demand on the peak load bus shown in Figure 7 would be supplied through the charger/trackers, up to the limit of maximum battery charge current; if this power were insufficient, the batteries would discharge, supplying the additional required peak load current through diodes D2.

During satellite nighttime, the mode selector would inhibit the "daytime" PWM regulator and the discharge regulator would supply all the regulated loads.

The primary advantage of the PFT system would be in a mission with numerous heavy loads occurring during solar illumination periods.

f. Direct Energy Transfer System (DET)

A functional block diagram of a boost-charger direct energy transfer system is shown in Figure 8. No series power conditioning device is required between the solar array and the spacecraft, thus providing practically no loss during normal transfer of source-to-load energy during daytime operation. The shunt regulator senses the load bus voltage, providing a shunt path to ground for excess array current in order to maintain the regulated voltage in the event that the batteries will not accept the difference between array and load current and the system tends to move toward a higher voltage operating point. Obviously then, a small dynamic range of regulation must be permitted to perform the shunting function. The mode selector senses the regulated voltage and keeps the discharge regulator inhibited as long as sufficient array current exists to maintain regulation. The DC-DC converter in series with each charge controller and battery raises the regulated bus voltage to a level sufficient to overcome the drop in the charge controller and provide charging current for the battery. If an increased load demand causes a slight reduction in regulated voltage, the mode selector will inhibit the charge controllers to provide more current to the loads. If even more load current is required, the regulated voltage will further decrease and the mode selector will now turn on the discharge regulator to allow the batteries to supply the additional load current required. The shunt regulator is inhibited by the mode selector when the load demand causes a reduction in charge current or when the battery discharges.

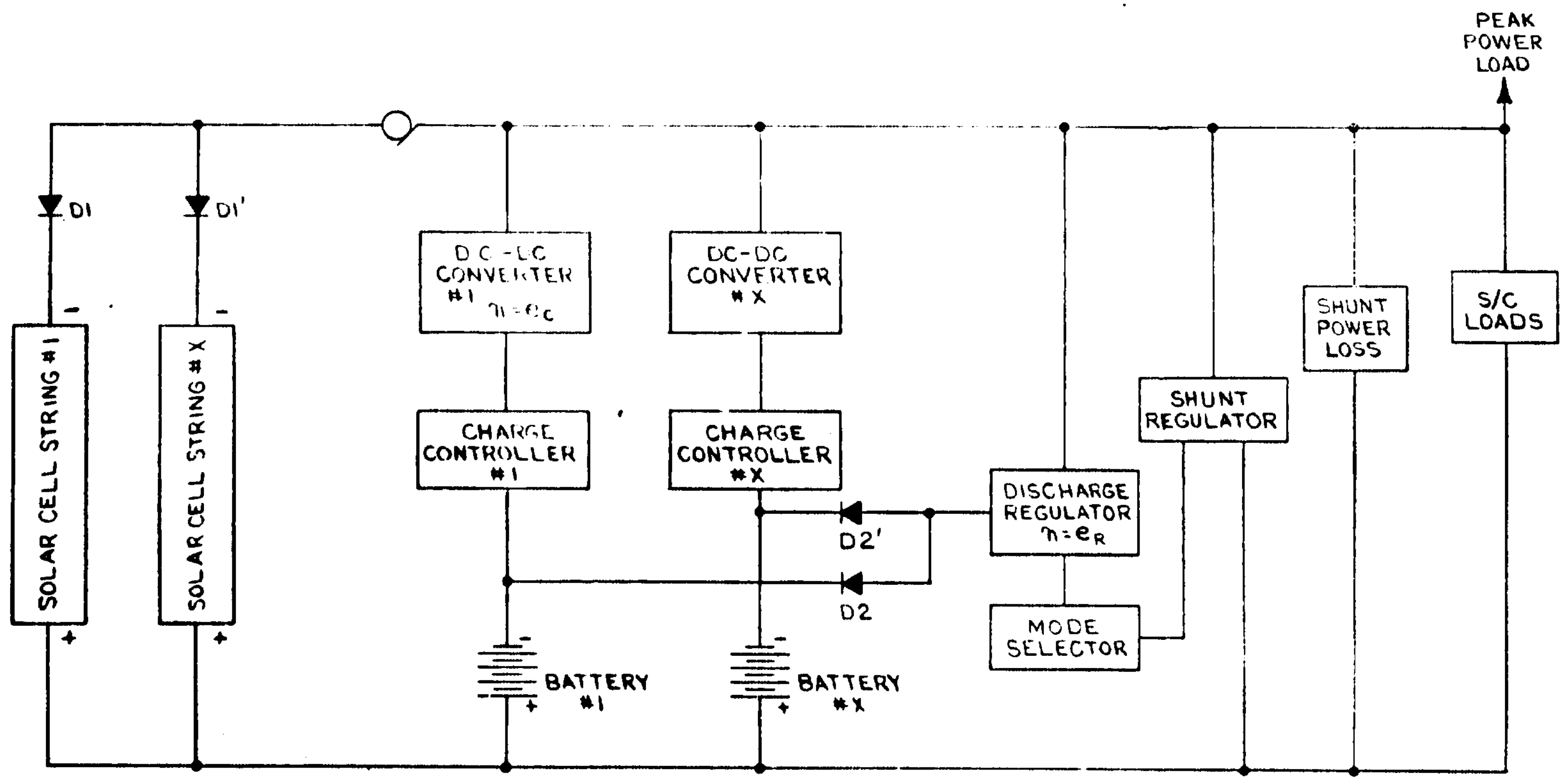

Figure 8. Direct Energy Transfer (DET)

During satellite nighttime, the shunt regulator is inhibited and the discharge regulator maintains regulation. The number of storage cells in each battery is selected so that the discharge voltage is always greater than the regulated voltage, providing better regulated bus performance and system efficiency by the down-converting method.

g. Parallel Part-Time/Full-Time Tracker (PPFT)

Figure 9 presents a functional block diagram of a parallel tracker configuration which provides full-time tracking without the necessity for a separate discharge regulator. The system differs from the earlier-described PPT in that all batteries are connected together through an additional set of discharge diodes D4 to provide a peak load bus separate from the unregulated (solar array) bus. PPFT system operation is identical to the PPT system during satellite nighttime and normal load daytime operation. When a heavy peak load demand is present, it receives current from the solar array bus through the charger/tracker units and diodes D4, up to the limit of array power not required by the main PWM load regulator. Note that the solar array bus is maintained at array maximum-power voltage by the duty cycle of the charger/tracker units since these components are tyring to satisfy what appears to be a battery charge current demand. If this available solar array power is insufficient for the peak load demand, the batteries will discharge through diodes D4 to supply the additional required peak load power.

The functional block diagrams for the seven system configurations discussed in paragraph a) through g) above show two batteries for each system. This is merely to demonstrate the points of parallel connection; any number of batteries may be connected in this manner in each system.

For power system configurations utilizing the F-3 type solar array, it is presumed that the 20-ampere PWM voltage regulator housed in the Nimbus B Control Module (Nimbus 4/4 module size) will be sufficient to provide regulation for the spacecraft loads. The regulator in the PFT and PPFT systems must be modified to accommodate the higher unregulated bus voltages encountered with these systems (up to -80 volts). This modification has been breadboarded and tested successfully at RCA and GSFC.

Power system configurations utilizing the bifold solar array (about 84 percent more array area than the F-3 type substrates alone) are specified as using two NB control modules to supply the spacecraft regulated loads. The primary reason for two regulators is that the approximately 10 percent efficiency loss in the regulator would result in excessive power dissipation in one bay if only

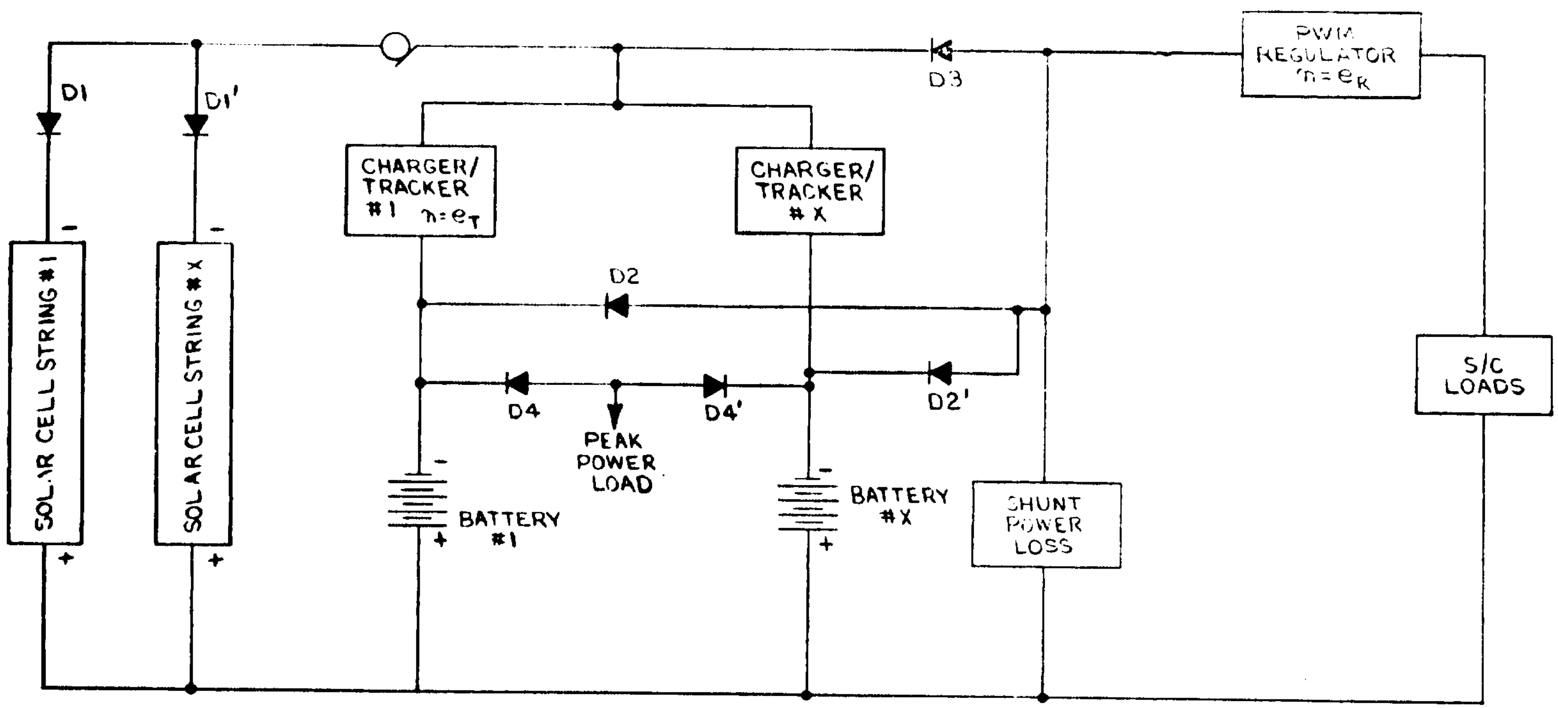

Figure 9. Parallel Part-Time/Full-Time Tracker (PPFT)

one regulator were used. Total load power capability of the bifold systems could be as high as 500W, orbit average. Spacecraft loads should be divided equally between the two regulators, providing a split-bus system with independent regulation control from each regulator. OR-gating of critical loads, such as attitude control, clock or command receiver, could easily be accomplished with diodes but may not be required since each NB control module already contains a completely redundant standby regulator with automatic switchover in the event that loss of regulation is sensed.

Both regulators would derive input power from a common unregulated bus, thus the functional block diagrams presented for the earlier-described F-3 array systems apply to the counterpart bifold array systems as well, with the addition of a parallel load regulator for each one shown in the diagrams, with the following single exception:

h. Direct Energy Transfer System with Split Bus

Figure 10 presents a functional block diagram of a boost-charger direct energy transfer system with a split regulated bus. This configuration differs from the single bus DET system in Figure 8 by the addition of a second discharge voltage regulator and the regulator isolation diodes D3. The spacecraft loads are assigned equally to each regulator, as in the other bifold array systems, to prevent excessive power dissipation in a single regulator bay. Diodes D3 are necessary to ensure that a slight difference in the output voltage of each regulator does not destroy the necessary equal load sharing. The penalties involved with the use of the regulator isolation diodes are a slightly greater system loss during daytime due to power losses in the diodes and a slightly greater voltage regulation band due to the changing voltage drop in the diodes caused by different load currents and diode temperatures.

The peak power loads must be diode OR-gated to the two regulated buses to ensure an adequate current availability for the heavy loads. As in the other bifold systems, the battery discharge bus forms a common input to the two regulators. Shunt regulator and mode selector voltage sensing is made at a single point common to both regulated buses on the solar array side of the regulator isolation diodes.

2. Energy Balance Equations

One of the most significant parameters needed to compare the various power subsystems is a reasonably accurate estimate of the load capability of each system. A fundamental representation of each system configuration

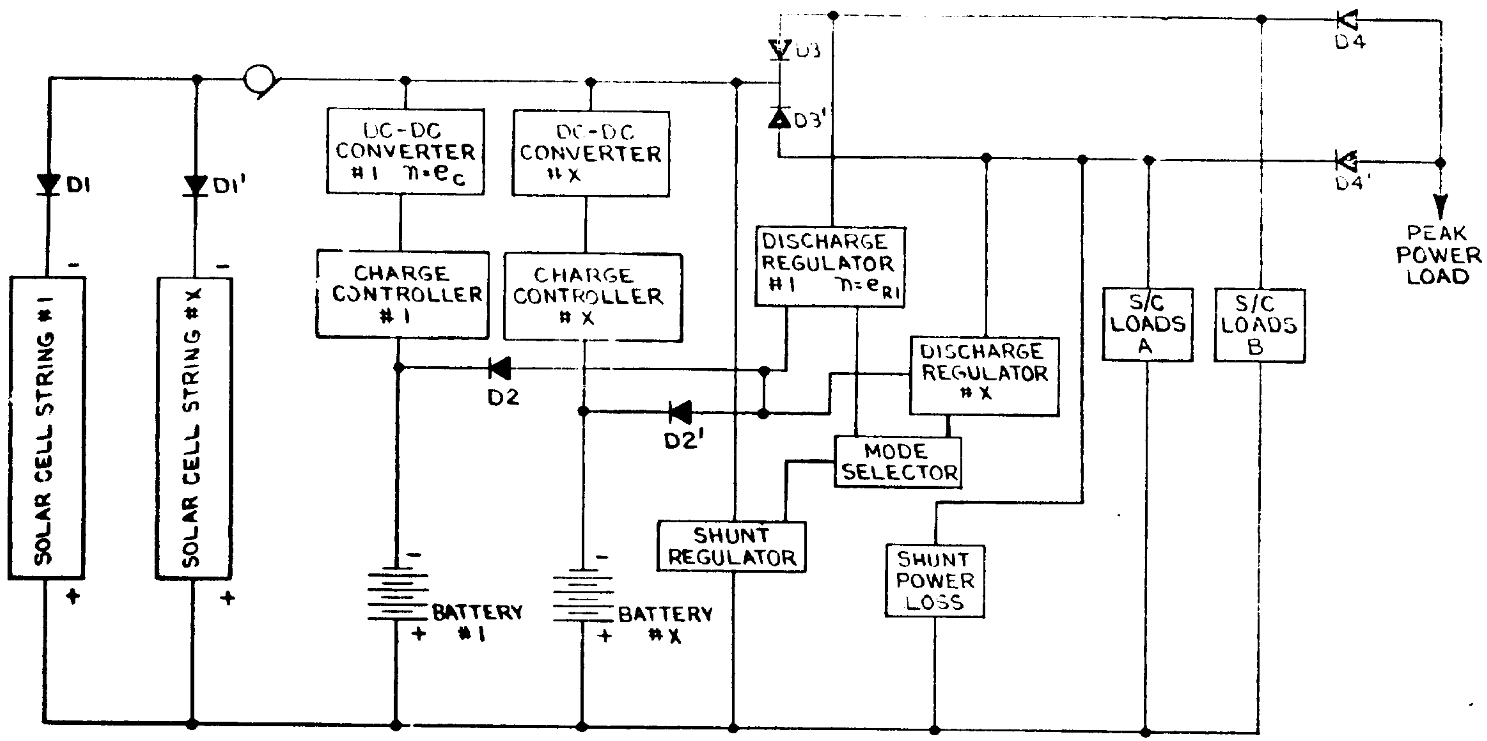

Figure 10. Direct Energy Transfer (DET) (Split Bus)

described earlier was prepared and either an ampere-minute balance equation or an energy balance equation was derived for each one. Some necessary assumptions were required in order to make the load power capability determination for the various systems, and are listed below:

a. Solar Array Power

Testing of the F-3 Solar Platforms has yielded an extrapolated AMO output current of about 13.5 amperes average during the daylight portion of the orbit. The temperature versus time profile reported by Nimbus II telemetry (-60°C to +50°C) was used to prepare the plot of solar array maximum power versus time during an orbit. The same temperature profile is applied to the Bifold section of the solar array. Bifold solar array power is defined by multiplying the F-3 power by a factor of 1.84, which is the ratio of the maximum number of solar cells that can be placed on the bifold substrate to the number of solar cells bonded to the F-3 substrate.

b. Load Profile

A constant load during the entire orbit with an additional peak load of 400 watts for 5 minutes occurring near the end of spacecraft day was assumed. This profile produces a battery discharge during the day for all systems considered, and is accounted for in the energy balance equations. Note that an estimate of the Nimbus B load capability was made on an earlier contract, yielding 228W orbit average plus a 73W peak load for 5 minutes. Thus the orbit average load power should be less for the present estimate, since the peak load energy is considerably greater.

c. Switching Component Efficiency

All switching components in the systems (PWM regulators, series trackers, tracker/charger units) have been assigned a nominal 90% power transfer efficiency, except the DC-DC converter used to obtain charge voltage in the DET system, which has an efficiency of 85%.

d. System Shunt Power Loss

When a PWM regulator efficiency of 90% is applied to the Nimbus B ampere-minute balance equation, an additional shunt power loss of 23 watts is required to make the results of the equation agree with measured values of maximum load power from system testing. This value of shunt loss (23 w) is included in the energy balance equation for all systems using the F-3 solar array; an arbitrary shunt loss increase to a total of 30 watts is assumed for all systems using the Bifold solar array.

e. SA Diode and Slip Ring Power Loss

The value of measured power loss in the SA isolation diodes and slip rings in the Nimbus B system, 24 watts, is applied to all systems using the F-3 array; corresponding power losses for the Bifold solar array are $1.84 \times 24 = 44$ w.

The fundamental system diagrams and energy balance equations are presented in the following figures.

Nimbus B	Figure 11
Series Tracker (single)	Figure 12
Series Tracker (multiple)	Figure 13
Parallel Part-Time Tracker	Figure 14
Parallel Full-Time Tracker	Figure 15
Direct Energy Transfer	Figure 16

Note that the parallel part-time/full-time tracker system (PPFT) would use the same energy balance equation as the parallel full-time tracker (PFT). The equations apply to the bifold array systems as well as the F-3 type array systems. Table I in Appendix II lists the parameter symbols used in the energy balance equations, their definition, and the value used in the evaluation of the equations.

The values of orbit average load power that each system configuration is capable of supporting with both the F-3 and bifold solar array, as determined by the energy balance equations, are shown below.

	F-3 Solar Array (w)	Bifold Solar Array (w)
Nimbus B	210	415
Series Tracker (single)	224	440
Series Tracker (multiple)	228	448
Parallel Part-Time Tracker	238	463
Parallel Full-Time Tracker	245	480
Direct Energy Transfer	232	457
Parallel Part-Time/Full-Time Tracker	245	480

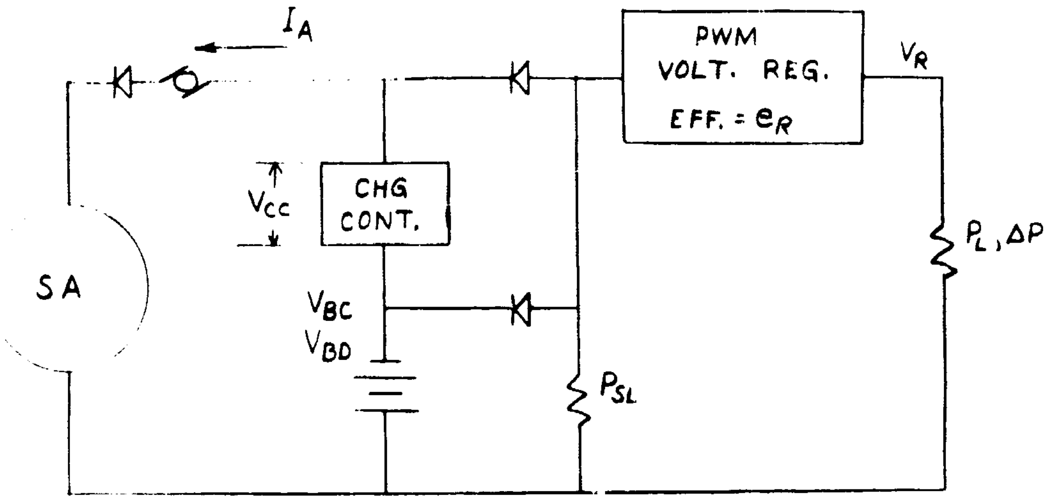

$$\frac{(TN)(C/D)}{V_{BD}}\left[\frac{P_L}{e_R}+P_{SL}\right]+\frac{(TD-TP)}{V_{BC}}\left[\frac{P_L}{e_R}+P_{SL}\right]+\frac{TP}{V_{BD}}\left[\frac{P_L+\Delta P/4}{e_R}+P_{SL}\right]$$

$$+\frac{(TP)(C/D)}{V_{BD}}\left[\frac{3/4\ \Delta P}{e_R}\right]=(I_A)(TD)$$

Figure 11. Nimbus B Ampere-Minutes Balance EQN

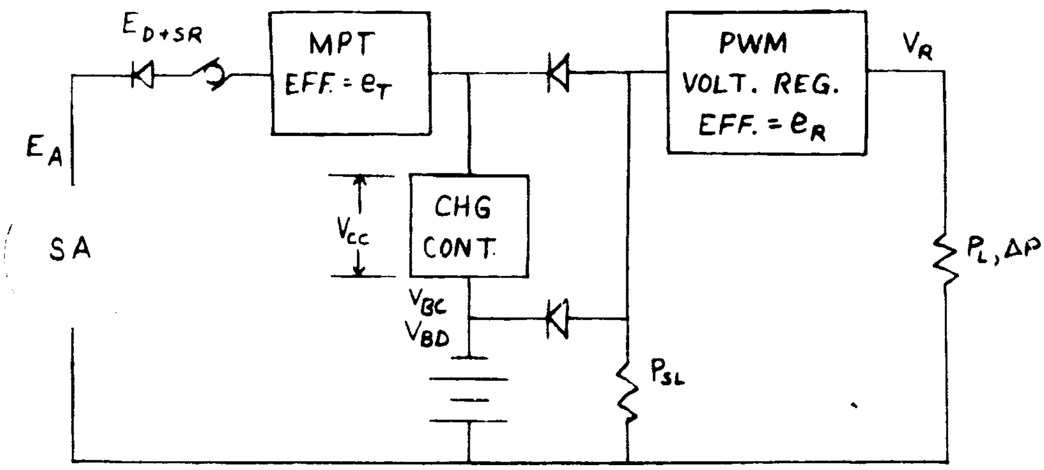

$$(TN)(C/D)\left(\frac{V_{BC}+V_{CC}}{V_{BD}}\right)\left[\frac{P_L}{e_R}+P_{SL}\right]+(TD-TP)\left[\frac{P_L}{e_R}+P_{SL}\right]+TP\left[\frac{P_L+\Delta P/2}{e_R}+P_{SL}\right]$$

$$+(TP)(C/D)\left(\frac{V_{BC}+V_{CC}}{V_{BD}}\right)\left[\frac{\Delta P/2}{e_R}\right]=e_T\left(E_A-E_{D+SR}\right)$$

Figure 12. Series Tracker (Single) Energy Balance EQN

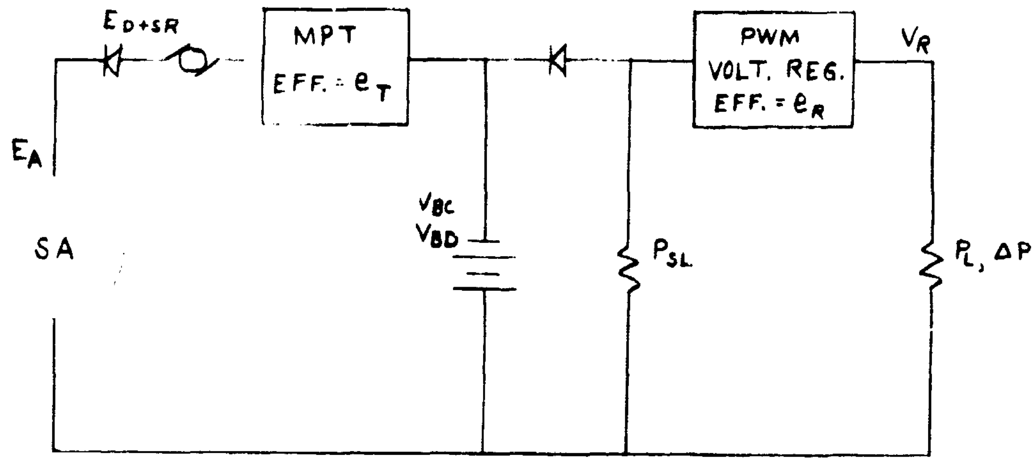

$$(TN)(C/D)\left(\frac{V_{BC}}{V_{BD}}\right)\left[\frac{P_L}{e_R}+P_{SL}\right] + (TD-TP)\left[\frac{P_L}{e_R}+P_{SL}\right] + TP\left[\frac{P_L}{e_R}+P_{SL}+\frac{1/2\,\Delta P}{e_R}\right]$$

$$+ (TP)(C/D)\left(\frac{V_{BC}}{V_{BD}}\right)\left[\frac{1/2\,\Delta P}{e_R}\right] = e_T\left(E_A - E_{D+SR}\right)$$

Figure 13. Series Tracker (Multiple) Energy Balance EQN

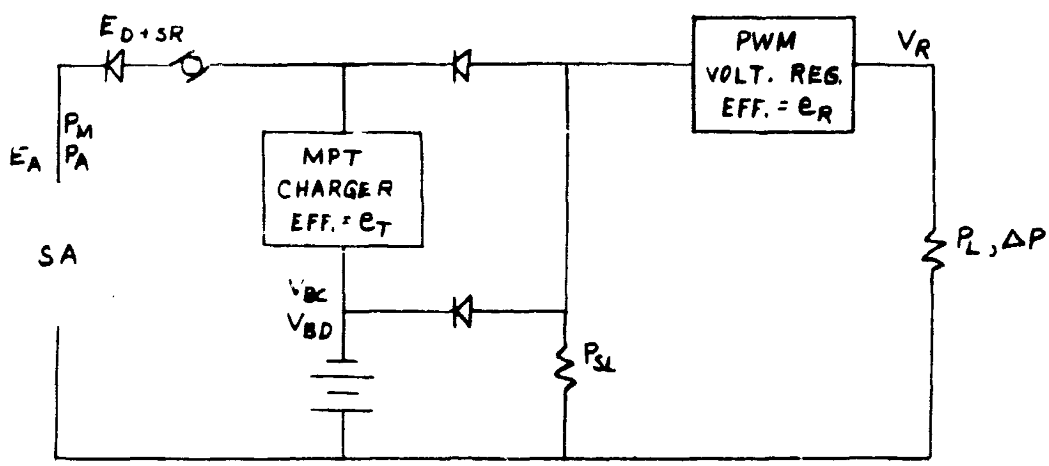

$$\frac{(TN)(C/D)}{e_T}\left(\frac{V_{BC}}{V_{BD}}\right)\left[\frac{P_L}{e_R}+P_{SL}\right] + (TD-TP)\left[\frac{P_L}{e_R}+P_{SL}\right] + TP\left[\frac{P_L}{e_R}+P_{SL}+\frac{1/4\,\Delta P}{e_R}\right]$$

$$+ \frac{(TP)(C/D)}{e_T}\left(\frac{V_{BC}}{V_{BD}}\right)\left[\frac{3/4\,\Delta P}{e_R}\right] = E_A - E_{D+SR} - TP(P_M - P_A)$$

Figure 14. Part-Time Parallel Tracker Energy Balance EQN

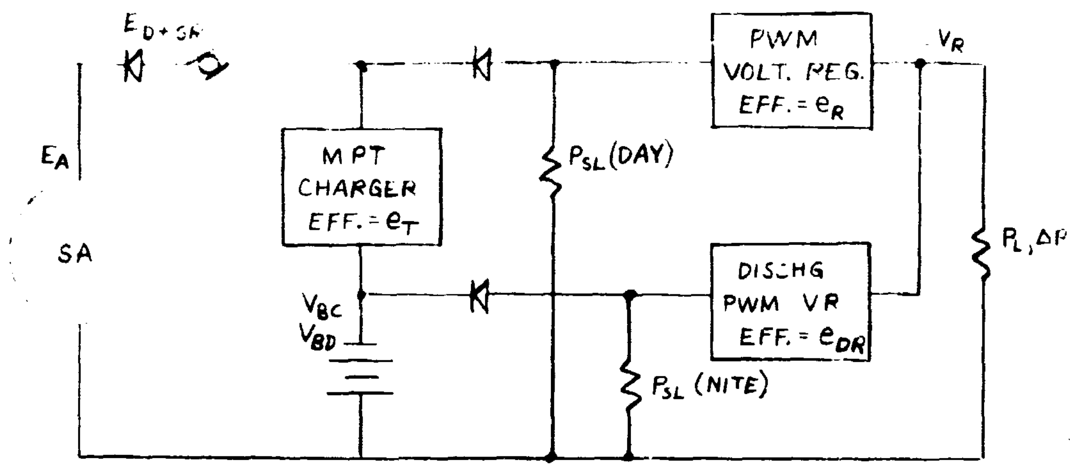

$$\frac{(TN)(C/D)}{e_T}\left(\frac{V_{BC}}{V_{BD}}\right)\left[\frac{P_L}{e_{DR}}+P_{SL}\right]+(TD-TP)\left[\frac{P_L}{e_R}+P_{SL}\right]+TP\left[\frac{P_L}{e_R}+P_{SL}+\frac{1/2\,\Delta P}{e_R}\right]$$

$$+\frac{(TP)(C/D)}{e_T}\left(\frac{V_{BC}}{V_{BD}}\right)\left[\frac{1/2\,\Delta P}{e_{DR}}\right]=E_A-E_{D+SR}$$

Figure 15. Full-Time Parallel Tracker Energy Balance EQN

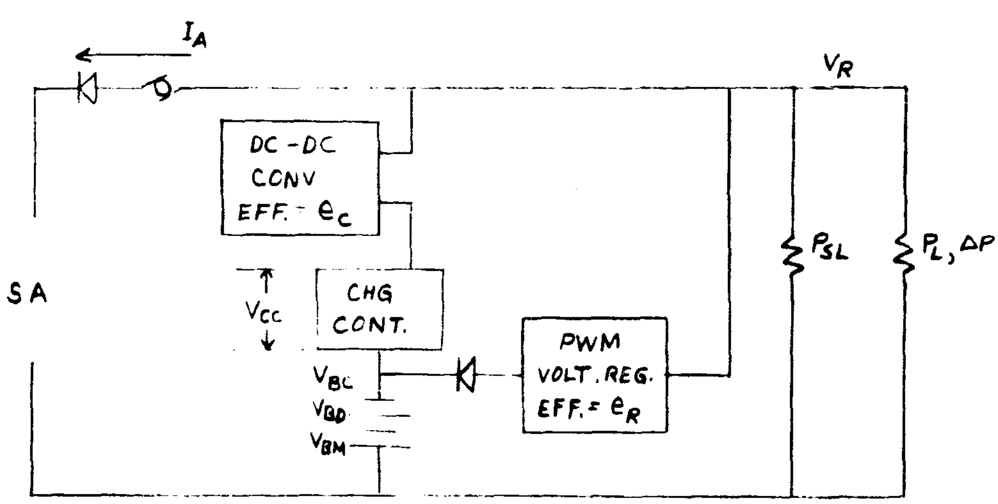

$$\left[\frac{V_R}{(V_{BM}+V_{CC})}+\frac{(V_{BM}+V_{CC}-V_R)}{e_C(V_{BM}+V_{CC})}\right]\left(\frac{C/D}{e_R}\right)\left(\frac{V_{BC}+V_{CC}}{V_{BD}}\right)\left[TN(P_L+P_{SL})+TP(1/2\,\Delta P)\right]$$

$$+(TD-TP)\left[P_L+P_{SL}\right]+TP\left[P_L+P_{SL}+1/2\,\Delta P\right]=(V_R)(TD)(I_A\,@\,V_R)$$

Figure 16. Boost Charger Direct Energy Transfer Energy Balance EQN

Values of maxir um load power shown above are approximate and based on use of the solar ce the F-3 array. Those systems selected for further detailed analysis onsidered with a new solar cell and array layout, which will somewhat inc...se the load power capability.

3. Comparison of System Configurations

It is necessary to compare the various characteristics of the seven types of power systems already described in order to proceed to a more detailed evaluation of those configurations which appear to be most suitable to a Nimbus mission requiring more load power than the Nimbus B system is capable of delivering.

Selection of several of the systems for further detailed analysis can be made on the basis of first-order tradeoffs since each of the seven configurations initially considered will show distinct advantages and disadvantages.

Table I presents a summary comparison of the significant system characteristics of the seven power system configurations, for both the F-3 type and the bifold solar arrays. Items in Table I are further discussed below.

a. Utilization of Nimbus B Storage Modules and Control Module

The check marks under each system indicate which of these already flight-qualified modules can be used to configure the system. Every system can use the Control Module; item 3 in the table shows the number of control modules required with each system. The parallel tracker configurations (PPT, PFT, and PPFT) require a high input voltage modification to the voltage regulator, and the regulator for use in the DET system must be modified to provide response to the mode selector input signals.

An increase in the maximum allowable charge current from the present C/4 rate to C/2 will allow the NB Storage Modules to be used in the series tracker systems. It is conceivable that the existing electronics in the storage module could not be adapted to the STM system, but the cells and packaging could be utilized. The DET system would use NB Storage Modules that were modified to respond to the charge inhibit signal from the mode selector.

b. Storage Capacity

Item 2 in Table I shows the required battery capacity needed to limit the depth of discharge to 20 percent with the maximum orbit-average load power derived from the energy balance equations. The number of ampere-hours does not include any redundancy. Thus, dividing the capacity by 4.5 would yield the number of NB storage modules required to supply the non-redundant, baseline system capacity.

c. Number of Cells, Batteries

The number of parallel batteries specified for each system is shown in item 4 of the table. All F-3 array systems that utilize the NB Storage Modules would use a total of 8, in order to supply the same redundancy that exists with the Nimbus B system. The bifold array systems using the NB modules are specified as having 12. This number is a compromise considering the excellent flight reliability of earlier Nimbus batteries, a significant spacecraft "real estate" demand by the batteries, and a small increase in depth of discharge in the event of one or two battery failures. All NB storage modules would use 23 4.5 A-H cylindrical NiCd cells.

The three parallel tracker systems require a completely new charge control electronics complement, as well as an additional cell in each battery. The additional cell is needed to ensure adequate unregulated bus voltage under end-of-life high temperature operation. The greater load capability of these systems requires more baseline capacity, and a new battery design utilizing 12 A-H prismatic cells provides a greater capacity/volume ratio. This real estate savings is important because of the need for one spacecraft bay to house the tracker control electronics and switching devices.

d. Power Dissipation

Of the seven system configurations initially considered, only the NB and DET systems are specifically designed to dissipate excess power. The NB shunt dissipator must be able to safely dissipate, at -38 volts, the array power when an unlikely failure mode occurs which opens one load regulator and prevents automatic switchover to the standby regulator. The temporary loss of regulated bus voltage would prevent battery charging and the resulting power that the shunt dissipator must accommodate is 420 watts with the F-3 system, and over 800 watts with the bifold system, as shown in item 5 of Table I. Similarly, in a very unlikely mode of operation, the DET shunt regulator would have to dissipate 391 and 790 watts, respectively, with the F-3 and bifold solar arrays.

In view of the greater load power capability of the systems being considered, the voltage regulator bay power dissipation would be in excess of 20 and perhaps

SYSTEM CHARACTERISTIC	F-3		
	NB	STS	STM
1. Nimbus B PWM Reg/Stor Mod (M = Modification Required)	√ / √	√ / $√_M$	√ / $√_M$
2. Battery Capacity (A-H) for 20% DOD, Based on Calculated Load Power	25.3	26.6	26.9
3. Number of Regulators (Steady-State Load)	1	1	1
4. Number of Batteries Cells per Battery Capacity per Battery (A-H)	8 23 4.5	8 23 4.5	8 23 4.5
5. Excess Power Dissipation Required (BOL Watts)	420	0	0
6. Charge Rate/Overcharge Control	C/4 V/T	C/2 V/T	C/2 V/T
7. Orbit Average Load Power (Watts)	210	224	228
8. Load Power Relative to Nimbus B	1.0	1.07	1.09
9. Regulated Bus Stability (G = Good, U = Unknown)	G	G	G
10. Array Bus Maximum Voltage (Volts)	-38.2	-76	-76
11. Development Status (FQ: Flt Qual, BB: Breadboard Tested)	FQ	BB	BB
12. Peak Load Tie-In Point	V_U	V_U	V_U
13. Total Number of Bays Required	5	6	7

FOLDOUT FRAME 1

TABLE I. COMPARISON OF SYSTEM CHARACTERISTICS

3 SOLAR ARRAY				
M	PPT	PFT	DET	PPFT
M	√ M	√ M	√ M / √M	√ M
9	27.9	28.6	27.4	28.6
	1	2	1	1
	3 24 12	3 24 12	8 23 4.5	3 24 12
	0	0	391	0
	C/2 V/T	C/2 V/T	C/4 V/T	C/2 V/T
	238	245	232	245
9	1.13	1.17	1.11	1.17
	G	U	U	G
	-76	-76	-24.5	-76
	BB	—	—	BB
	V_U	V_B	V_R	V_B
	5	7	$6\frac{1}{2}$	5

BIFOLD SOLAR ARRAY						
NB	STS	STM	PPT	PFT	DET	PPFT
√ / √	√ / √M	√ / √M	√ M	√ M	√ M / √M	√ M
47.9	50.5	51.4	53.1	54.9	52.5	54.9
2	2	2	2	4	2	2
12 23 4.5	12 23 4.5	12 23 4.5	5 24 12	5 24 12	12 23 4.5	5 24 12
839	0	0	0	0	790	0
C/4 V/T	C/2 V/T	C/2 V/T	C/2 V/T	C/2 V/T	C/4 V/T	C/2 V/T
415	440	448	463	480	457	480
1.98	2.09	2.13	2.20	2.28	2.17	2.28
G	G	G	G	U	U	G
-38.2	-76	-76	-76	-76	-24.5	-76
FQ	BB	BB	BB	—	—	BB
V_U	V_U	V_U	V_U	V_B	V_R	V_B
3	10	11	8	10	$9\frac{1}{2}$	8

even 30 watts, orbit average. It is recognized that this factor, plus an even greater dissipation in the series tracker units, could impose a serious thermal problem. This problem will be specifically investigated during the detailed analysis later in the study report.

e. Load Power

Items 7 and 8 of Table I show the maximum orbit average load power that each system can support, as determined by the energy balance equations, and the relative value of load power compared to the Nimbus B system. Note that the load values are constant during the orbit; the additional peak load of 400 watts for 5 minutes was also accounted for in the equations.

f. Regulated Bus Stability

Item 9 of Table I lists the regulated bus stability as good for all systems except the parallel full-time tracker and the direct energy transfer system. This is because the function to supply a transient with the other systems is the same as in Nimbus B, which was capable of meeting the spacecraft requirements. Both the PFT and DET systems, however, must rely on turning on a discharge regulator as well as inhibiting other functions, which will produce what must be considered an unknown effect on bus stability at this time. In addition, the DET system depends on a wider regulation range in order to provide proper operation of its shunt regulator, charge controllers and discharge regulator.

g. Solar Array Bus Voltage

Item 10 in the table summarizes the maximum expected operating voltages on the solar array bus, as described earlier for each system. The tracker systems would incur the highest voltage since their operation could be near open-circuit voltage of even of a cold solar array, during special loading conditions. The DET system would always maintain its operating point at the regulated voltage, within the limits of regulation and transient susceptibility. The highest operating voltage with the NB system would occur when the batteries are in a tapered charge condition, the regulated bus power demand is low, and the shunt dissipator is actuated at slightly above the threshold voltage, -38.0 volts.

h. Development Status

Only the components comprising the NB system have been flight qualified by RCA. Components of the tracker systems have been successfully breadboard tested, but the system configurations of the DET and full-time parallel tracker (PFT) have not undergone the same degree of testing. It is strongly recommended that any system under serious consideration should be initially breadboard tested and packaged in an engineering model of the flight configuration, in order to uncover and solve in a timely manner any problems that may arise.

i. Peak Load Tie-In Point

The point at which the connection of the peak power load is made, resulting in the highest efficiency in transferring power to that load, is shown in item 12 of Table I. The DET system utilizes the regulated bus, the PPFT system uses a battery peak load bus and the other systems use the unregulated bus as the peak load connection point. At this time it is uncertain what the power and time duration requirements of the mission peak loads will be. If they are both small, the peak loads could of course be taken from the regulated bus in all systems without greatly affecting system load capability. Peak loads having considerable magnitude and duration could exceed the main regulator current capability, impair regulated bus stability or create an excessive power dissipation in the main regulator bay, or a combination of these effects.

j. Number of Spacecraft Bays Required

Item 13 of Table I presents an estimate of the combined number of full spacecraft bays (4/4) required by each system. The numbers for the F-3 type array systems are well defined; it is possible that the actual number for the bifold systems would be greater, if more battery capacity were required or power dissipation in bays containing the series tracker units or DET shunt regulator was excessive.

4. Advantages and Disadvantages of Power Systems

Table II presents a summary of the advantages and disadvantages of the seven power system configurations initially considered. Most items in this table show a relative comparison to Nimbus B. The advantages and disadvantages shown were obtained from the system descriptions and comparisons presented earlier in this report. Table 2 is intended to show the most readily apparent

TABLE II. ADVANTAGES AND DISADVANTAGES OF POWER SYSTEMS

Advantages	Disadvantages
NIMBUS B	
1) No Design or Dev. Required 2) Dwg, Specs Completed 3) All Components Space Qual. 4) Min. Integration Effort 5) High Reliability 6) Good Reg. Bus Stability 7) Min. Bays Required	1) Least Efficient 2) High Excess Power Dissipation
SERIES TRACKER (SINGLE)	
1) Min. Excess Power Dissipation 2) Utilize NB SM 3) 7% Load Power Improvement 4) Min. Des. & Dev. Required 5) High Reliability 6) Good Reg. Bus Stability	1) Qual. Required for Tracker Unit 2) High Pwr Diss in Tracker Bay 3) Requires 1 Additional Bay
SERIES TRACKER (MULTIPLE)	
1) 9% Load Power Improvement 2) Min. Excess Power Dissipation 3) Good Reg. Bus Stability	1) Largest Number of Bays Req'd 2) Tracker Dev. & Qual. Required 3) Heaviest System 4) High Pwr.Diss in Tracker Bay (55W)
PARALLEL PART-TIME/FULL-TIME TRACKER	
1) Most Efficient (17% Load Pwr Increase) 2) Min. Excess Power Dissipation 3) Min. Bays Required 4) Good Reg. Bus Stability 5) Breadboarded Dev. Completed	1) High Input Voltage Reg. Mod. Req'd 2) New Battery Dev. & Qual. Req'd 3) C/T Des. & Qual. Req'd
PARALLEL PART TIME TRACKER	
1) 13% Load Power Improvement 2) Min. Excess Power Dissipation 3) Min. Bays Req'd 4) Good Reg. Bus Stability 5) Breadboard Dev. Completed	1) Reg. Redesign for Hi Input Voltage Req'd 2) New Battery Dev. & Qual Req'd 3) C/T Des. & Qual. Req'd 4) Peak Load Regulator Must Handle High Voltage Input

TABLE II. ADVANTAGES AND DISADVANTAGES OF POWER SYSTEMS (Continued)

Advantages	Disadvantages
PARALLEL FULL TIME TRACKER	
1) Most Efficient (17% Load Power Improvement) 2) Min. Excess Power Dissipation	1) Requires Additional Bays 2) Reg. Bus Stability Unknown 3) Complex Circuitry 4) Reliability Unknown 5) New Battery Dev. & Qual. Req'd 6) C/T Dev. & Qual. Req'd 7) Reg. Redesign for Hi Voltage Input Req'd
DIRECT ENERGY TRANSFER	
1) 11% Load Power Improvement 2) Utilize NB SM 3) All Loads At Reg. Bus	1) High Excess Power Dissipation 2) Additional S/C Bays Req'd 3) Reg. Bus Stability Unknown 4) DC-DC Conv Dev. & Qual. Req'd 5) Shunt Reg. Dev. & Qual Req'd 6) Mode Selector (Complex) Req'd 7) Additional Slip Ring Capacity Req'd 8) SM and CM Mod. Req'd for Mode Sel.

qualities of each system, and is limited to first-order considerations only, since a specific design study of each system would be required to perform a more complete and accurate evaluation.

B. SELECTION OF SYSTEMS FOR DETAILED STUDY

After considering the information already presented in this report and as a result of several technical discussions with NASA-GSFC, the following power system configurations were selected for further detailed evaluation during this study:

F-3 Type Solar Array Systems

1) Nimbus B (NB)

8 NB Storage Modules, 1 NB Control Module, Optimized solar cell layout, Peak Load Regulator.

2) Parallel Part-Time/Full-Time Tracker (PPFT):

3 New-design 12 A-H batteries, 2 Tracker Control Modules, 1 Modified NB Control Module, Optimized solar cell layout, Peak Load Regulator.

3) Series Tracker, Single Tracker Unit (STS):

8 Modified NB Storage Modules, 1 NB Control Module, 1 Series Tracker Unit, Optimized solar cell layout, Peak Load Regulator.

Bifold Solar Array Systems

1) Nimbus B (NB):

12 NB Storage Modules, 2 NB Control Modules with Split Regulated Bus, Optimized solar cell layout, Peak Load Regulator.

2) Parallel Part-Time/Full-Time Tracker (PPFT):

5 New design 12 A-H Batteries, 2 modified NB Control Modules with Split Regulated Bus, Optimized solar cell layout, Peak Load Regulator.

3) Series Tracker, Single Tracker Unit (STS):

12 modified NB Storage Modules, 2 NB Control Modules with Split Regulated Bus, 2 Series Tracker Units, Optimized solar cell layout, Peak Load Regulator.

The three selected system configurations have all exhibited good performance during breadboard and/or flight acceptance testing. Regulated bus stability (regulation, transient response) is excellent and a minimum amount of development effort would be required to qualify these systems for either F-3 or bifold array applications. The NB, PPFT and STS systems represent the widest range of load power capability of all the configurations considered, and they provide minimum spacecraft real estate demands. Identical solar array layouts can be used for both the STS and PPFT tracker systems, since trackers inherently optimize the energy utilization from a solar array as long as a maximum-power voltage is provided which exceeds a certain minimum requirement. Both tracker systems have minimum excess power dissipation, which can be a significant advantage during orbits with minimum bus loading, particularly with a bifold system.

The four remaining system configurations exhibit less of an advantage in the Nimbus application for various reasons. The basic parallel part-time tracker (PPT) becomes the selected PPFT system with the addition of the extra battery discharge diodes providing the peak load bus, yielding a disti ct load power capability advantage. The parallel full-time tracker (PFT) can supply the same load as the PPFT configuration, but at the expense of an extra spacecraft bay for the discharge regulator, the need for a mode selector and circuit modifications to the "daytime" PWM regulator to ensure its maintaining system operation at the array maximum-power voltage during peak load battery discharge. Because of the inherent load sharing difficulty with the multiple series tracker system (STM), each of the multiple series tracker units must be capable of supplying the entire regulated bus load. This greatly increases the complexity compared to the STS design. Additionally, charge control circuitry must be designed and incorporated into each series tracker unit of the STM system. The slight load advantage of the STM over the STS system does not trade off the extra spacecraft bay and circuit complexity required.

The direct energy transfer (DET) system offers a moderate load power increase over Nimbus B. However, it too is a high-excess-power dissipation system. The DET would require the greatest development effort of all systems considered, in view of the new shunt regulator, multipurpose mode selector, DC-DC converters and modification to the NB storage and control modules required. The voltage regulation band is greater than any other system, and transient response of the regulated bus is inherently slower since several sequential functions must be initiated to induce battery discharge to supply a peak demand. These disadvantages, plus a need for six and one-half spacecraft bays (4 for batteries, 1 for the modified NB control module, 1 for the high power dissipating switching shunt regulator and a half bay for the mode selector circuitry and its redundancy requirements) would make the DET system a relatively poor choice for the Nimbus spacecraft.

C. DETAILED DESCRIPTION OF SELECTED SYSTEMS

This section discusses a more detailed functional block diagram of each of the three selected system configurations (NB, PPFT and STS), the most significant system electrical requirements, electronic components characterization, packaging considerations, a summary of component and system weight and volume and recommended telemetry and ground command provisions.

1. System Functional Block Diagrams

a. Nimbus B (NB)

A detailed functional block diagram of the Nimbus B-type power subsystem is shown in Figure 17. Note that a section of the diagram labeled AUXILIARY LOAD CONTROLLER is supplied by the integration contractor. The auxiliary load function shown in this portion of the diagram is not essential to the proper and safe automatic operation of the subsystem.

Critical loads are OR-gated to the auxiliary regulator output and the -24.5V regulated bus. Under normal operation the -23.5V power is used within the power system only. Each of the eight batteries provides a fuse blow tap which becomes forward biased if the main bus voltage drops below approximately -18 to -20 volts. Battery voltage limiting and trickle charge functions are inhibited or actuated simultaneously for all 8 batteries with one ground command. Batteries may be individually disconnected but can only be connected simultaneously. Shunt dissipator pass transistors are mounted on a heat sink in each storage module; the power dissipating resistors in their collector circuits are externally mounted on the Auxiliary Load Panels.

Much thorough documentation has been prepared on the Nimbus B power subsystem description and operation; therefore, further detail will be omitted from this report.

b. Parallel Part-Time/Full-Time Tracker (PPFT)

Figure 18 presents a detailed functional block diagram of the PPFT power subsystem. The Voltage Regulator Module shown in the figure is the NB Control Module modified to accommodate the -80 volt unregulated bus input voltage. The redundant auxiliary regulators no longer derive power from the unregulated bus, but from the peak load bus which remains at battery voltage. Note that there is no requirement for the NB shunt dissipator circuitry in the control module or the storage modules. There is also no longer a need for an Auxiliary Load Controller or Load Panels, saving space and a significant number of formerly required ground commands.

The fuse blow tap arrangement is essentially the same as in the NB system, still relying on a total of 36 ampere-hours of storage capacity to provide fuse blowing capability. The diagram shows the low power sensing and control circuitry for the charger/tracker functions packaged in Tracker Control Module I, and the high-power-dissipating tracker pass elements in Tracker Control Module II. Also contained in the second module are the filtering components for the square-wave-operated tracker pass elements. A more complete description of these considerations is presented in a later discussion of component packaging.

Two of six storage modules are shown in Figure 18; two storage modules connected electrically in series comprise one of the three parallel batteries in this system. Each battery has its own charge control function and protection functions operated completely independent of the other two batteries.

Figure 19 presents the nominal value of maximum storage cell charge voltage as a function of temperature. This relationship is identical to that used on the Nimbus B flight subsystem and provides a safe voltage limit for charging the battery in the over-charge state. In order to implement a minimum power dissipating condition in the batteries, the voltage limit of course must be considerably reduced, but this could present a severe problem in trying to replace even the minimum required amount of charge. The technique utilized in the PPFT system to permit full recharge and yet ensure minimum dissipation once the battery has been fully recharged is an electronic ampere-hour counter function which would reduce battery charge current to a low value of trickle charge current when the required ampere-hour C/D ratio has been achieved.

Figure 20 presents the recommended battery C/D ratio, as a function of temperature, that should be obtained to ensure full recharge of the battery. The ampere-hour counting technique being considered would reset a digital counter to zero at the end of each orbit sunlight period, probably with a signal from the solar array current telemetry circuit. The counter would "count up" during discharge, and "count down" during charge. The gain of the charge current signal amplifier would be reduced during charge, so that the slower "counting down", or charge, process would effectively incorporate the C/D ratio, and the value of the bits in the counter would always reflect the true state of charge. The gain reduction during charge would be a function of battery temperature, to accommodate the proper C/D ratio. When the charge counter reaches zero, full recharge has been achieved, and the charge current is reduced to a low dissipation, trickle-charge value.

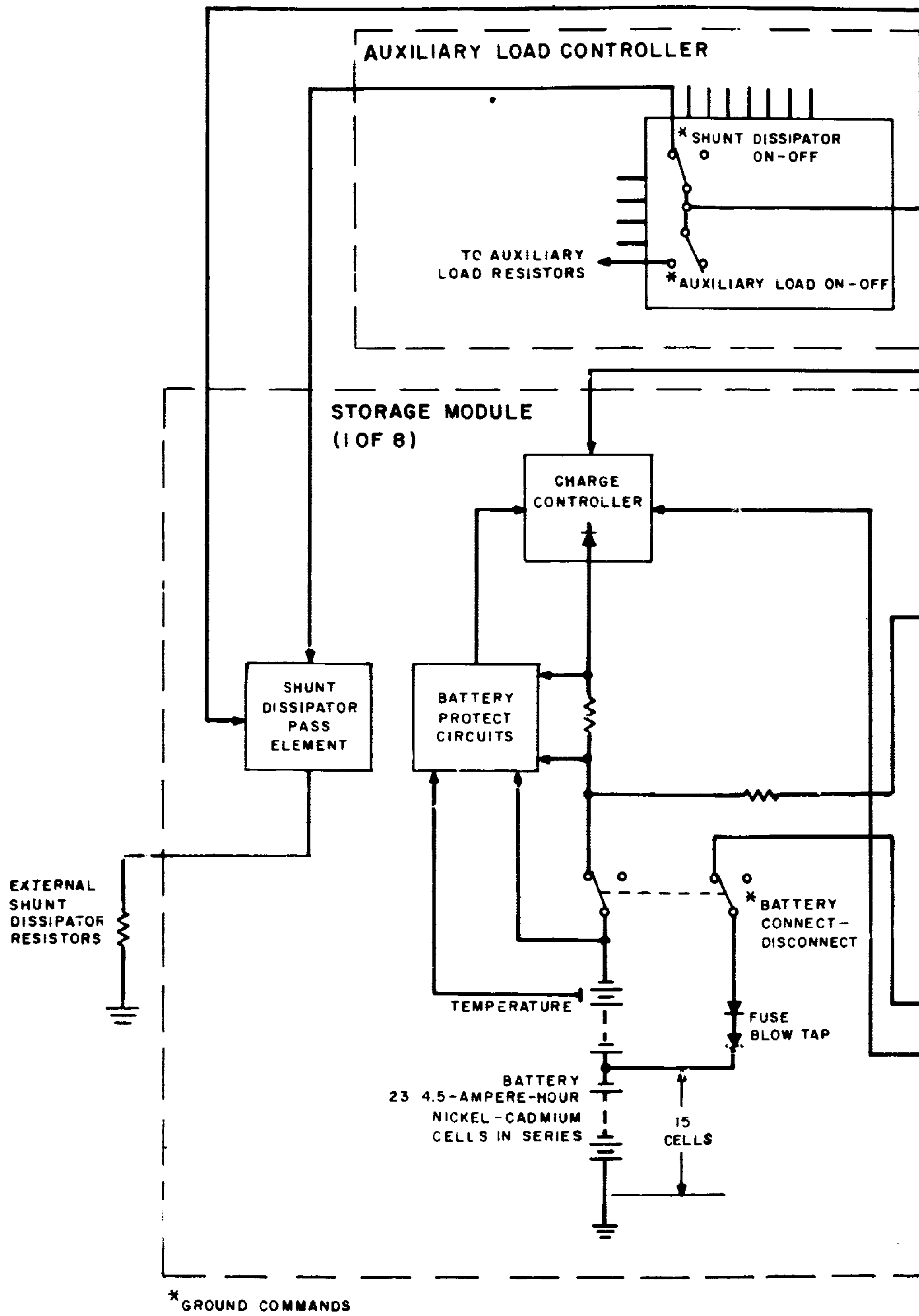

FOLDOUT FRAME 1

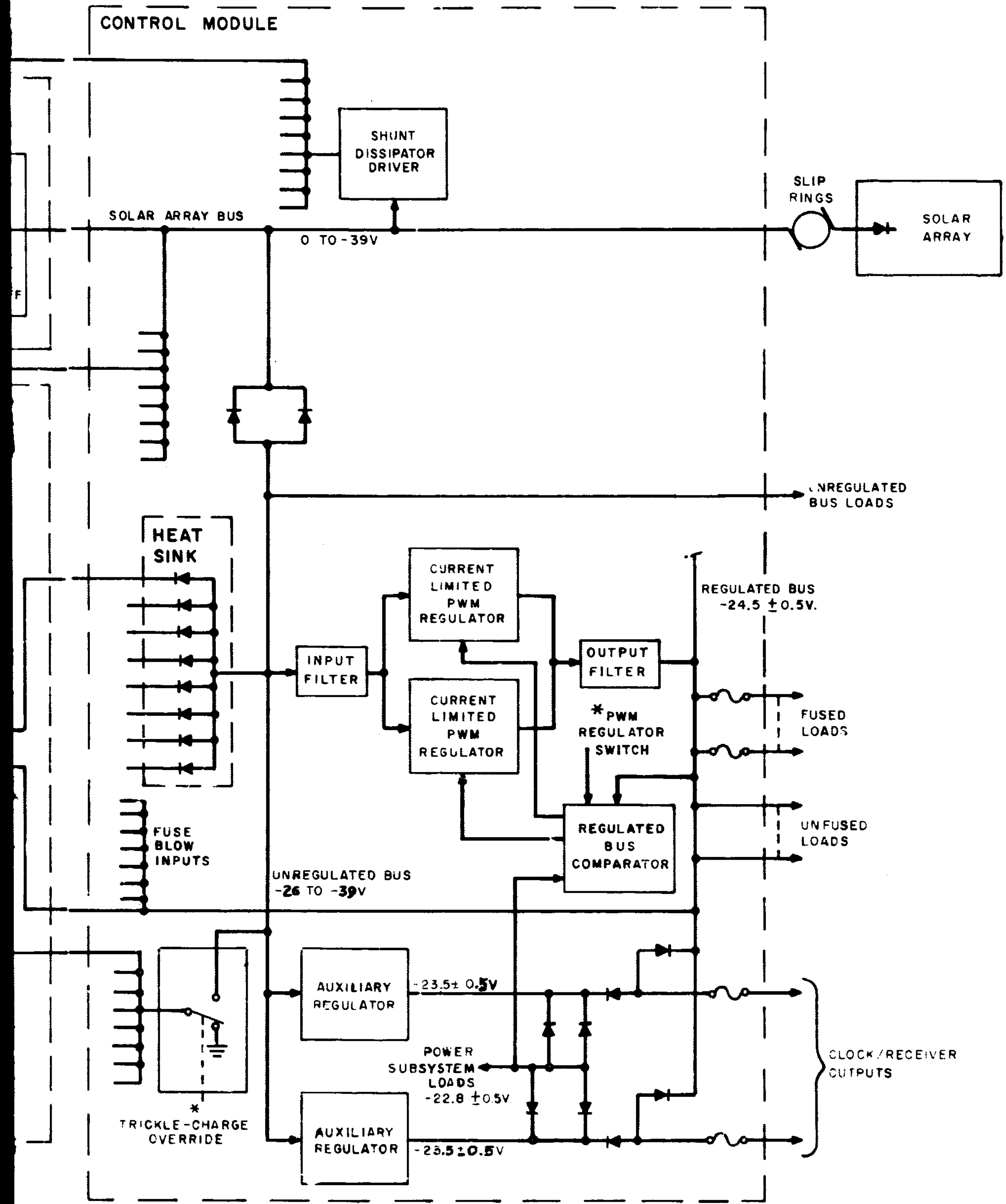

Figure 17. Functional Block Diagram for Nimbus B Type Power Subsystem

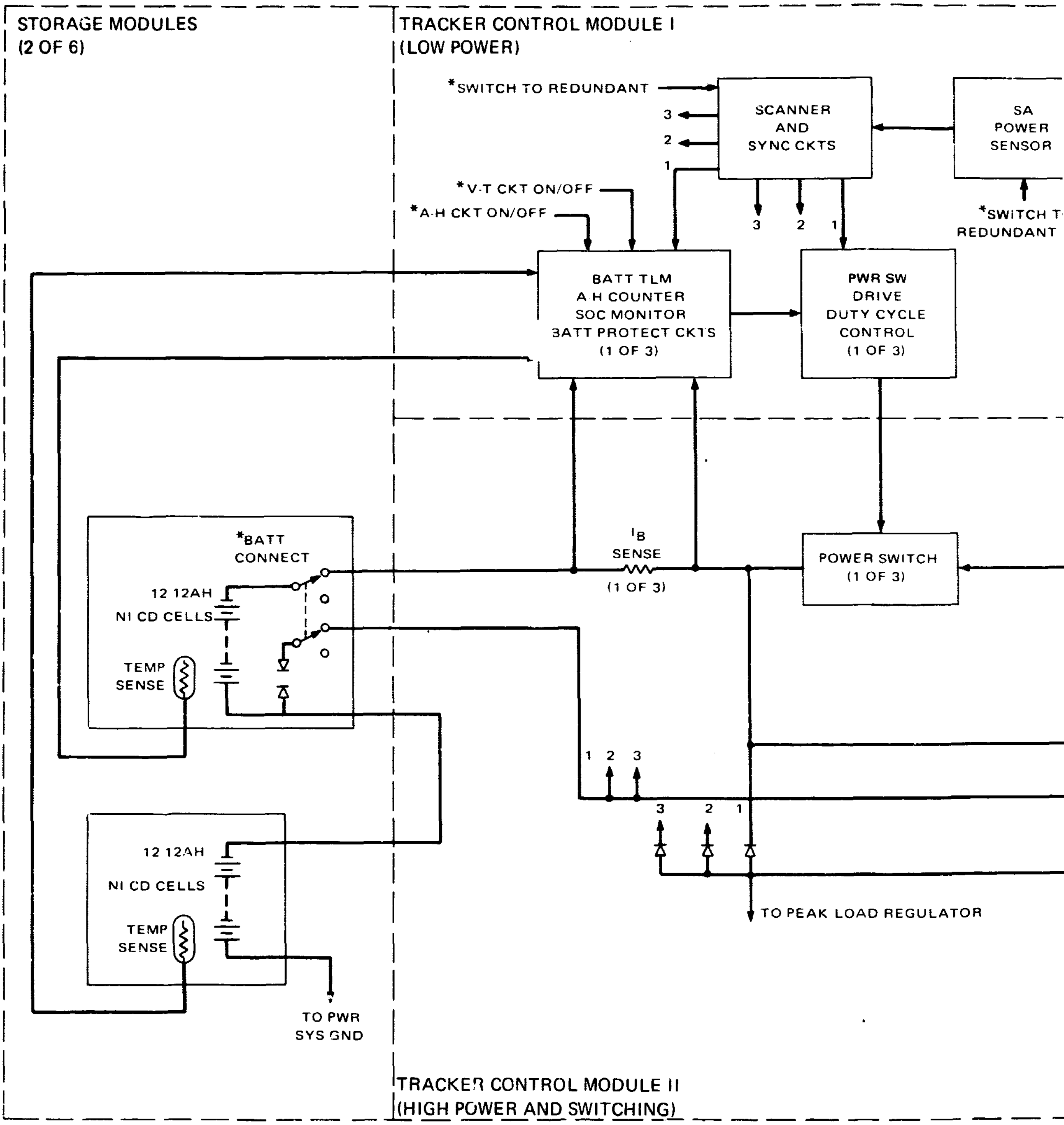

*GROUND COMMAND

FOLDOUT FRAME 1

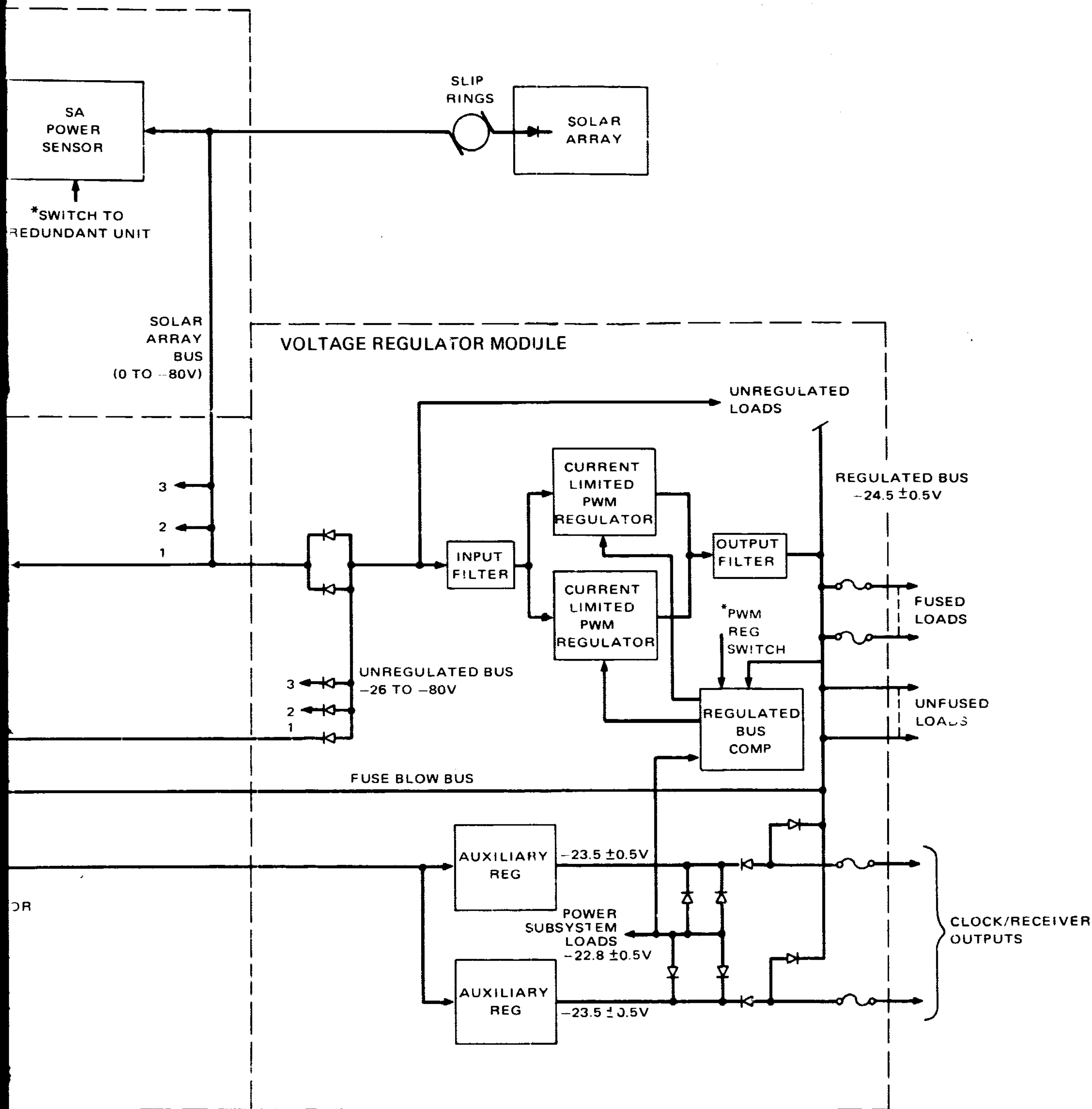

Figure 18. Functional Block Diagram, Nimbus Parallel Maximum Power Tracking Subsystem

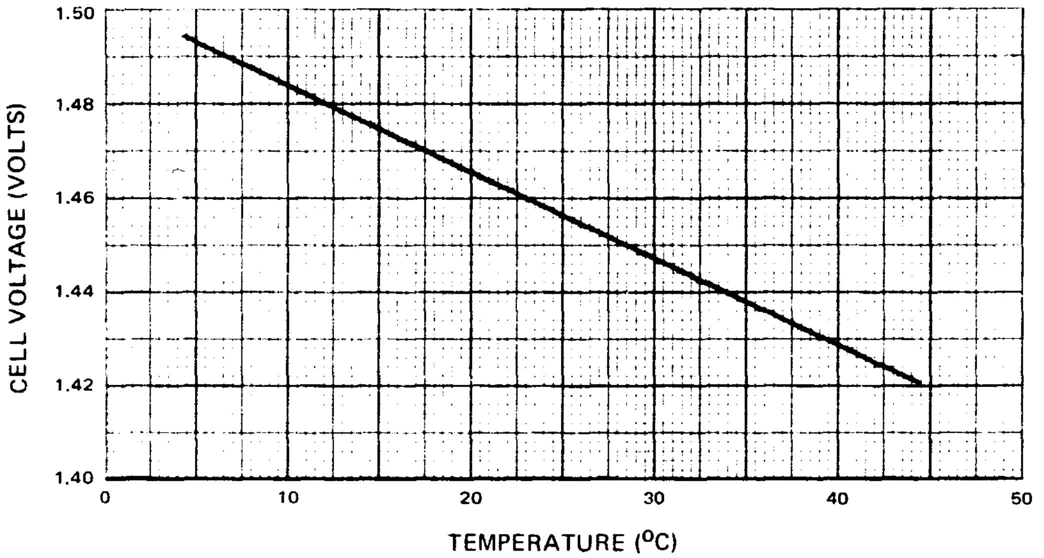

Figure 19. Nominal Cell Charge Voltage Limit Versus Temperature

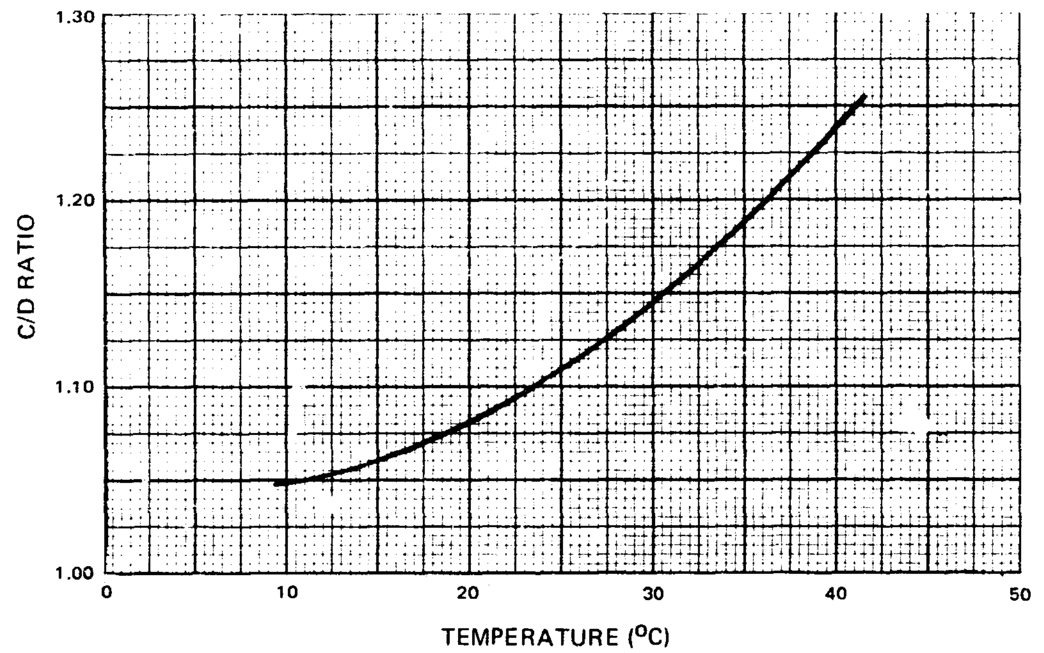

Figure 20. Minimum Ampere-Minute C/D Ratio Versus Temperature For Beginning-Of-Life Ni-Cd Storage Cells

Figure 21 presents several battery current profiles during an orbit with a low value of spacecraft load. Battery discharge current for the 35-minute night-time is identical for all systems using the NB PWM load voltage regulator. When the solar array becomes illuminated, the NB system will allow battery charging at the maximum current limit, 8.8 amperes, if this much charge current is available from the solar array. Actual Nimbus test data has shown that the batteries will reach their limiting voltage at about the same time that the minimum required ampere-hour C/D ratio has been achieved, at this nominal battery operating temperature of 25°C. When the limit voltage is reached, a reduced current is effected to charge the battery at its limit voltage, thus the name "tapered charging". It may be approximated, with the present Nimbus B voltage-limiting circuitry, that all of the power into the battery during the voltage-limited portion of the charge period is converted to heat energy. It is recognized that the state-of-charge of the battery at which voltage limiting will occur is a function of charge rate as well as temperature and the particular voltage-vs-temperature curve that is designed into the circuitry. Thus, for a given voltage limit, a tracker system will cause charge current tapering at a somewhat lower state-of-charge, because of the higher charge rates provided by the tracker, producing the charge current curve labeled "MPT rechg" in Figure 21. If the MPT system utilizes only the voltage-limiting charge control technique, it will also introduce a "tapered charge" condition at about the time full recharge has been achieved, thereby allowing power dissipation in the overcharged battery for an even longer period of time than with the NB system. If however, the MPT system also has an ampere-hour counting function, the battery will be placed in a trickle-charge condition as soon as full recharge is achieved, resulting in the very small overcharge dissipation shown under the curve labeled "MPT A-H Counter" in Figure 21.

The particular voltage-temperature limit curve for use in a tracker battery control function would of course be selected after a detailed analysis during the design phase of a hardware program, ensuring a high enough voltage limit to allow the batteries to charge to a full state of charge, and still provide protection against the possible effects of charging at too high a rate, particularly when the battery is near a full state of charge or in overcharge.

The omission of current-sharing circuitry for the multiple batteries in this system is intentional. If all batteries had identical charge and discharge characteristics, capacity and operating temperature, charge current sharing would be desirable. However, these conditions cannot exist. Recent experience with system testing of the Nimbus B-2 power system at RCA included maximum-load cycling with 6 "old" and 2 "newer" storage modules, the latter having more capacity, higher discharge voltage and lower charge voltages. As was expected with the common charging bus (solar array bus) and discharge (unregulated) bus arrangement used with Nimbus B and specified for the PPFT system, the higher

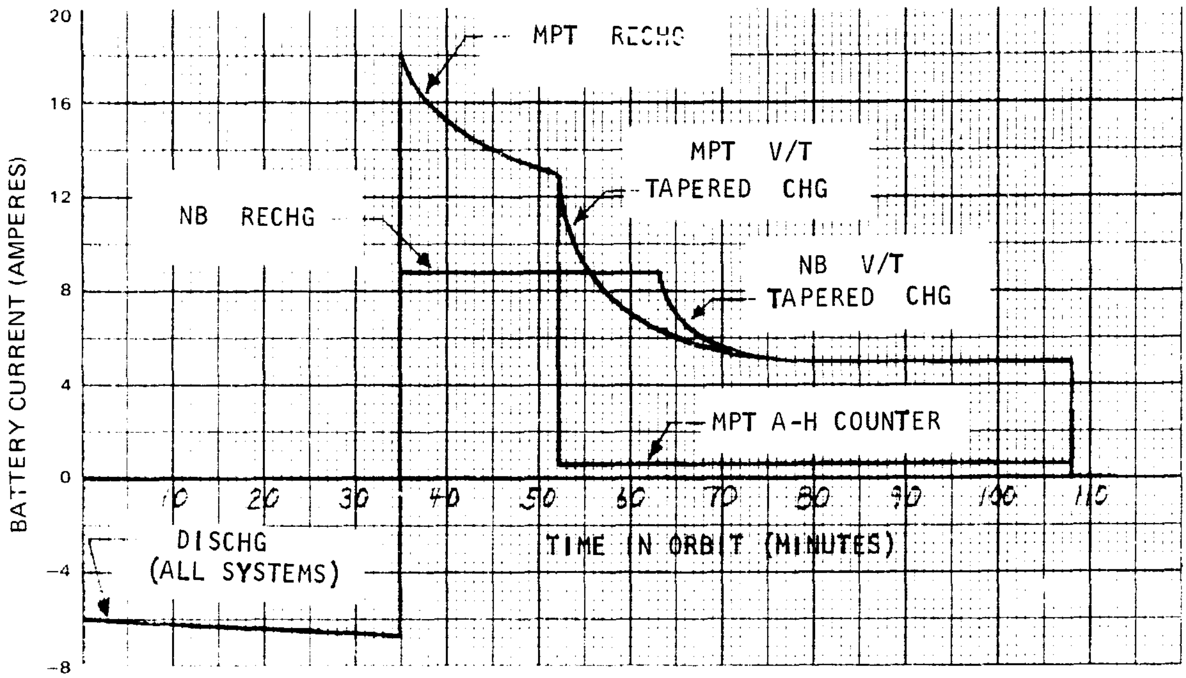

Figure 21. Battery Current Profiles For Three Types of Systems

capacity modules supplied more energy during the nighttime discharge. This cannot be prevented and actually results in approximately the same depth-of-discharge for all modules. During charge, the lower voltage of the newer batteries permitted greater charge currents, such that the same C/D ratio for each of the eight batteries was maintained. This would have been impossible with forced charge current sharing.

In addition, the ampere-hour counter used to reduce charge current to a trickle value in each battery as it reaches its proper C/D ratio in the PPFT system will ensure that no one battery will receive excessive overcharge, even without charge current sharing. Furthermore, each battery will receive its required C/D ratio in the PPFT system since the spacecraft load will be limited to that which will permit power system energy balance during each normal orbit.

c. Series Tracker, Single Tracker Unit (STS)

Figure 22 presents a detailed functional block diagram of the STS system. This system is identical to the NB system with the following exceptions.

(1) No shunt dissipator or auxiliary load circuitry is required,

(2) A series tracker unit is placed in series between the solar array and the rest of the power subsystem, and

(3) Battery charge current limit is increased from approximately a C/4 rate to a C/2 rate to take advantage of the additional solar array energy delivered by the series tracker unit.

All protective, redundant and ground command functions in the STS system operate just as in the NB system. The tracker output voltage is limited to about -37 volts to eliminate the need for high-voltage modification to the control and storage modules. Unlike the PPFT system, the STS configuration required that the PWM regulator load power as well as the battery charge power be processed through the series tracker unit. This is responsible for a considerable amount of power dissipation in the tracker unit. The dissipation may be serious enough to restrict the use of this system configuration; further discussion will be presented in the System Performance Analysis section of this report.

2. System Electrical Requirements

Table III lists the most significant electrical parameters applicable to each of the selected power subsystems.

Regulation, ripple and transient response specifications for the -24.5V regulated bus shall be, for all systems, identical to those of the flight Nimbus B subsystem. Power transfer efficiency of the PWM load regulator, series tracker unit and charger/tracker units shall be as high as possible, with a design goal of at least 90% efficiency. Recommended telemetry and ground command functions for the three systems are presented in a later section of this report.

3. Electronics Characterization

a) Nimbus B. A complete description of the equipment and functions for the Nimbus B power subsystem electronic components can be found in the RCA Performance Specifications:

RCA Drawing No.	
PS 1846666	Nimbus B Power Subsystem
PS 1759580	Nimbus B Storage Module
PS 1759712	Nimbus B Control Module

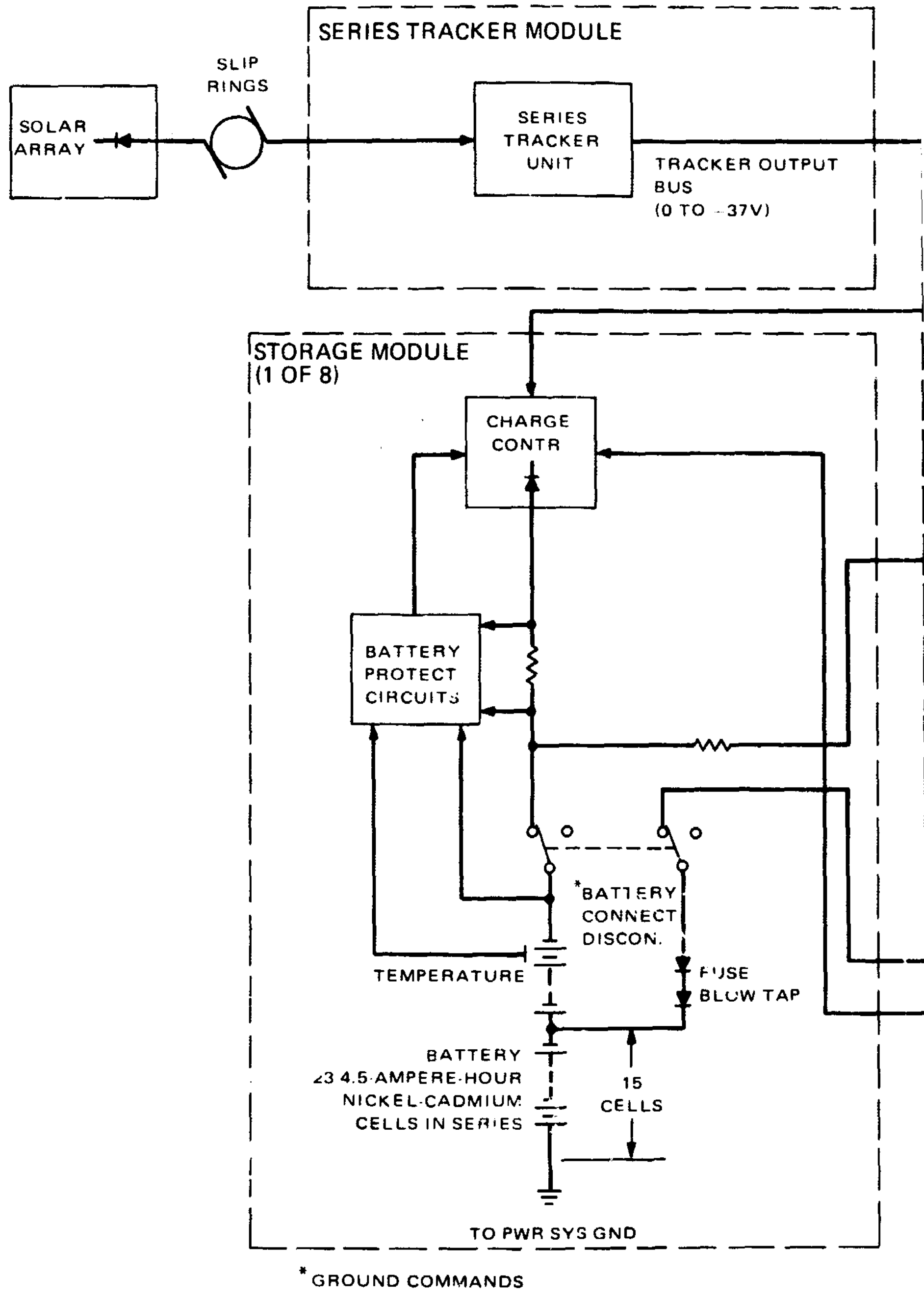

FOLDOUT FRAME 1

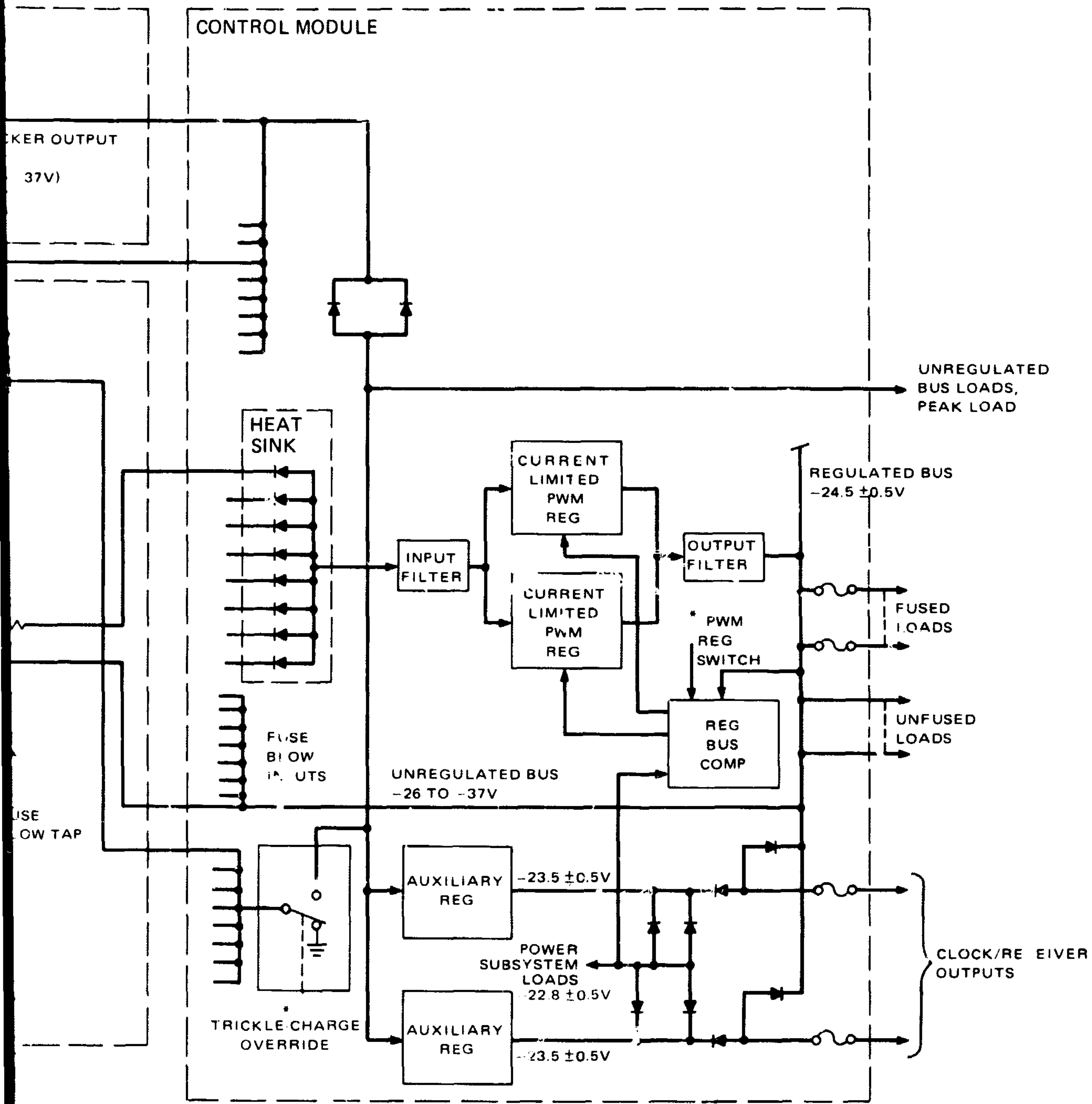

Figure 22. Functional Block Diagram Nimbus Series Maximum Power Tracking Subsystem

TABLE III. APPLICABLE ELECTRICAL PARAMETERS

Parameter	NB	PPFT	STS
Solar Array Voltage	0 to 38V	0 to 80V	0 to 80V
Unreg Bus Voltage	0 to 38V	0 to 80V	0 to 37V
Solar Array Current	0 to 14A	0 to 14A	0 to 14A
No. of Batteries	8	3	8
No. of Cells per Batt.	23	24	23
Storage Cell Capacity	4.5 AH	12 AH	4.5 AH
Max. Chg Current	1.1 A per batt	6.0 A per batt	2.25 A per batt
Trickle Chg Current	150 mA per batt.	250 mA per batt	150 mA per batt
Overchg Protection	Volt.-Temp Limit	Volt.-Temp Limit Amp-Hr. Counter	Volt.-Temp Limit
Batt Volt. Range	26.5 to 34.0 V	26.5 to 35.4 V	26.5 to 34.0 V
Fuse Blow Tap	Yes	Yes	Yes
Isolated Common Return (Gnd)	Yes	Yes	Yes
Reg Bus Voltage	-24.5 V	-24.5 V	-24.5 V
Reg Bus Current	2 to 20A	2 to 20A	2 to 20A

b) PPFT System

Battery Charge Electronics. The function of the Battery Charge Electronics is to provide for the maximum transfer of energy from the source (Solar Array) to the energy storage devices (batteries). This is done taking into account the requirements of the batteries as determined from the previous orbital dark period, the limitations of the batteries and the capability of the source. The various operating modes are as described below. A functional block diagram for the Battery Charge Electronics is presented in Figure 23.

(1) Charge Mode. The normal charge mode occurs during the daylight portion of the orbit and can be considered for three conditions of source capability. The first is the capability of the solar array to supply more power than the batteries and spacecraft loads require; the second occurs when the array

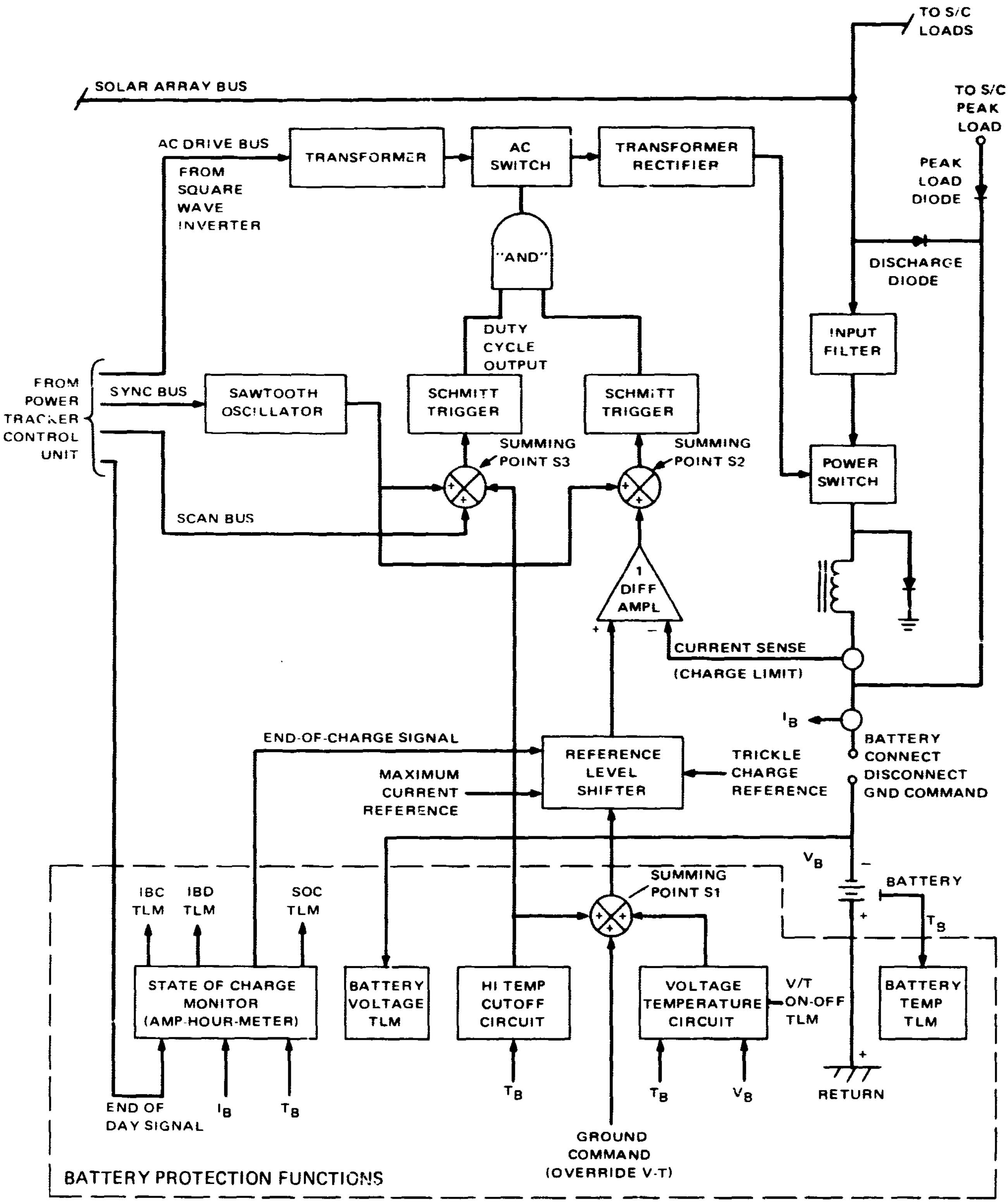

Figure 23. Battery Charge Electronics - Functional Block Diagram (Parallel Tracker System)

can supply both the battery and load requirements only if active control of the operating point is used; and the third is that in which the array can no longer satisfy the requirements of both loads and batteries.

(a) Excess Array Capability. In this condition, the source has more power available than the loads and the batteries require, and the array is operated (off the maximum power point) on its I-V characteristic at a point determined by the actual system load requirements. This is essentially a fixed operating point operation.

The operation of a battery module is as follows: (See Figure 23) In this mode, the battery voltage and temperature are assumed to be within the acceptable limits and no signal is applied to the reference level shifter from the battery protective function(s). The array is activated as the spacecraft enters the daylight portion of the orbit and the batteries begin to charge. The reference-level-shifter output senses that the maximum charge current is allowable.

Since there is excess array power available, the batteries will charge at the maximum allowable rate. The charge-current sensor provides an analog output which is applied to difference amplifier No. 1 where it is compared with the signal from the reference level shifter. If the current sensed is greater than maximum allowable current, then the output to summing point S_2 decreases. Also at point S_2, the synchronized sawtooth signal which determines operating frequency is added to the charge-current-error signal. This combined signal is threshold detected by Schmitt trigger No. 2. The Schmitt trigger output controls the a-c switch which applies and removes the drive from the power switch. A decreasing output from difference amplifier No. 1 results in an increasing off time of Schmitt trigger No. 2, thereby decreasing the on time of the power switch, which in turn, tends to decrease the charge current.

The scanner and sawtooth signals are added to the summing point, S_3. The total signal at point S_3 determines the duty cycle of the power switch when the protection functions are inactive. Since the array power is greater than the load demand, the deliverable current (if the array were operated at the maximum power point) is greater than the limiting current, as determined by the protection function. The AND function input to the a-c switch allows the Schmitt trigger (modulator), to be activated for a shorter period of time to control the power switch duty cycle. Therefore, the current limiting protective function (which requires a shorter duty cycle) controls the power switch, causing the maximum power tracking function (Schmitt trigger No. 1) to be inhibited.

An automatic adjustment is made to the charge rate when the protection functions detect overvoltage, high temperature conditions, overcharge, or when a ground command is applied. At this time a signal is generated which causes the reference level shifter output to provide a reduced charge rate reference to difference amplifier No. 1. When this decrease in maximum allowable charge current occurs, the action of all functions is as described above, except that the system is operated at a lower power (higher solar array voltage) point.

Summary:

The operation under conditions of excess array capability can be summarized as follows: The charge current is limited to preset values which have been established for safe battery charging. The source is biased to a point which satisfies the demands of both the loads and the batteries. The condition would normally occur during the beginning of a mission (before the array has degraded) or later in the mission if load power requirements are unusually low. Note that transition between this operating condition and those to be discussed below is automatic.

(b) Sufficient Array Capability. In this state, the solar array (source) has enough power capability to satisfy the requirements of the loads and charge the batteries, if active control is exercised over its operating point. If a fixed operating point were to be used, the batteries might not be fully recharged each orbit and the spacecraft would not be in positive energy balance.

The battery module circuits act in response to sensed battery conditions, and duty-cycle control information received from the power-tracker control unit.

In this mode, it is assumed that the battery voltage and temperature are within the acceptable limits and that the charge current is less than the maximum allowable value as determined by the high-charge-limit reference. The duty-cycle required by the signal level at summing junction S_2 is greater than the duty-cycle required at summing point S_3, thus the inputs to point S_3 will control the system operation.

The duty cycle of the power switch is determined by the signal output of summing junction S_3. The inputs to S_3 are: scanner-inhibit signal from battery-protection function, synchronized sawtooth which determines operating frequency, and the scanner signal which determines the approximate duty cycle.

If the charge current should become greater than the maximum allowable value, as determined by the reference-level-shifter, then the current-limiting action will occur as described previously.

Summary:

The operation under the conditions of sufficient array capability can be summarized as follows: The load demand is satisfied and the remainder of the maximum available power is used to charge the batteries. This is true, because the battery electronics actively track the maximum point of the source and adjust the operating point to coincide with that point. This condition would normally occur throughout the major portion of the spacecraft lifetime.

(c) Insufficient Array Capability. In this case, the source power is not adequate to supply the loads and fully recharge the batteries during each orbit. The maximum power point controls are operating and the source is operated at its maximum power point.

The operation of the battery modules is controlled by the battery conditions and the power tracker control unit in the same manner as described in Paragraph (1) (b).

Summary:

The significant difference between insufficient source capability and the previous operating modes is that the total ampere-hour discharge of the batteries is greater than the ampere-hour charge (per orbit) and the power system is not in positive energy balance.

(2) Protection Functions. In order to ensure operation of the power system within the design parameters, certain protective functions have been incorporated into the battery module electronics. These functions automatically hold the system operation within established safe limits. Protected modes occur when certain system parameters do not agree with limiting or allowable values as determined by the system and black-box design specifications. These modes serve to protect the power system from premature failures due to improper operation.

(a) Battery Voltage-Temperature Limit: The maximum end-of-charge voltage characteristic of the battery and its variations with temperature are known. Sensing of the battery voltage to ensure that a maximum value is not exceeded is accomplished by the voltage-temperature circuit. If the battery voltage-temperature combination is greater than the allowable maximum, then the reference level shifter functions to reduce the maximum charge-current to some value less than the maximum rate. This condition is essentially a linear, battery-voltage regulation mode. System action is as previously described in Paragraph (1) (a).

(b) Battery Current Limit: The maximum charge current must be limited to a safe rate which is determined from battery considerations. The charge current is limited by the maximum current-reference signal applied through the reference-level shifter. This process has been described in Paragraph (1) (a).

(c) Battery High Temperature Cutoff. The battery charging process must be limited if the battery temperature exceeds a safe limiting value. A temperature-sensitive component is physically located on, or near, the battery to sense temperature. If battery temperature exceeds a preset limit, a signal is applied to the reference level shifter which immediately establishes the trickle charge rate as the maximum allowable current. This output is also applied to summing junction S_3, to inhibit battery module operation in response to the scanner signal. The high-temperature protection function automatically resets when the battery temperature decreases below the preset safe value. A small amount of hysteresis is present to further protect the battery and prevent an oscillating condition.

(3) State-of-Charge Monitor

(a) Function: The state-of-charge monitor will measure and store the ampere-hour charge and discharge of a battery, making corrections for battery temperature and efficiency, and will provide a signal indicating when the full-charge condition is reached. This is accomplished by an ampere-hour meter with an accumulator and logic circuits as shown in Figure 24.

(b) Operational Description: The battery current is sensed by a resistor in series with the battery and is amplified to provide a workable signal level. This analog signal is fed to the "current direction sensor" which develops an output signal indicative of the mode of the system, i.e., either charge or discharge. If the battery is discharging, the "gain control network" transfer function has a relative gain of unity, and the discharge current telemetry output is enabled. If the system is charging, then the "gain control network" transfer function has a relative gain less than unity, and the charge current telemetry output is enabled. The actual transfer function of the gain control network is determined by the battery temperature, and the required C/D ratio from Figure 20. By this technique, the input to the current integrator is weighted to compensate for battery characteristics and environment.

The current signal is digitalized by a voltage controlled oscillator consisting of an integrator and a limit detector. Output pulses are generated proportional to the number of ampere-minutes measured. Each pulse resets the integrator and is accumulated in the counter.

The counter logic distinguishes between charge and discharge pulses and resets the accumulator each orbit. The orbit begins with the onset of spacecraft night with fully-charged batteries. As the batteries begin to discharge, the reversible 10-bit counter (1024 counts) begins counting discharge pulses while the digital-to-analog

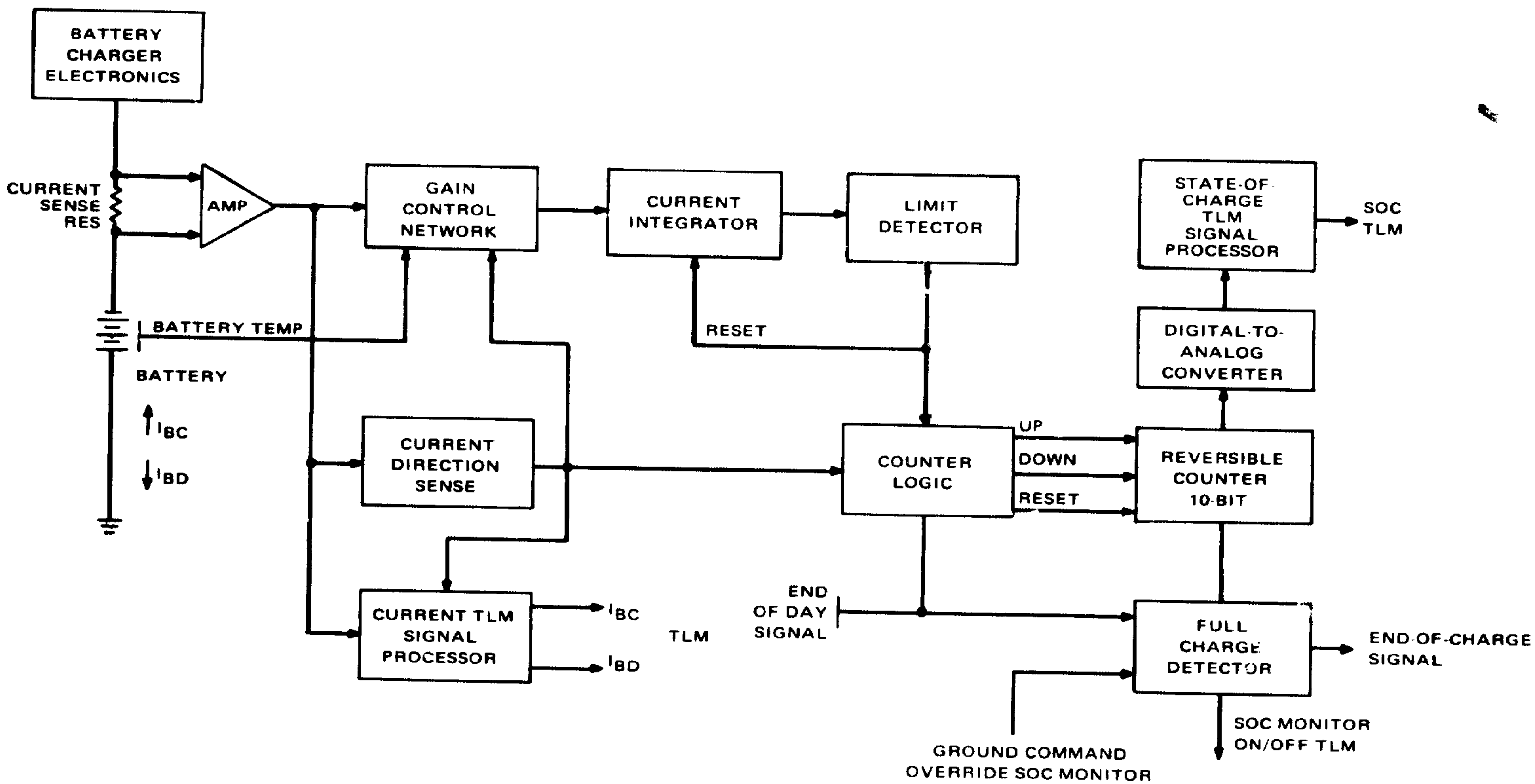

Figure 24. Functional Block Diagram, Battery State-of-Charge Monitor

converter simultaneously converts the counter's digital information to an analog signal, which is the battery state-of-charge indication. At the start of spacecraft day, the batteries begin to charge and the counter logic causes the accumulator to count charge pulses by subtracting them from the total discharge count. When the entire discharge count is cancelled (battery is fully recharged), the counter reads zero once again and the full charge detector generates an end-of-charge signal which puts the batteries in trickle charge. At the end of spacecraft day, the counter is reset to 1 by the "end-of-day" signal. Introducing a count of 1 (a tolerable error of less than 0.1 percent) into the register, instead of resetting to zero, allows the full-charge detector to be reset also. This countdown, count-back-to-zero, and reset-to-one cycle repeats each orbit.

(4) Telemetry and Ground Commands. As a further protective feature, the battery module electronics contains both telemetry indications and ground command capability. All critical subsystems functions are telemetered. These include:

a) Battery charge current

b) Battery discharge current

c) Battery voltage

d) Battery temperature

e) State-of-charge

f) V-T on-off

g) State-of-charge monitor on-off

Transducer circuits convert each of the above parameters to proportional voltages for transmission.

The following ground commands are also available:

a) State-of-charge monitor override

b) V-T circuit override

c) Battery connect-disconnect

(5) Discharge Mode. The discharge mode occurs during the dark or night portion of the orbit. The beginning of spacecraft night is characterized by the source (array) output becoming essentially zero. The solar array bus voltage falls until it is slightly lower than the battery voltage, at which time the discharge diodes become forward biased. The batteries supply the load power requirements through these diodes. Note that with the discharge diodes conducting, the battery charge electronics cannot function.

For peak loads, which may cause the load power requirements to exceed the array capabilities, the peak load diodes conduct the peak power. In this way, periods of battery discharge during spacecraft day do not cause the battery charge electronics to be inhibited and operation at the maximum power point of the array is maintained.

(6) Specifications fc ³attery Charge Electronics. A summary of the major electrical parameters specified for the PPFT Battery Charge Electronics functions is listed below:

(1) 12 A-H Battery

(2) C/2 (6A) Max. Chg. Current Limit

(3) Input Voltage 80V Max.

(4) Minimum Line drop for 6A: Typically 1.5V (non-tracking operation)

(5) Power transfer efficiency @40V Input

6A, 33V output: typically 92%
(does not include -24.5V shunt losses)

(6) -24.5V. Shunt losses: 4 watts for each battery

Tracker Control Electronics

The function of the Maximum Power Tracker Control Electronics is to detect the maximum power point of the solar array and to exercise control over the Battery Charge Electronics such that the source is operated at or near that point. A functional block diagram for the Control Electronics is shown in Figure 25. A detailed functional description is presented below.

(1) Functional Description. The array voltage sensor and array current sensor provide signals which are multiplied together to yield the instantaneous power at the array operating point.

When source power peak is detected, the peak detector reverses the direction or sense of the scanner.

The scanner generates a signal which is capable of varying the duty cycle from 0 to 100 percent which corresponds to all possible source operating points. The scanner is free-running and automatically reverses if it reaches 0 or 100 percent duty cycle before maximum power is detected.

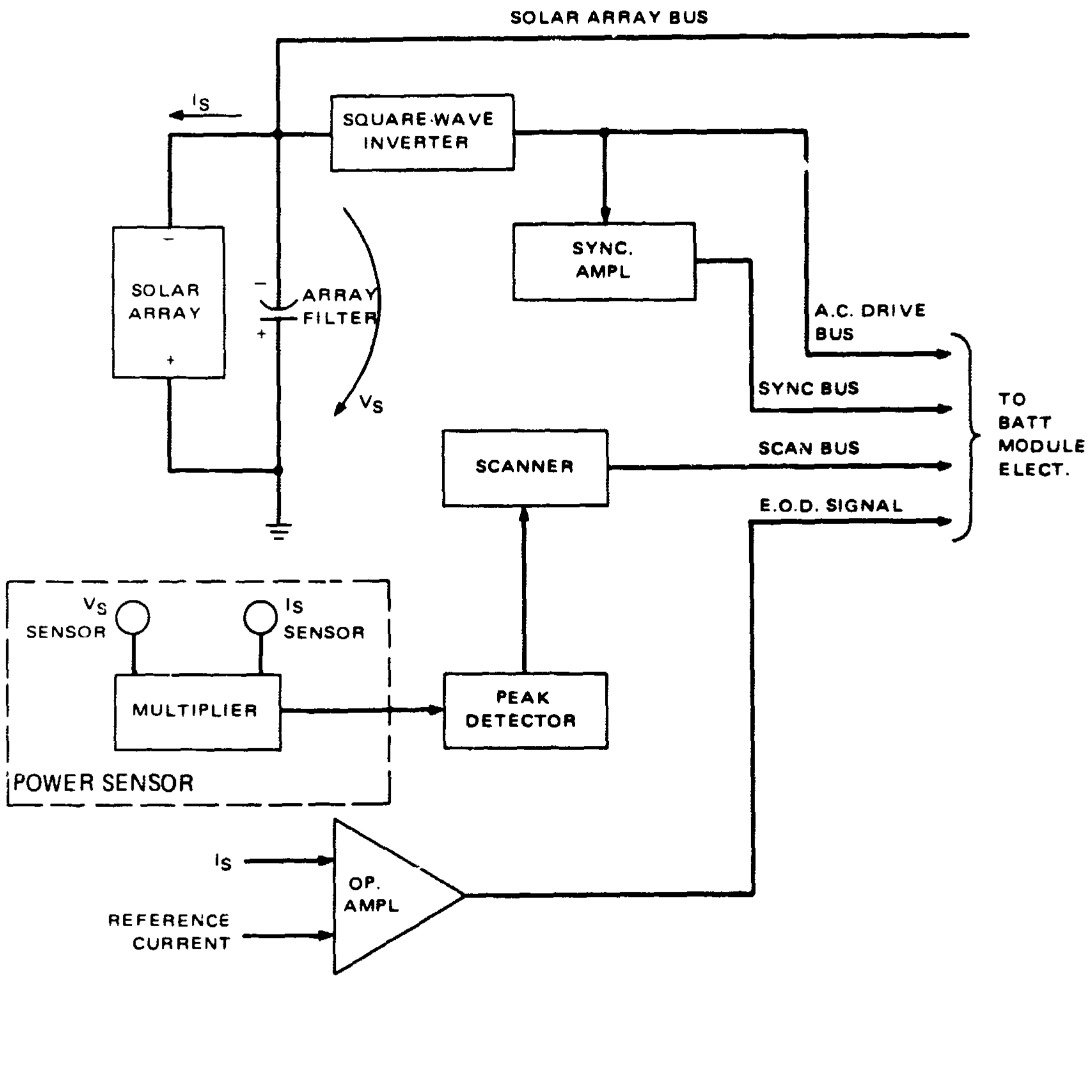

Figure 25. **Parallel MPT Control Electronics, Functional Block Diagram**

Noting that the battery module contains a pulse-width-modulated switch, and an averaging filter, the output (battery) voltage is proportional to the input (array) voltage by a factor equal to the power switch duty cycle. The output voltage is essentially fixed by the battery, so that by varying the duty cycle the solar array voltage may be controlled. The operating point of the source is controlled by the duty cycle which is derived from detection of the source maximum power point as indicated by the power sensor output.

To understand the acquisition and tracking of the maximum power point, assume that the scanner is indicating zero percent duty cycle and its output is changing towards an indication of 100 percent duty cycle. As the scanner output changes, the duty cycles of the battery module power switches are increasing and the source voltage decreases as determined by battery voltage and duty cycle. It is necessary to assume that the source has a point of maximum power and that this point is at some voltage greater than the battery voltage. As the source voltage decreases, the source power output increases. The instantaneous output power is sensed and fed to the peak detector which compares this level to the previous level which was sensed. If the most recent sensed level indicates an increase in source power output over the previous level, then the new level replaces the previous one in a memory device and the process repeats. If the most recent sensed level indicates a decrease in source output power, then a signal is generated which causes the scanner to reverse direction (towards zero percent duty cycle) and the most recent sensed power level is stored in the memory device. Note that it is necessary to pass through the maximum power point in order to detect the peak power and that as the duty cycle now decreases, the source output power is again increasing and the entire process repeats. In this manner the source operating point continually makes small excursions to either side of the maximum power point, thereby tracking that point, while performing system adjustments automatically. Operation does not depend on the initial conditions of the scanner.

The square wave inverter is used to provide drive and synchronization for all battery modules. The operational amplifier generates the end of day signal when the array current falls below a predetermined value.

(2) Reliability Considerations - Parallel Tracker System. To enhance power system reliability beyond that attained by standard derating policies, and conservative, worst case design, certain key functions are made redundant. In the present Nimbus system, there is standby redundancy of both the PWM load bus regulator and the auxiliary regulator, as well as active redundancy in the battery modules. Considering the parallel tracker system, the control electronics provides a vital function, and therefore redundancy should be considered.

Two of the four outputs of the tracker control electronics must be sensed, in order to detect a failure in the control electronics. These two outputs are the sync bus and the scan bus. Each could be made independently redundant, with little penalty in weight or size over the system with single redundancy, where all functions are replaced when a failure in any one occurs. This could be implemented by either ground command, automatic switchover, or both.

(a) Square Wave Inverter and Sync Amplifier - Sync Bus. A failure in either the square wave inverter or the sync amplifier could be sensed by a pulse absence detector (PAD) as shown in Figure 26. With no output from the sync amplifier, the PAD would set a flip-flop which switches a latching relay to replace the failed function with its redundant spare. This flip-flop can also be triggered by ground command.

(b) Power Sensor, Peak Detector, Scanner - Scan Bus. An automatic switchover scheme for the power sensor, peak detector, and scanner is shown in Figure 27. Absence of a scan signal (i.e., failure of the scanner to reverse), causes switchover by allowing the counter to accumulate the count required to set the flip-flop. This changes the state of the relay, disconnecting the faulty circuitry, and enabling its redundant spare. Ground command switchover control is also provided.

(c) End-of-Day Indicator. A third output from the control electronics, the end-of-day signal, provides a critical function and should be made redundant. Active redundancy can be used for the end-of-day signal generator by "or" gating the outputs of two identical circuits.

(d) Effect of Redundancy. The total weight and volume of the MPT control electronics with redundant controls and failure detection circuits will approximately double. Total shunt loss should increase slightly, since only one of the redundant functions is powered at a time, and the failure detection circuits will consume little power.

(3) EMI Considerations. Compatibility among the various elements of an electronic system is of prime importance. It is clear that the portions of the system which carry heavy AC currents (such as the power switching networks) will display a much greater tendency to produce EMI than will the low-level electronics (such as differential amplifiers). It is advantageous to arrange components so that the low-level circuits are protected from the fields produced by high-current

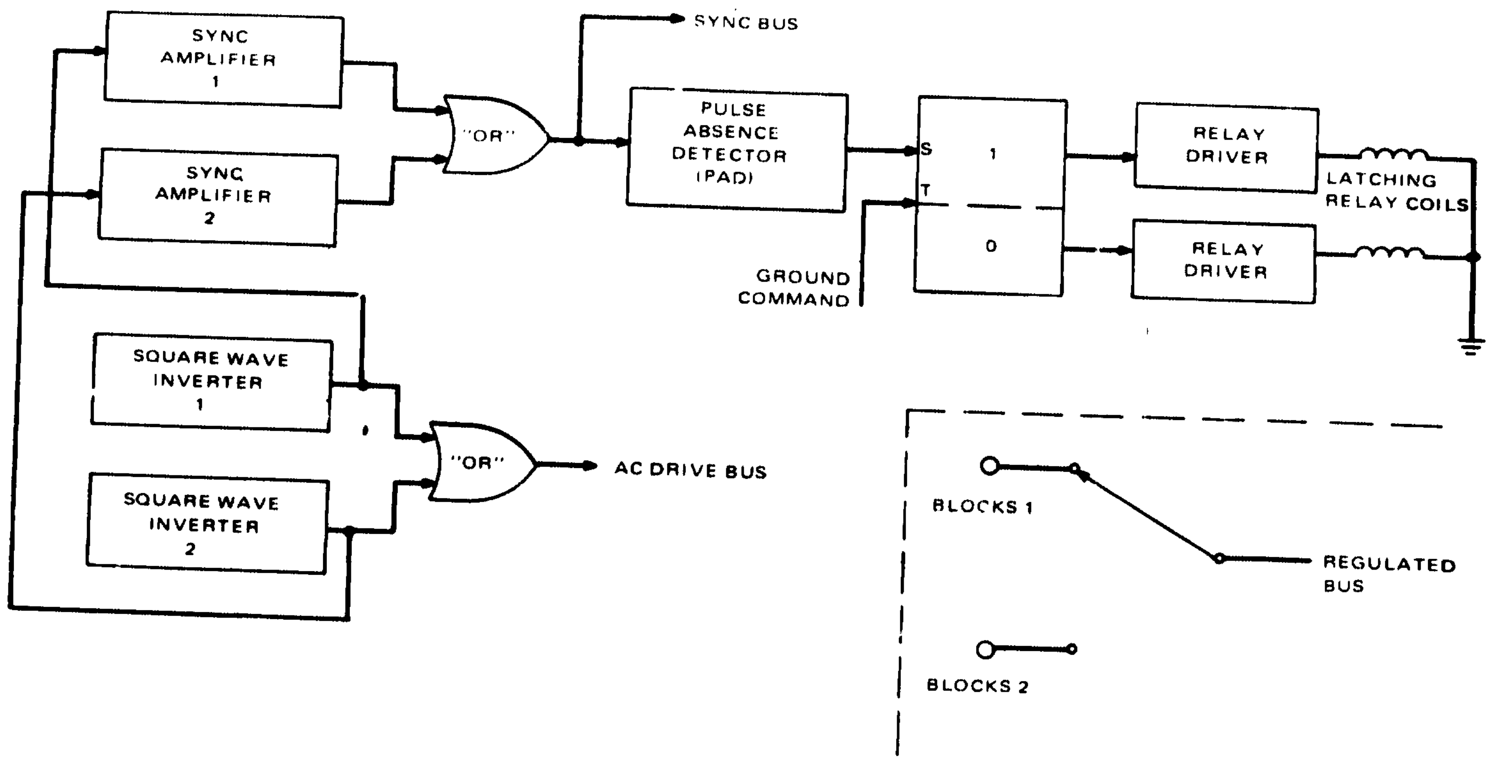

Figure 26. Functional Block Diagram - Square Wave Inverter and Sync. Amplifier, Switchover Circuit

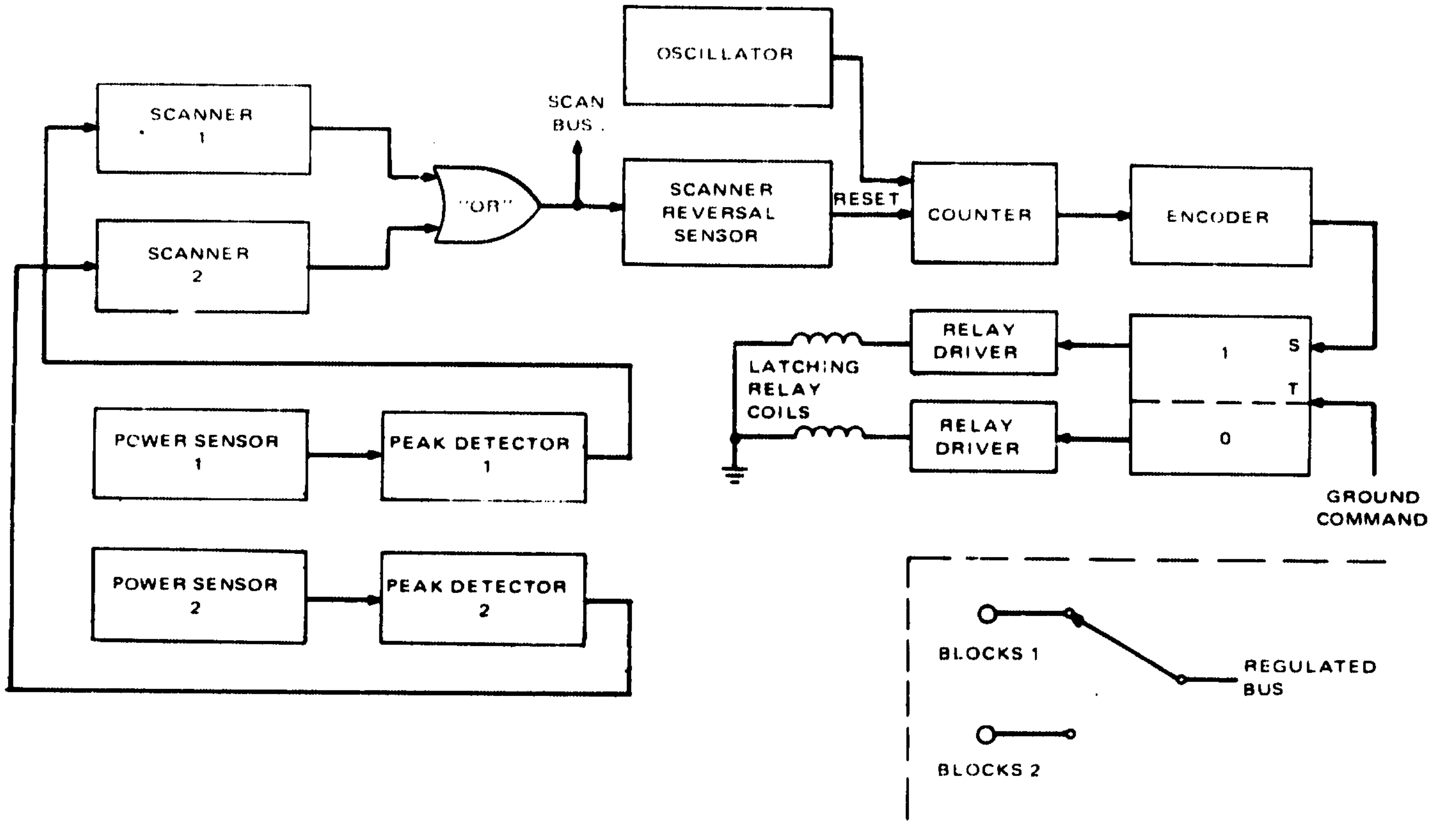

Figure 27. Functional Block Diagram - Scan Bus Switchover Circuit

sections, as well as to contain these fields within the equipment. This might be accomplished by creating separate compartments to house the most obvious EMI offenders. These "EMI Vaults" should be completely sealed. All leads penetrating the walls of the vault should be provided with EMI filters.

Since both implementation and optimization of techniques to eliminate EMI are of an extremely complex nature, further detailed analysis and testing will be required in this area, similar to that done on the Nimbus B Program.

(4) Required Changes. The following is a discussion of the changes required in the present Nimbus B Control Module for Parallel Tracker System Operation.

(a) Auxiliary Regulators. In the present Nimbus Power System, the auxiliary regulators are operated from the unregulated bus. If this were the case in the parallel tracker system, the auxiliary regulators would require redesign, since the maximum unregulated bus voltage is -80V. Because these regulators are of the series type, operation under this condition would be most inefficient and therefore undesirable.

A better approach would be to operate the auxiliary regulators from the peak load bus, since this is compatible with their present input requirements, and no circuit modifications are required.

(b) PWM Load Bus Regulator. In the parallel tracker system, the input voltage of the PWM load bus regulator can be as high as -80 volts. This circuit is presently designed to operate at a maximum input voltage of -39 volts. Therefore, some circuit modifications will be required to make the regulator compatible with the parallel tracker system.

To reduce the power dissipation (heat) produced by the drive circuits for the high voltage PWM regulator power switch, a means of transformer drive should be used. The switching transistor must be changed to a higher voltage unit, with a greater margin for second breakdown protection. The two modifications described above, plus substitution of higher voltage capacitors in the regulator input filter, constitute the only major changes to the existing Nimbus B Control Module. Implementation of the above requires an additional component volume of about 5.50 cu. in., and an increase in total weight of approximately 0.50 lb., with some minor housing modifications.

(5) Specifications for Tracker Control Electronics. A summary of the major electrical parameters specified for the PPFT Tracker Control Electronics functions is listed below:

(1) Tracking error ±2%

(2) Shunt loss 1.5 watts*

c. STS System

The series tracker system utilizes the NB Control Module without modification and the NB Storage Modules with a change in the maximum charge current from 1.1A to 2.25A. The only new electronics component required for the STS system is the series tracker unit.

(1) Summary. The series maximum power tracker unit (STU) is located in series with the solar array. Its function is to provide the maximum transfer of energy from the array to the energy storage devices and spacecraft loads. This requires efficient conversion of array power to an unregulated bus voltage compatible with the Nimbus B Storage and Control Modules to be used in this system.

(2) Functional Description. A functional block diagram of the STU is shown in Figure 28. The array current and voltage are sensed and multiplied to provide a signal which is proportional to instantaneous array power. When the source power peak is detected, the peak detector reverses the direction of the scanner.

The scanner generates a signal capable of varying the power switch duty cycle from 0 to 100 percent, which corresponds to all possible source operating points. The scanner is free-running, and automatically reverses if it reaches either limit before maximum power is detected.

The series tracker module contains a pulse-width-modulated switch and an averaging filter. Thus, the output (unregulated bus) voltage is proportional to the input (array) voltage and the power-switch duty cycle. The unregulated bus voltage is limited by the over-voltage protection function, so as to be compatible with the existing Nimbus B Power System Components. The operating point of the array is controlled by varying the power-switch duty cycle as determined from detection of the maximum source power by the power sensor and peak detector.

* Without redundancy

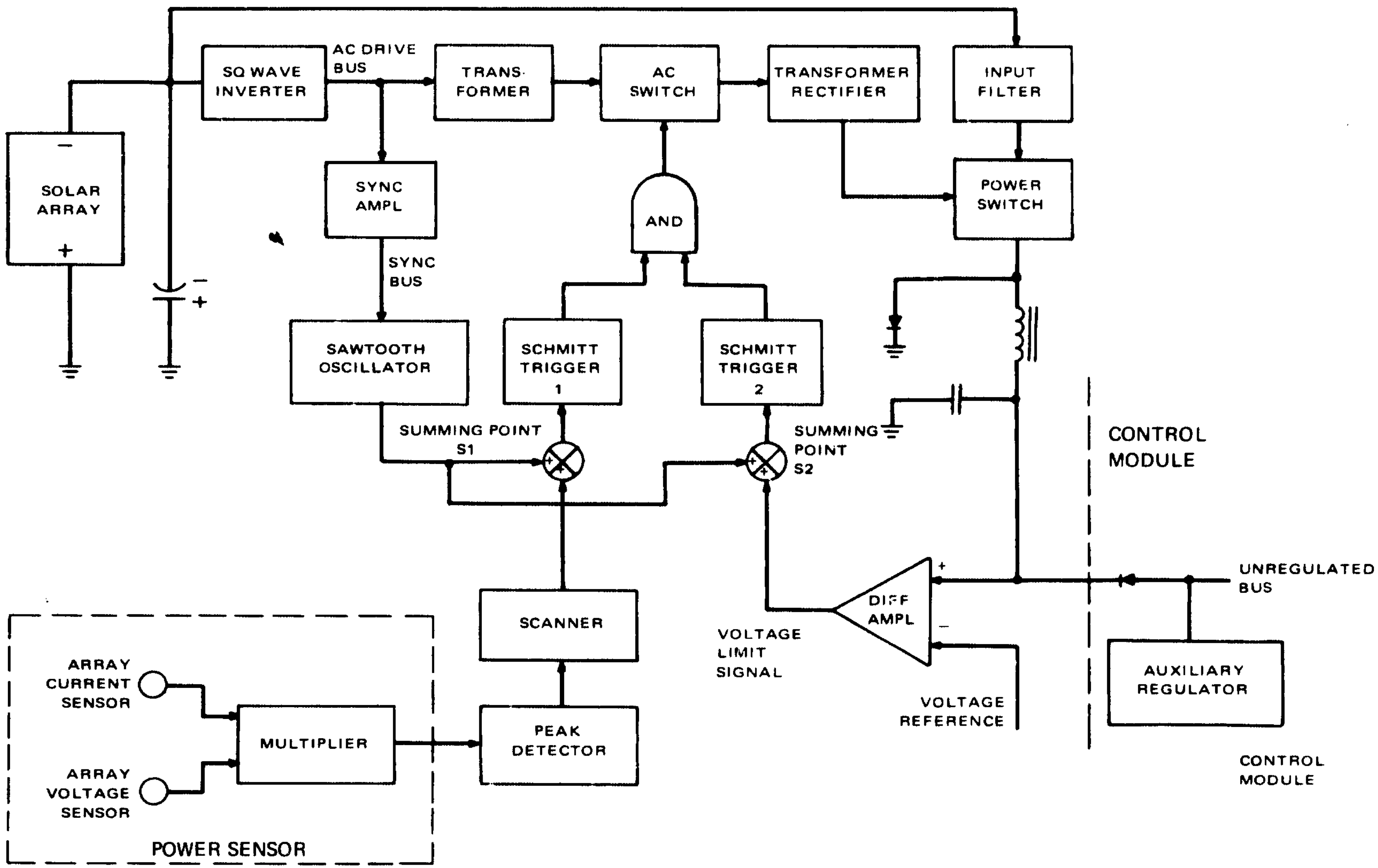

Figure 28. Series Tracker Unit, Functional Block Diagram

For proper system operation, it is only necessary to assume that the source has a point of maximum power, and that this point is at a higher voltage than the unregulated bus.

To understand the acquisition and tracking of the maximum power point, assume that the scanner is indicating zero percent duty cycle and its output is changing towards an indication of 100 percent duty cycle. As the scanner output changes, the duty cycle of the power switch is increasing and the source voltage decreases. As the source voltage decreases, the operating point shifts towards the maximum power point and the source power output increases. The instantaneous source power is sensed and fed to the peak detector, which compares this level to the previous level sensed. If the most recent sensed level shows an increase in source power over the previous level, then the new level becomes the reference and the process continues. If the most recent sensed level shows a decrease over the previous level, then a peak detector signal is generated which reverses the scanner, (towards zero percent duty cycle) and the most recent sensed power level becomes the new reference. Note that it is necessary to pass through the maximum power point in order to detect the peak power and that as the duty cycle now decreases, the source output power is again increasing and the entire process repeats. In this manner, the source operating point continually makes small excursions to either side of the maximum power point, effectively tracking that point. The system is adaptive in that it makes system adjustments automatically in response to source, load and environmental changes. Operation does not depend on the initial conditions of the scanner or any other functions.

The square wave inverter provides drive and synchronization for the tracker module. The synchronized sawtooth signal, applied to both summing points, determines the operating frequency. The scanner and sawtooth signals are added at summing point S_1. This signal determines the duty cycle of the power switch when the voltage limit loop is inactive. The "and" gate input to the A-C switch forces the Schmitt Trigger (Modulator) input which requires the shorter duty cycle to control the power switch. Therefore, the voltage limit protection function (which acts by reducing the duty cycle) causes the maximum power tracking function (Schmitt Trigger No. 1) to be inhibited when the unregulated bus voltage exceeds the established limit.

(3) Reliability Considerations. Because of the critical nature of a failure in the series tracker unit, redundancy should be provided. Improved reliability is attained by dividing the STU into three basic parts, each having independent standby redundancy. This can be accomplished with little penalty in weight or size over a system with single redundancy, where the entire module is replaced when a failure occurs.

The three independently redundant parts shall be:

1) Square wave inverter and sync. amplifier

2) Power sensor, peak detector and Scanner

3) Power switch, drive circuitry, pulse-width modulator and voltage limit circuit

Redundant functions shall be actuated by automatic switchover or ground command.

(a) Square Wave Inverter and Sync Amplifier. A failure in either the square wave inverter or the sync amplifier could be sensed by a pulse absence detector (PAD) as shown in Figure 29. With no output from the sync amplifier, the PAD would set a flip-flop which switches a latching relay to replace the failed function with its redundant spare. This flip-flop can be triggered by ground command.

(b) Power Sensor, Peak Detector, and Scanner (Scan Bus). An automatic switchover scheme for the power sensor, peak detector, and scanner is shown in Figure 30. Absence of a scan signal (i.e., failure of the scanner to reverse) causes switchover by allowing the counter to accumulate the count required to set the flip-flop. This changes the state of the relay, which disconnects the faulty circuitry, and enables its redundant spare. Ground command switchover control is also provided.

(c) Power Switch, Drive Circuitry, Pulse Width Modulator, and Voltage Limit Circuit. Automatic switchover to a standby power switch, drive circuit, pulse-width-modulator, and voltage limit circuit shall be provided, as shown in Figure 31. The unregulated bus under voltage detector provides an output if the unregulated bus voltage is below the solar bus voltage by a pre-determined amount and no power switching is occurring. The unregulated bus over-voltage detector provides an output whenever the unregulated bus exceeds -37 volts. These two outputs are "or" gated to set a flip-flop which changes the state of the relay thereby switching in the redundant spares. Ground command control is also provided.

(4) EMI Considerations. Compatibility among the various elements of an electronic system is of prime importance. It is clear that portions of the system which carry heavy AC current (such as power switching networks) will display a much greater tendency to produce EMI than will the low level electronics (such as differential amplifiers). It is advantageous, therefore, to arrange components so

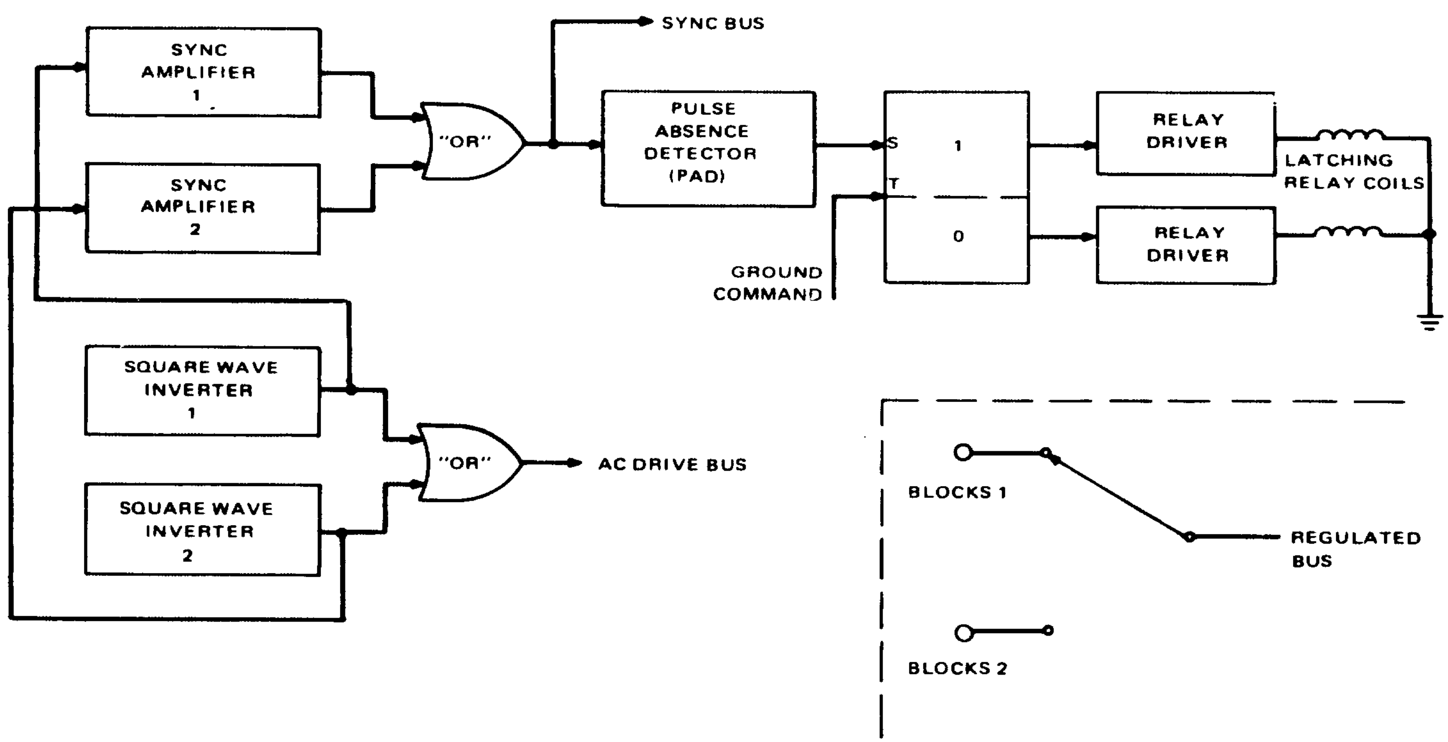

Figure 29. Functional Block Diagram - Square Wave Inverter and Sync Amplifier Switchover Circuit

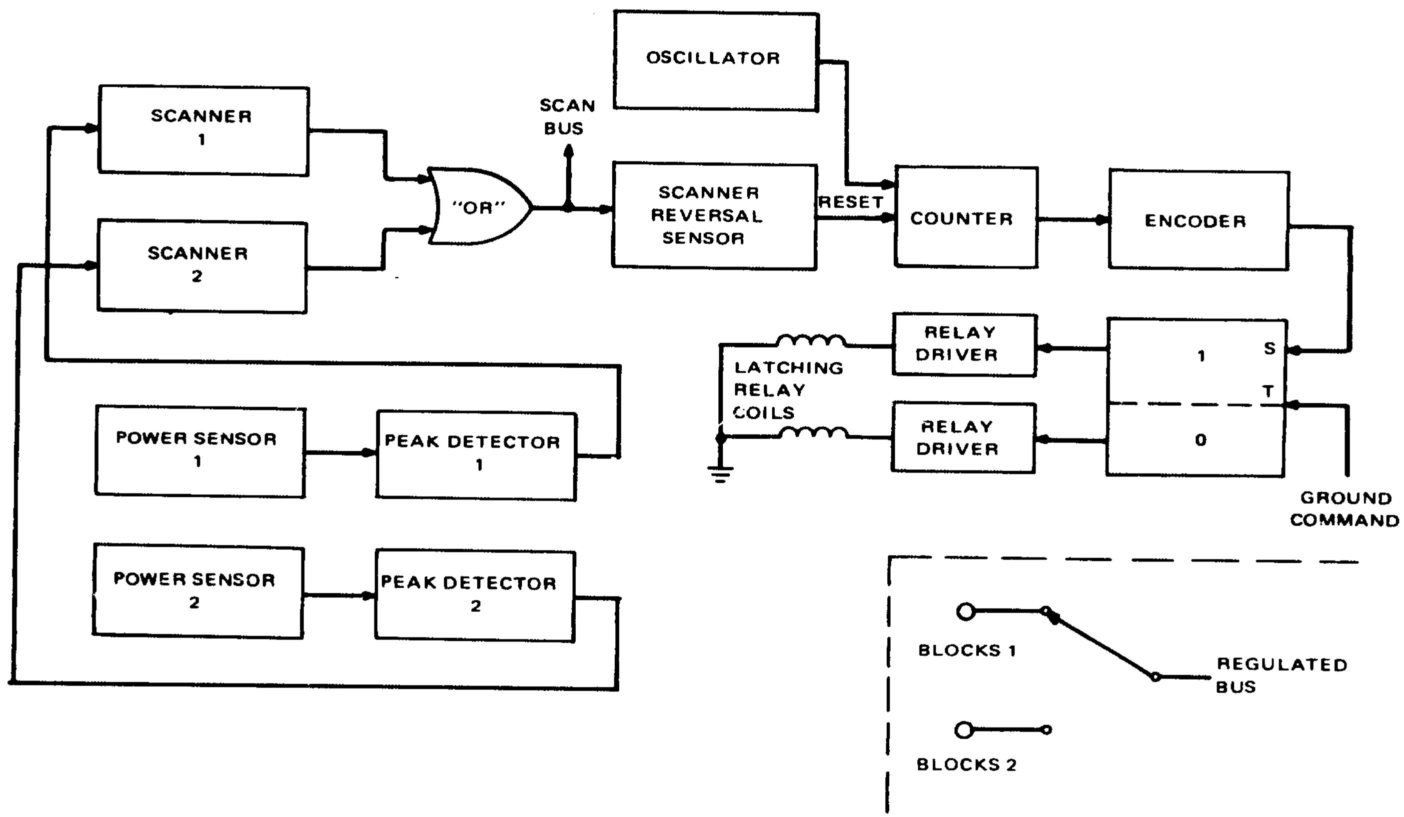

Figure 30. Functional Block Diagram - Scan Bus Switchover Circuit

that the low-level circuits are protected from the fields produced by high-current sections, as well as to contain these fields within the equipment. This might be accomplished by creating separate, sealed EMI compartments to house the most obvious offenders, with EMI filters provided on all leads penetrating the walls of the compartments. To further enhance power system compatibility, synchronization shall be provided between the series tracker unit and the -24.5 volt load bus regulator.

Since both implementation and optimization of techniques to eliminate EMI are of an extremely complex nature, further detailed analysis and testing shall be required.

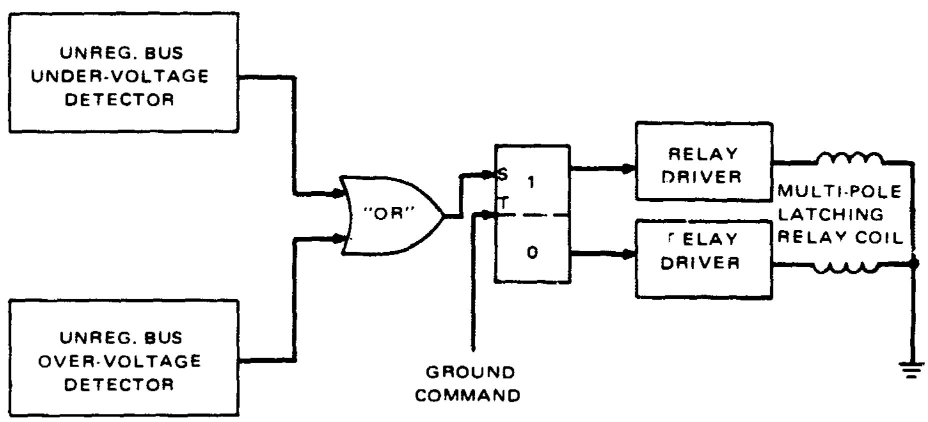

Figure 31. Functional Block Diagram - Switchover Circuitry for Power Switch and Associated Circuitry

(5) Telemetry and Ground Commands. The only additional telemetry required in the series tracker system, other than that which exists in the Nimbus B design is telemetry that defines which of the redundant circuits are operational.

Three additional ground commands shall be required to override automatic switchover to redundant spares in the STU.

(6) Storage Modules and Control Module. There are no major changes required in either the storage modules or the control module (Nimbus B types) when used in the series tracker system, since they are operated off a comparable unregulated bus. The maximum charge current limit in the storage modules would be increased from the present 1.1A to 2.25A to accommodate the higher available charge current in the series tracker system.

(7) Specifications for the STS Series Tracker Unit (with redundancy). A summary of the major electrical parameters specified for the STS Series Tracker Unit is listed below.

1) tracking error ±2%
2) power transfer efficiency 90%
3) -24.5V shunt loss 15 watts (daytime)
6 watts (nighttime)
4) estimated package weight 31 lbs.
5) estimated package size 6" × 8" × 13"
6) maximum input power (tentative) 840 watts
7) output voltage range -27 to -36 volts
8) output voltage limit @37V

4. Solar Array

a. Environmental

The environmental conditions that both the F-3 type and the bifold solar arrays for the NB, PPFT and STS Systems must accommodate are the same as for the flight Nimbus B. Figure 32 presents the solar array temperature versus time profile during an orbit, as measured by Nimbus II telemetry data near beginning-of-life with a nominal value of solar intensity. The high temperature of about + 50°C and the equilibrium temperature of about +40°C are the same as predicted for the Nimbus array. A cold temperature extreme of -74°C was predicted, as compared with -60°C reported by telemetry. The accuracy of the temperature telemetry at the cold extreme, on Nimbus II, is uncertain. However, since the advantage of a maximum-power tracker system is emphasized with a colder array, the more conservative, warmer temperature profile was selected to provide a more objective comparative evaluation of the various system configurations. It is estimated that the bifold array section will have essentially the same thermal properties as the F-3 array, and therefore the profile in Figure 32 will apply to both sections of the array. This profile was subsequently used in the energy balance computer program for system load capability analysis.

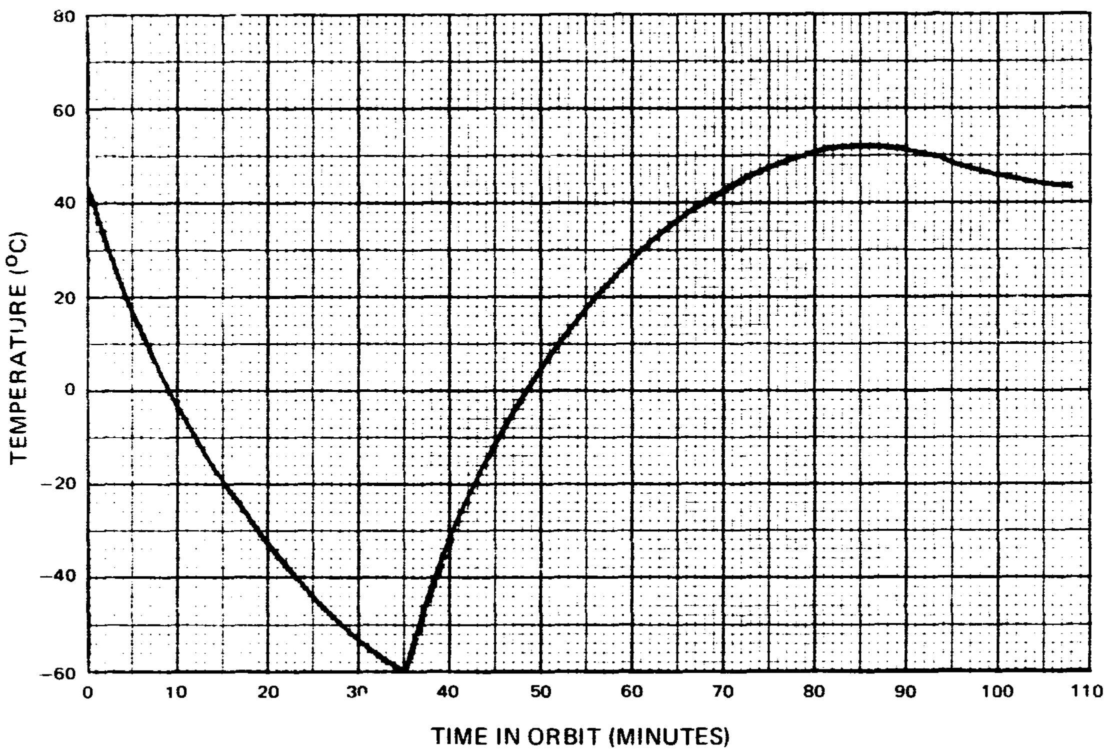

Figure 32. Nimbus Solar Array Temperature Versus Time Profile

A ground rule of this study was that the orbital charged particle environment predicted for Nimbus B shall be considered as the basis for solar cell irradiation degradation. Without the damaging fluxes introduced by the RTG, the natural environment produced an estimated damage-equivalent, normally incident 1-MeV electron flux of 3.16×10^{14} e/cm^2/yr and 6.32×10^{14} e/cm^2 for the two-year mission.

b. Solar Cell Selection

The solar cell selected for use in this study is the nominal 1 ohm-cm, 2 × 2 cm, 14 mil thick Centralab silicon N on P cell with solderless silver-titanium contacts in the conventional configuration, having an air mass zero efficiency of 11.4%, measured at 0.46 volt on the cell I-V curve at a temperature of 28°C, before glassing. This, of course, is the cell selected by RCA for the Nimbus D solar array redesign on the basis of extensive tradeoffs considering temperature, irradiation, module assembly techniques, array storage and procurement costs. The coverglass is 6 mils of microsheet (Corning 0211) with an anti-reflective coating on the sun side and a blue-reflective optical filter on the solar cell side. Approximately 1 mil of Sylgard 182 silicone adhesive is used to bond the coverglass to the cell. It is recommended that costs of larger area cells be reviewed before final commitment to a flight hardware design, as these may show a more significant cost savings at that time.

Figure 33 shows the above-described solar cell I-V curve at beginning of life and at 3, 6, 12 and 24 months in orbit, demonstrating the effect of charged particle degradation on cell output.

c. Series-Parallel Arrangement

The energy balance computer program was run for the three system configurations having end-of-life worst-case degradation. The number of series-connected solar cells was changed after each run, in order to determine the number of cells required to produce the greatest load power capability. The resulting series-solar cell requirement is 94 for the NB system and 102 for both the PPFT and STS tracker systems. These numbers apply to both the F-3 and bifold sections, since both will have approximately the same temperature-versus-time profile.

An outline drawing was prepared for both the F-3 and bifold array substrates, and a solar cell layout was designed which provides the greatest number of parallel cell strings, minimizes magnetic dipole net effects and provides an economical manufacturing task, utilizing the expanded silver mesh cell interconnections widely adopted in solar array designs at the present time. Figure 34 presents the solar cell layout for the F-3 and bifold sections for the NB systems (94 series cells); Figure 35 presents the 102 series-cell layouts for the STS and PPFT systems. These layouts have been prepared as RCA Drawings SK1976440 (102 series cells) and SK1976443 (94 series cells).

d. Mechanical Considerations

The solar cell layouts on SK1976440 (Figure 35) and SK1976443 (Figure 34) were made using the bifold dimensions and configuration shown on Fairchild Stratos drawing D512-00-00011. It should be noted that the bifold section is not notched to mate the clearance notch on the F-3 platform. If the notch is required, the number of parallel strings of solar cells on the bifold will be reduced from 42 to 41 on SK1976440 and from 46 to 45 on SK1976443.

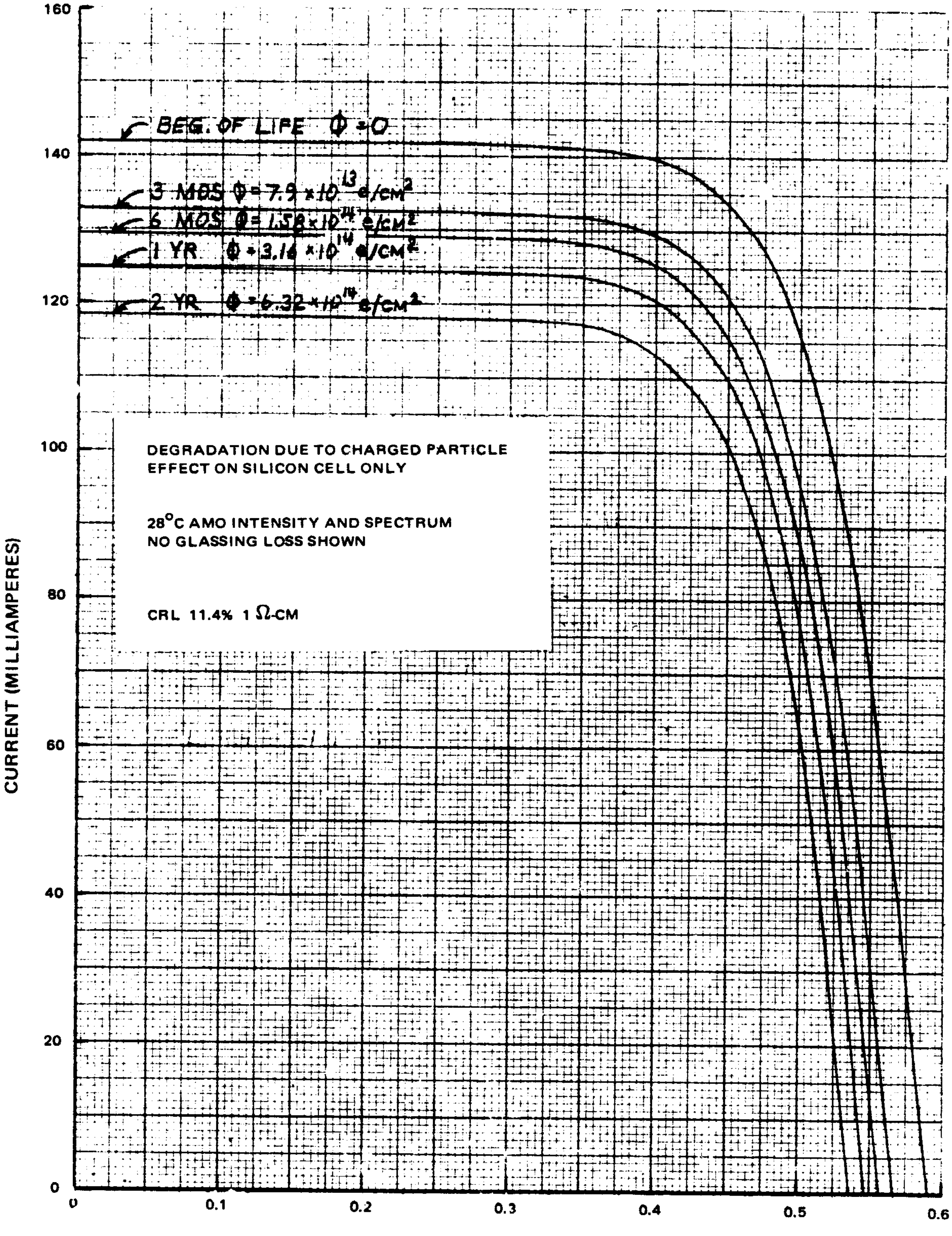

Figure 33. Solar Cell I-V Curves at Various Times in Orbit

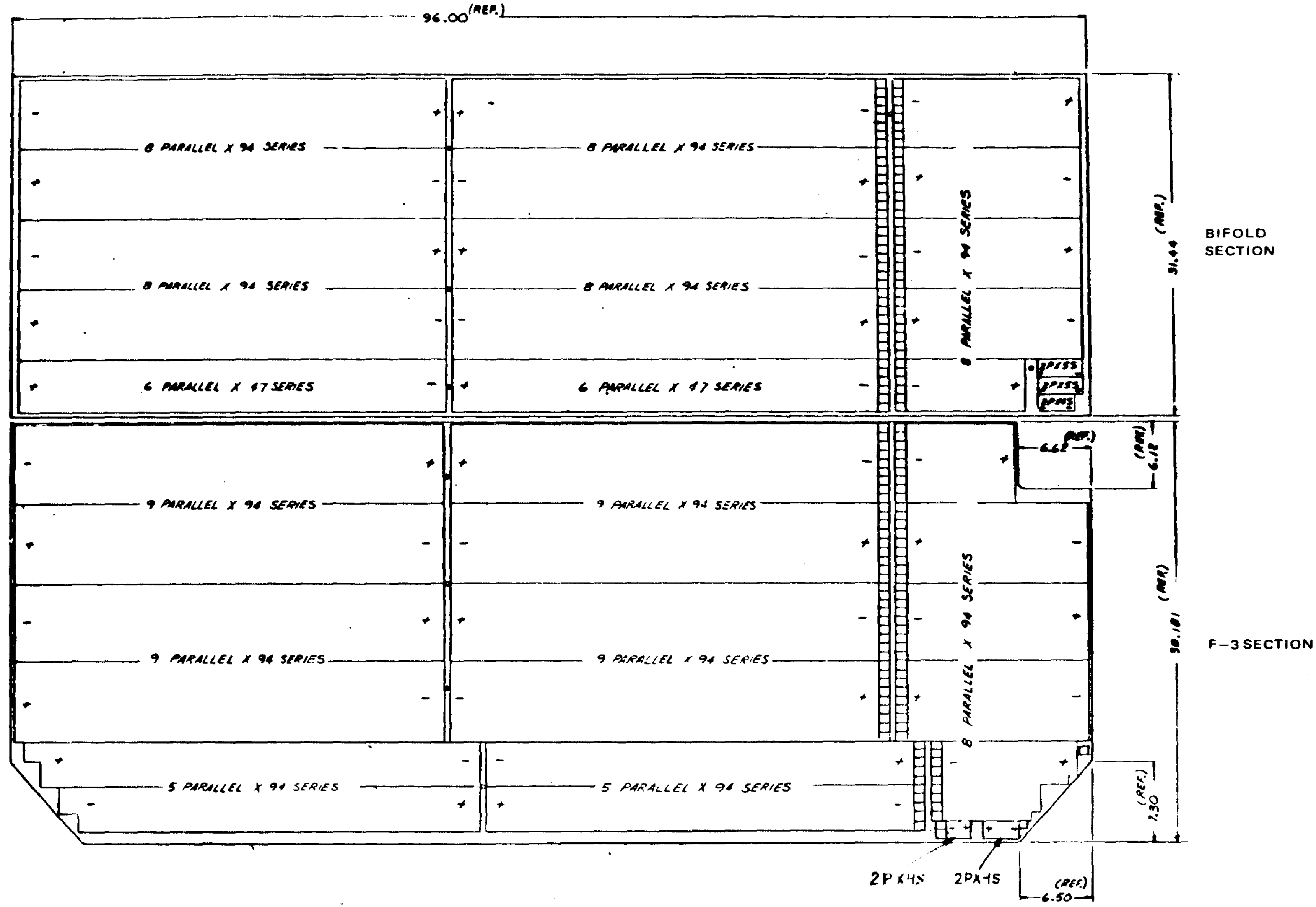

Figure 34. Solar Cell Layout for NB Systems (94 Series Cells)

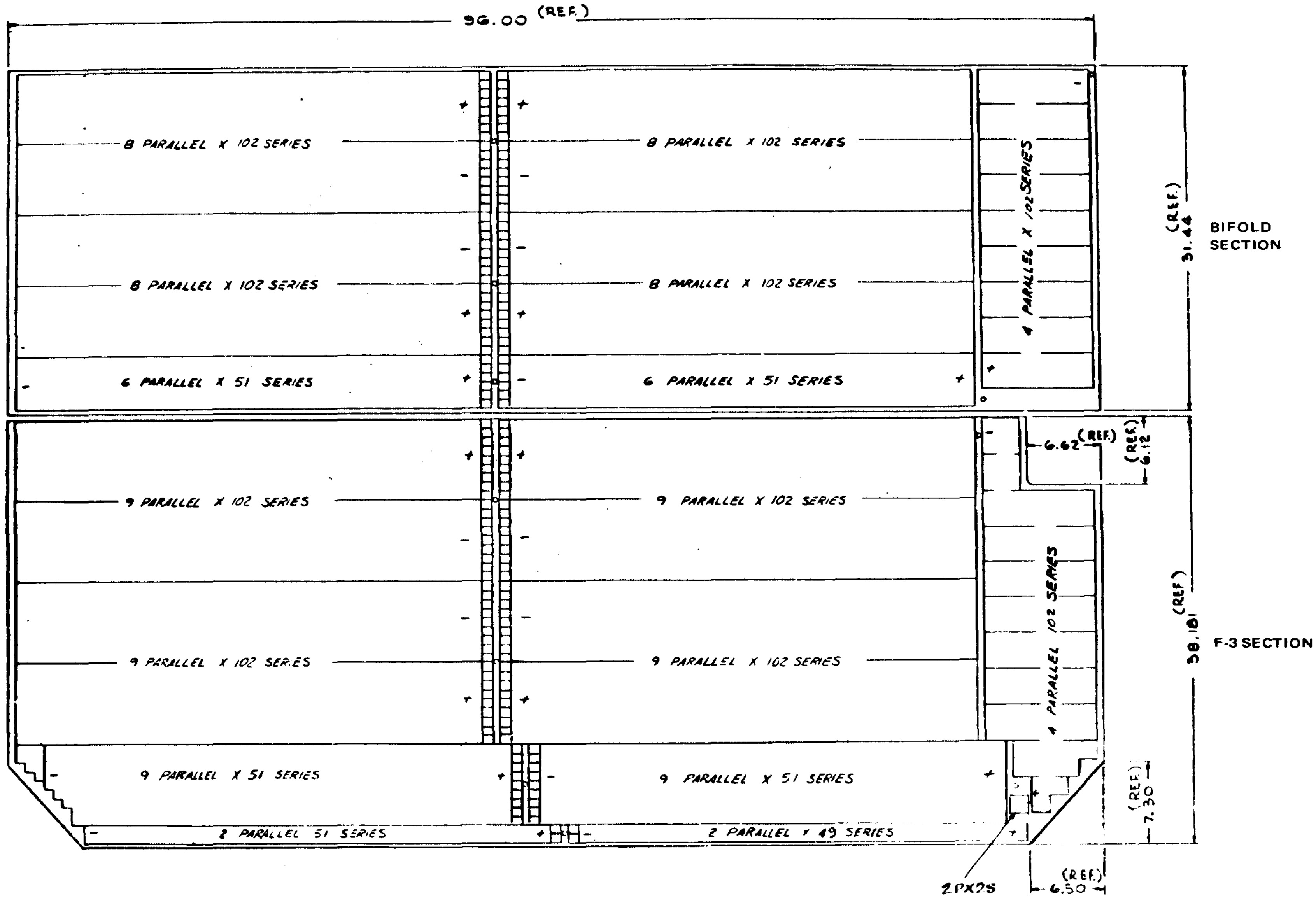

Figure 35. Solar Cell Layout For MPT Systems (102 Series Cells)

Notches along the panel hinge line were not delineated on the Fairchild drawing. The array layouts on the referenced sketches require that notches shall not protrude more than 0.20 inch into the indicated array bonding area.

Cell dimensions used in making the referenced layouts were 0.788 inch by 0.788 inch nominal. Nominal spacing between cells in parallel was 0.016 inch and nominal spacing between cells in series was 0.032 inch. These are the normal spacings used by RCA for solar array layouts. An additional allowance was made in the series direction to compensate for expandion of the solar cell modules prior to bonding due to the length of the module involved.

e. Slip Rings

All solar array power and telemetry circuit connections are made through a slip-ring assembly which is located around the solar platform driveshaft in the NIMCO controls housing. Performance of the power and signal slip rings on the Nimbus II satellite have demonstrated excellent performance after more than two years in orbit, therefore the basic design of this assembly appears to be quite adequate. Table IV below lists the existing F-3 type slip ring complement and recommended slip ring provisions and current ratings for the F-3 and bifold systems considered in this study.

Note that the recommended power slip rings allow one redundant ring for the positive and negative solar array bus as a reliability enhancement. It is uncertain what the bifold section unfold mechanism will require in regards to electrical power; it may be necessary to provide for more than the two sets of unfold motors normally used with the F-3 type arrays.

TABLE IV. RECOMMENDED SLIP-RING PROVISIONS

Slip Ring Function	Flight NB, B-2	Recommended F-3	Recommended Bifold
SA Power (+)	2 (10A)	2(15A) or 3(10A)	4(15A) or 6(10A)
SA Power (-)	2 (10A)	2(15A) or 3(10A)	4(15A) or 6(10A)
TLM Return	1 (1A)	2 (1A)	2 (1A)
-24.5V (TLM only)	1 (1A)	2 (1A)	2 (1A)
TLM Signal	2 Temp 4 Volt (1A)	2 Temp 4 Volt (1A)	4 Temp 4 Volt (1A)
S/C Ground	1 (1A)	1 (1A)	2 (1A)
-24.5V (Motors)	3 (1A)	3 (1A)	At least 3 (1A)

5. Batteries

During this study it was necessary to select a new battery design for the parallel tracker system and to characterize both the new battery and the Nimbus B storage cells in order to provide a battery model for use in the energy balance computer program.

a. Nimbus B System

Figures II-1 through II-9 in Appendix II present a set of curves showing charge and discharge voltage at several charge and discharge rates as a function of cell recharge and cell discharge for the Nimbus 4.5 A-H cylindrical nickel-cadmium storage cell. The curves are for three different temperatures, 15, 25 and 35°C, which is the expected temperature range of the batteries in the Nimbus spacecraft, and for three times in life: beginning of life, one year and two years in orbit. Repetitive cycling of the cells to approximately 20 percent depth-of-discharge is assumed in the preparation of these curves. Data observed from testing this type of cell at Crane, Indiana and at RCA as well as data from other NiCd cell testing has formed the basis for these estimated performance curves.

The "UVL" and "LVL" lines on the figures are the recommended upper and lower voltage limits for use in limiting battery voltage during recharge (tapered charging).

b. Series Tracker System

Since the STS system will utilize the NB Storage Module, the cell data described above also applies to the series tracker application. Note that a recharge rate of 2.25 amperes for the 4.5 A-H cell is shown in Figures II-1 and II-2. This is the C/2 rate which is allowed in the STS system to utilize the available energy from the solar array during the initial minutes of spacecraft sunlight illumination.

c. Parallel Tracker System

Table I presented the baseline storage capacity for each power system configuration that would produce a 20 percent depth of discharge. The PPFT system has the greatest capacity requirement since it is capable of supplying the greatest load energy through effective utilization and transfer of solar array energy. Since the PPFT requires an entirely new complement of battery electronics (the charger/tracker functions) which will require separate packaging because of the probable EMI generation due to the switching circuitry and the unavoidable heat generated as a result of conditioning solar array energy for the batteries, it was considered desirable to design a more efficient storage cell packaging arrangement.

The 12 ampere-hour prismatic cell was selected for several reasons:

1) Three 12 A-H batteries can supply the nominal beginning-of-life load at about a 17% depth of discharge, which is quite conservative for even a two-year mission, with active battery temperature control and adequate overcharge control. Although battery failure is considered highly improbable in the Nimbus mission, two batteries could support the same load with about a 25% depth of discharge at beginning of life, which would be reduced to about 20% after six months because of expected solar array degradation. These values of depth of discharge are based on spacecraft loading to the greatest amount which will permit power system energy balance; actual spacecraft loading will be somewhat less.

2) A large amount of electronics functions can be eliminated with a minimum number of parallel batteries. This is considered a significantly advantageous tradeoff in view of the high reliability that properly-controlled batteries have exhibited in over two years of Nimbus II operation.

3) A considerable cost savings will probably be realized with a three-battery system over an eight-battery system since the cost of cells is relatively independent of capacity and fabrication and testing costs will be proportionally reduced.

4) Use of a cell larger than 12 A-H would result in a significantly increased weight for a three battery system, with more capacity than is considered necessary for the mission. Larger cells in a two-battery system configuration would yield less flexibility in proportioning the heavy battery weight around the sensory ring, in addition to a somewhat reduced redundancy provision.

An additional series-connected storage cell in each battery, for a total of 24 cells per battery, is specified for the PPFT system. The higher load capability of this tracker system will exercise the batteries at a slightly greater depth of discharge than the NB and STS systems, such that an extra cell will ensure adequate unregulated bus voltage during nighttime discharge periods at end of life with a high temperature (+35°C) battery. Provision for the twenty-fourth cell is easily made, since the 12 A-H battery will be packaged in two 12-cell storage modules, each occupying half of a spacecraft bay (0/4 module size).

The charge and discharge voltage data in Figures II-1 through II-9 provide a very good approximation for the 12 A-H cell, the second (higher) set of charge and discharge rates indicated on the figures apply to the higher capacity cell.

d. Battery Charge Control

The battery charge control for the Nimbus B power system has been thoroughly discussed, notably in the "Instruction Manual for the Nimbus B Solar-Conversion Power-Supply Subsystem", RCA report No. AED M-2105, prepared for NASA-GSFC under Contract No. NAS5-9668, and issued June 30, 1967. The tapered charge provided by the limit voltage versus temperature curve shown in Figure 19, a maximum charge current limit of 1.1 ampere for each 4.5 A-H battery, and an automatic reduction of charge current to a trickle-charge value of 150 mA per battery, actuated on an individual battery basis by sensing a temperature above 51°C constitute the battery protection features of the NB system.

Battery protection in the STS system is identical to that for Nimbus B, with a maximum charge current limit increased from 1.1A to 2.25A in the series system to allow charging with the increased available array power.

As described earlier in the PPFT system description, the parallel tracker battery protection technique employs the NB voltage-limiting function and high-temperature cutoff. Maximum charge current is limited to a C/2 rate (6.0 A per battery) in the parallel tracker; computer simulation of power simulation shows that this rate cannot be obtained when operating at the maximum energy-balance regulated bus load value. In addition, the state-of-charge monitor (ampere-hour counter) circuitry associated with each battery will reduce the charge current to a trickle value when the designed value of temperature-sensitive C/D ratio has been achieved. A plot of the recommended C/D ratio as a function of temperature has been shown in Figure 20. The ampere-hour counter circuitry must be designed such that circuit function due to worst-case deviation will still permit the desired minimum recharge.

Note that the four protection functions will operate independently on each of the three batteries. The four protection functions (high current limit, high voltage limit, high temperature cutoff and ampere-hour counter current reduction) shall be sensing simultaneously and any one shall be allowed to control the charge, depending on which is automatically actuated first. Additionally, each battery shall have its own connect-disconnect ground command, as well as its independent command to enable or disable either or both the voltage-limiting and ampere-hour counting circuits.

c. Consideration of Other Storage Cell Types

An investigative effort was made to consider the use of third electrode storage cells and suitable charge control techniques for their application. After a review of literature on "third electrode" and "fourth electrode" cell studies, it has been concluded that the disadvantages inherent in the applications of the currently available control electrodes outweigh the advantages. That is, the use of auxiliary electrodes is not recommended for use in the Nimbus application at the present time due, primarily, to the following factors:

1. When a "third electrode" signal electrode is used, the residual oxygen from the previous charge can give a premature signal during repetitive cycling. This effect has a greater possibility of occurrence in a short orbit period, like the 108-minute Nimbus orbit, as compared to a longer duration orbit where more time exists for recombination of the oxygen. It may be possible, depending on the design of the charge control system, to overcome the premature signal problem.

2. When an "oxygen scavenger" electrode is used to overcome the above problem, the cell charges efficiently only at higher charge rates and becomes quite inefficient at lower charge rates, such as C/10. Data has been reported* which shows that cells equipped with this electrode exhibit only 73 percent of their rated capacity after charging from a shorted condition for 16 to 20 hours at a C/10 rate. A general RCA practice during conditioning of conventional cells is to charge from a shorted condition for 16 to 20 hours at a C/10 rate; the resulting capacity is, almost without exception, equal to or greater than rated capacity.

It is concluded that the use of the "third electrode" signal electrode and the "oxygen scavenger" electrode, in the light of the above mentioned problems, requires a more detailed study than the scope of this contract allows. Therefore, the auxiliary electrodes cannot, at the present time, be recommended for use in the design of a Nimbus power system.

A second consideration involved the use of silver zinc cells. With the present state-of-the-art silver zinc cells could not be considered to have any degree of reliability for a requirement of 10,000 cycles or even 5,000 cycles. Some experimental test results have reported as high as several thousand cycles but a review of the recent literature indicates that silver zinc cells, neither sealed nor unsealed, are available that can be repetitively cycled to an appreciable depth of

* Final Report for Characterization of Recombination and Control Electrodes for Spacecraft Nickel-Cadmium Cells, prepared by Gulton Industries, Inc., for NASA-GSFC under Contract No. NAS5-10241.

discharge for thousands of cycles. It has also been reported that in addition to the basic limitations of the life characteristics of both the silver and zinc electrodes the silver zinc cells are subject to radiation damage when in orbit. (Silver zinc batteries on Explorer XXXII are reported to have been caused to short by the electron irradiation which they received in orbit.)

6. Packaging Considerations

Hardware designs qualified for the Nimbus B program will, of course, be used for both the control and storage modules for the NB systems. New designs for the 12 A-H storage cell packaging and for the battery and tracker control electronics packaging in the parallel tracker (PPFT) system are required. The following paragraphs present the packaging concepts that appear to be most advantageous when considering the new parallel tracker system.

a. 12 A-H Storage Module Packaging Concept

Each of the six storage modules comprising the three batteries in the PPFT system will be packaged in a standard size Nimbus zero over four (6 × 8 × 6.5 inch) spacecraft module. The twelve 12 ampere-hour prismatic cells that are contained within this volume are assembled using a technique that has had much success on the Lunar Orbiter, TIROS and other classified spacecraft which utilized the prismatic cell configuration: the "tension-member" battery. A sketch of the Nimbus version of this design is shown in Figure 36.

Battery cells are relatively heavy spacecraft components, and as a consequence, one of the prime objectives of this packaging design is to group and hold the individual cells together while adding a minimum of weight. The "tension-member" packaging concept enables us to meet this objective in that the lateral clamping forces generated as the cells act on each other are sufficient to cause large frictional forces in the vertical plane which prevent cell movement. In this design, it may be said that the cells retain themselves and take an active part in the structural design of the unit. The estimated weight for each of the six modules is 18.0 lbs. out of which 14.9 lbs. are for cells, electronics parts, connectors and wire.

End and side plates of the module will be fabricated from aluminum alloy extrusions. The mounting base and the top cover will be formed from aluminum alloy sheet. Cells, separators and end plates will be assembled utilizing stainless steel flat head screws and dowel locating pins to assure that critical module dimensions are maintained.

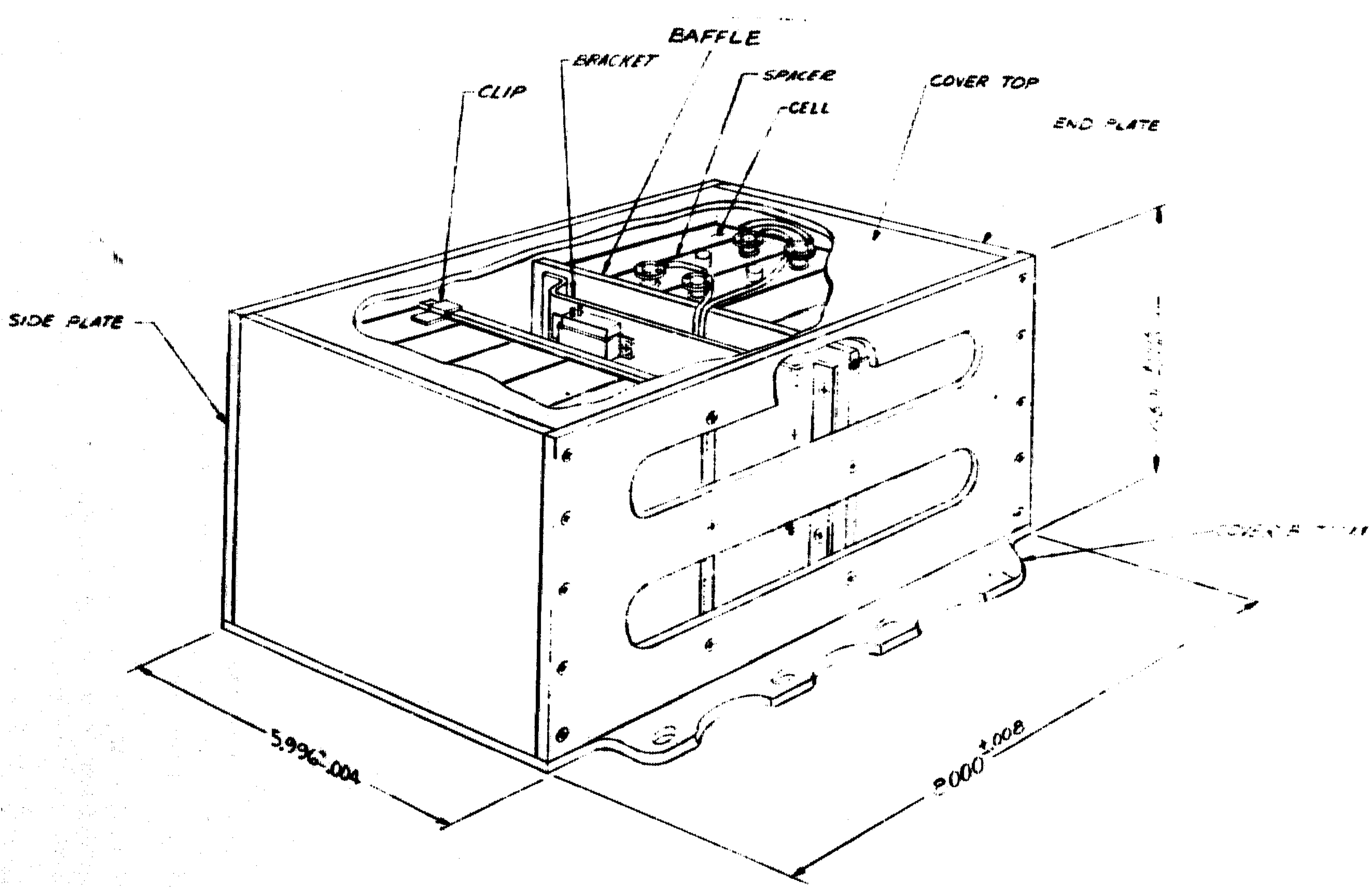

Figure 36. Packaging Concept for PMPT 12 Amp-Hr Storage Module

Provisions for mounting the battery disconnect relay and the battery fuse blow tap diodes will be made in each storage module. Since two modules form a spacecraft battery, these parts will only be assembled in three out of the six proposed storage modules.

b. Tracker and Battery Control Electronics Packaging Concept

The MPT power system control electronics has been packaged into two standard Nimbus zero-over-four (6 × 8 × 6.5 inch) modules. The tracker control circuitry has been separated into those functions which are at a low power level and those functions which have relatively high thermal dissipations and are a source of electromagnetic interference. This separation and the packaging of the circuitry into two modules has been done for the following reasons:

1) To provide a positive isolation of that circuitry which contains electromagnetic interference generators.

2) To provide units that have a consistent, single purpose internal design compatible with the unit function. Normal packaging objectives for low power circuitry are high density and low weight. Packaging objectives for high power level circuitry are usually isolation and good thermal paths.

3) To permit the use of a deep-drawn aluminum alloy container which is presently being developed as a standard RCA/AED spacecraft module to realize design and manufacturing cost savings.

4) To provide greater flexibility in locating the modules in the spacecraft sensory ring without paying any volume or weight penalty.

Tracker Control Module I, containing the low level circuitry, is shown in Figure 37. It is estimated that twelve 5 × 5 inch printed circuit boards will be used to package this electronics group which consists of approximately thirteen hundred parts. The board assemblies are interconnected by insertion into a hard-wired connector plate which is so designed that wiring changes are relatively simple to accomplish in the development stage while rapid, automatic wiring connection using tape controlled equipment is possible in production.

Module unit connectors (two Cannon series D-M are proposed per unit) are wired and mechanically assembled to the connector plate. A board separator assembly will be used to assure boards remain at their intended spacing before and after assembly into the unit container.

As seen in Figure 37, board integration and unit assembly uses a packaging design somewhat different from the rigid-mounted Nimbus A, or "Birtcher" spring-clip-mounted Nimbus B component boards. Mounting is accomplished using foam spring

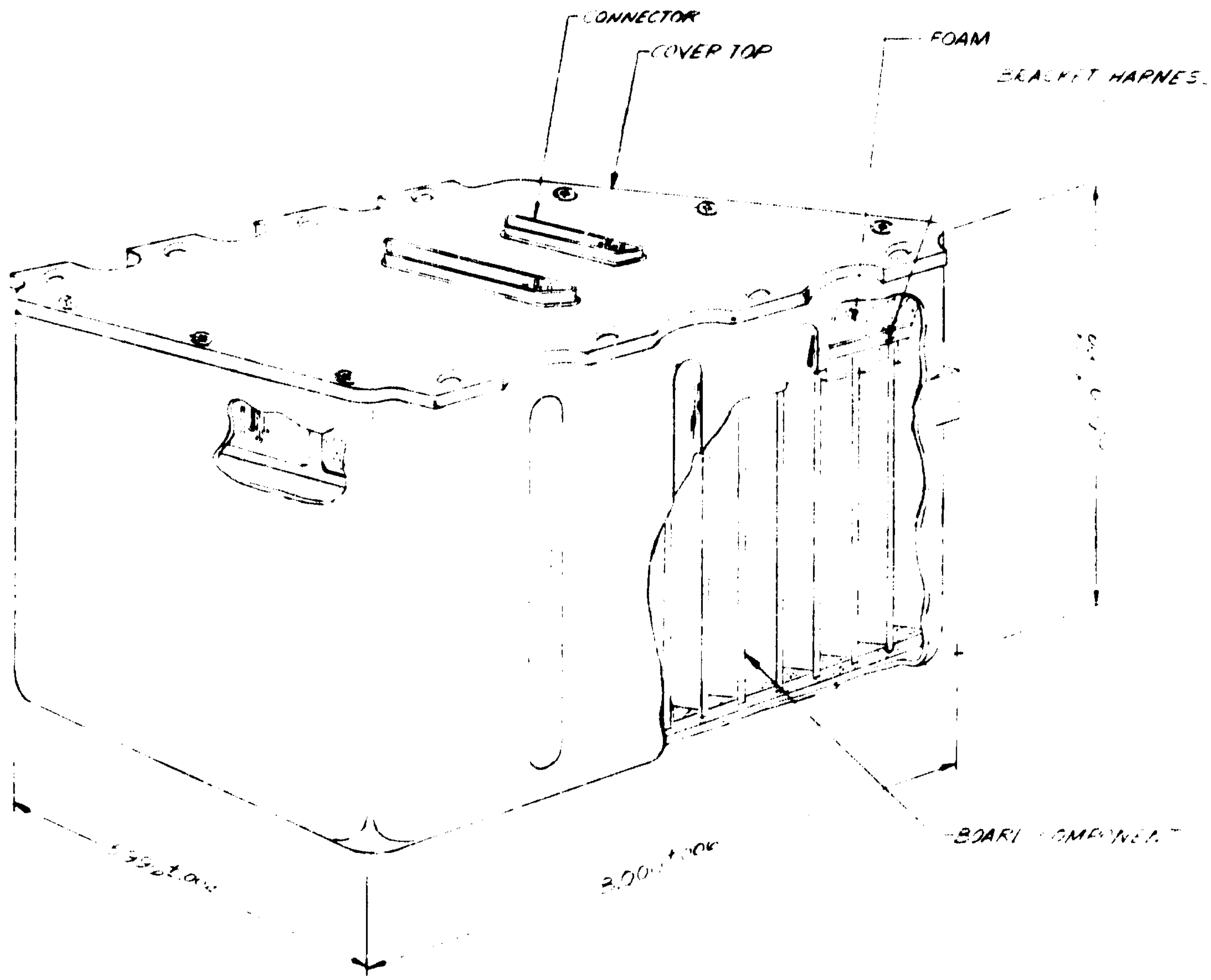

Figure 37. Packaging Concept for PMPT Tracker Control Module I (Low-Power Circuitry)

isolation or suspension. This technique has been selected because it offers many advantages, the major of which are 1) the elimination of tight internal board assembly control and therefore reduction of the unit fabrication and assembly costs, and 2) positive, design controlled vibration isolation of the central mass (the boards and connector plate assembly) from any external forces on the container. Essentially, the printed circuit boards, connector plate and unit connectors are all vibration isolated from the enclosure. By maintaining a margin between the natural frequencies of the central mass and the enclosure and including damping, the transmissibility (ratio of response to input forces) may be controlled and the electronics circuitry protected to any desired degree. Although thermal dissipations are expected to be small (about 5 watts orbit average) in this group of electronics, a good conductive path from any specific component or group of components can be provided via added copper foil on the printed circuit board, to the foam (loaded to improve conductivity if necessary) and then to the container. The unit board arrangement will be such that those boards with highest average dissipations will be positioned nearest the container thermal interface wall, thereby assuring best utilization of radiative paths.

Other advantages, although more subtle, include a shortening of packaging schedules since enclosure design and development may proceed as soon as the number and weight of the component boards has been established. Another advantage is the elimination of major board or unit rework due to cross-talk or capacitive coupling problems since boards may be assembled and interconnected in their final assembly configuration while still in the breadboard stage.

As mentioned previously, the Tracker Control Module I enclosure will be fabricated as a precision, deep-drawn aluminum alloy container to meet the Nimbus Spacecraft module requirements. Sheet aluminum alloy covers and mounting flanges will complete the assembly. The estimated unit weight is 14.2 lbs. out of which 11.8 lbs. are electronic components and circuit board materials.

Tracker Control Module II is shown in Figure 38 and contains an estimated 70 stud or screw mounted electronic components. The internal configuration and subassembly technique in this unit is similar to Tracker Control Module 1 except that the central mass is visualized as a space frame upon which the components can be mounted and which provides a good thermal conductive path to the enclosure. By proper selection of an electromagnetic interference (EMI) suppression gasket material, the lower portion of the assembly, between the feed-thru filters and the bottom cover, will form an EMI free compartment and all conductors entering or leaving the unit will be filtered. Major heat dissipating components such as switching transistors will be mounted on the spaceframe near its outboard surface to provide the shortest conductive path to the prime thermal interface.

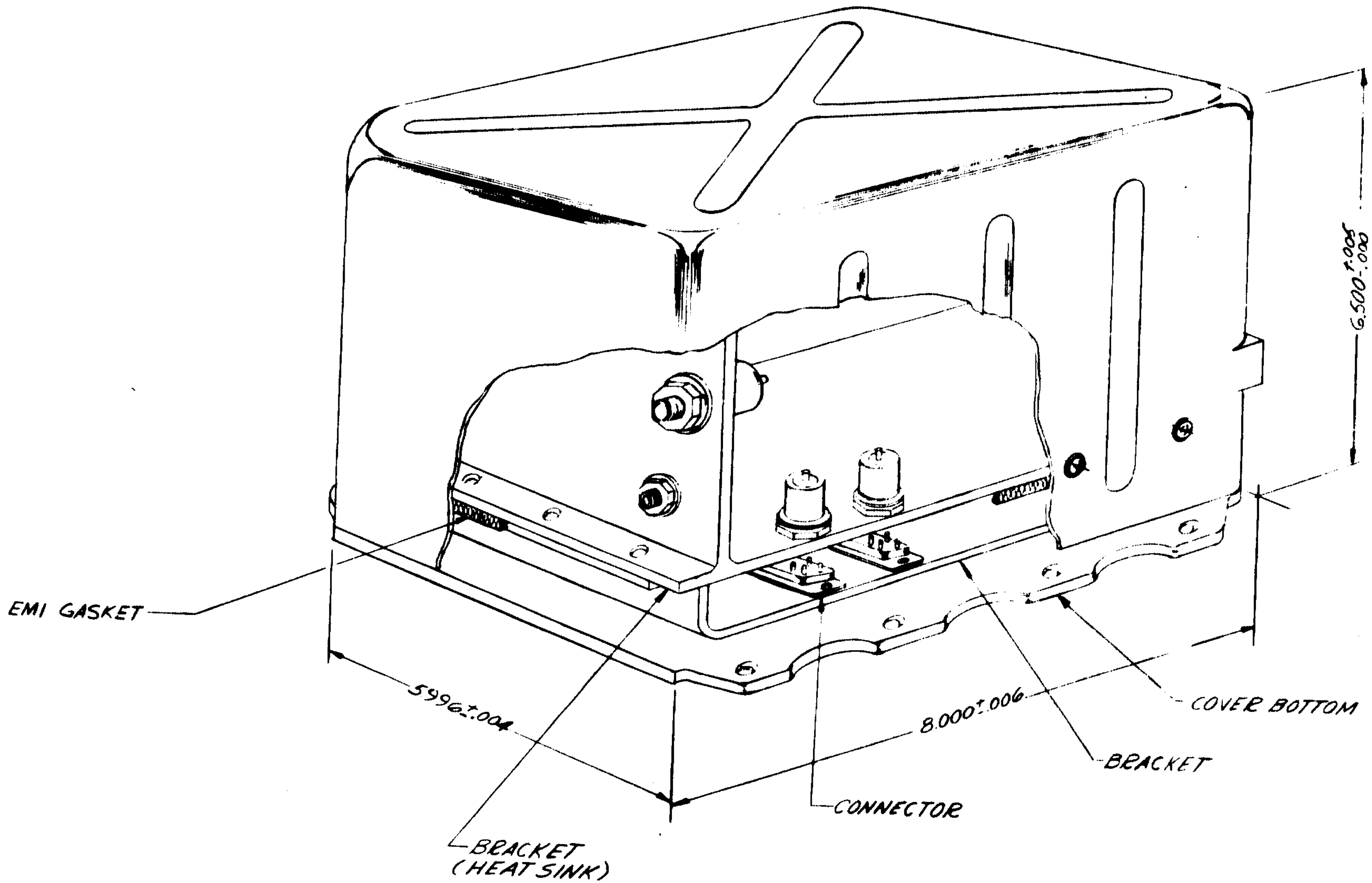

Figure 38. Packaging Concept for PMPT Tracker Control Module II (High Power and Switching)

The module housing will again consist of the deep-drawn aluminum alloy container, modified to mount the spaceframe, together with an aluminum alloy sheet mounting cover and flanges. The estimated unit weight of Tracker Control Module II is 9.3 lbs., of which 6.5 lbs. are electronic components.

c. Series Tracker Component Packaging

The STS system would utilize the existing Nimbus B Storage and Control Module packaging design, and would require a new packaging design only for the series tracking unit. The systems performance analysis, described in the following section of this report, has shown that the orbit average power dissipation in the series tracker unit is in excess of 50 watts, which exceeds by a considerable margin the desirable maximum 20 watts dissipation per spacecraft bay. This severe limitation, plus the fact that no load power advantage of the STS system over the NB system exists for the two year mission, has brought about the realization that the STS system is not particularly advantageous in a typical Nimbus mission. As a result, the conceptual packaging effort for the series tracker unit was curtailed.

7. Component and System Weight and Volume

A summary of the weight and module size of the components comprising the NB, PPFT and STS systems is presented in Table V. Components for the NB system reflect actual measured values; weights of the new components resulting from this study are the best, realistic estimates available at this time.

Using the component weights and sizes shown in Table V, the total system weight and sensory ring bay requirement can be estimated:

System	F-3 Array		Bifold Array	
NB	SA	74.0	SA	110.0
	8 S/M @ 15.2	121.6	12 S/M @ 15.2	182.4
	1 C/M @ 21.5	21.5	2 C/M @ 21.5	43.0
		217.1 lbs. (5 bays)		335.4 lbs. (8 bays)

System	F-3 Array		Bifold Array	
PPFT	SA	74.0	SA	110.0
	6 S/M @ 18.0	108.0	10 S/M @ 18.0	180.0
	1 C/M @ 21.5	21.5	2 C/M @ 21.5	43.0
	1 TCM I @ 14.2	14.2	1 TCM I @ 14.2	14.2
	1 TCM II @ 9.3	9.3	* 1 TCM II @ 14.0	14.0
		227.0 lbs. (5 bays)		361.2 lbs. (8 bays)
STS	SA	74.0	SA	110.0
	8 S/M @ 15.2	121.6	12 S/M @ 15.2	182.4
	1 C/M @ 21.5	21.5	2 C/M @ 21.5	43.0
	1 STU @ 31.0	31.0	2 STU @ 31.0	62.0
		248.1 lbs. (6 bays)		397.4 lbs. (10 bays)

* With the PPFT Bifold System, it is estimated that the additional circuitry required for the 2 batteries might be located in the high power Tracker Control Module. If this is not feasible, a full bay would be required for the low power TCM, making a system total of $8\frac{1}{2}$ bays instead of 8.

8. Telemetry and Ground Command Requirements

The following table lists the recommended telemetry and ground command requirements for both the F-3 and Bifold versions of the three selected power system configurations. The list contains all the telemetry points needed to perform a complete performance evaluation in orbit, as well as status reporting, verification of execution of ground commands and an analysis of all but the most serious type of failure modes.

Note that the ground commands are a manual back-up provision for normally automatic functions in all cases except the battery connect or disconnect function, which has no automatic provision.

It is strongly recommended that the specified ground commands be provided under all circumstances; the essential number of telemetry points could, for each system, be somewhat reduced if a severe limitation on available T/M channels exists.

Ground Commands	NB		PPFT		STS	
	F-3	Bifold	F-3	Bifold	F-3	Bifold
Batt Connect	1	2	3	5	1	2
Batt Disconnect	8	12	3	5	8	12
Volt.-Temp Ckt ON/OFF	1	2	3	5	1	2
PWM Reg Switchover	1	2	1	2	1	2
A-H Counter ON/OFF	-	-	3	5	-	2
Scan Bus Switchover	-	-	1	1	1	1
Sync Bus Switchover	-	-	1	1	1	1
MPT Pass Element	-	-	-	-	1	2
Total Gnd Cmnds:	11	18	15	24	14	22

Telemetry Points	NB F-3	NB Bifold	PPFT F-3	PPFT Bifold	STS F-3	STS Bifold
V Solar Array	4	4	4	4	4	4
I Solar Array	1	2	1	2	1	2
T Solar Array	2	4	2	4	2	4
V battery	8	12	3	5	8	12
I battery chg	8	12	3	5	8	12
I battery dischg	8	12	3	5	8	12
T battery	8	12	3	5	8	12
V unreg	1	1	1	1	1	1
V aux reg	2	2	2	2	2	2
V reg bus	1	2	1	2	1	2
I reg bus	1	2	1	2	1	2
PWM Reg ON/OFF	2	4	2	4	2	4
Volt.-Temp Ckt ON/OFF	1	2	3	5	1	2
A-H Counter ON/OFF	-	-	3	5	-	-
Batt State of Chg	-	-	3	5	-	-
Scan Bus 1, 2	-	-	1	1	1	1
Sync Bus 1, 2	-	-	1	1	1	1
MPT Power Switch 1, 2	-	-	-	-	1	2
V pkld bus	-	1	1	-	-	-
V trckr output	-	-	-	-	1	1
Total TLM Points:	47	71	38	59	51	76

TABLE V. WEIGHTS & SIZES OF COMPONENTS USED IN NB, PPFT, AND STS SYSTEMS

Components	Weight	Size
Solar Array (F-3 type, including transition piece but no GE latch-line hardware)	37.0 lbs. each platform with transition	38.2 × 96.0 inches (approx., no transition piece)
Bifold Solar Array Section (including small allowance for deploy mechanism)	18.0 lbs. per section	31.4 × 96.0 inches (approx)
NB Storage Module	15.2 lbs. each	0/4 (one-half S/C bay)
12 A-H Storage Module	18.0 lbs. each	0/4 (one-half S/C bay)
NB Control Module	21.5 lbs. each	4/4 (full S/C bay)
PPFT Tracker Control Module I	14.2 lbs. each	0/4 (one-half S/C bay)
PPFT Tracker Control Module II	9.3 lbs. each	0/4 (one-half S/C bay)
Series Tracker Unit	31.0 lbs. each	4/4 (full S/C bay)

PRECEDING PAGE BLANK NOT FILMED.

SECTION III

SYSTEM PERFORMANCE ANALYSIS

Following the component characterization for the three selected systems and the development of the energy balance computer program, a system performance analysis was conducted to evaluate orbital effects on the F-3 and Bifold solar array output characteristics and on the system maximum load capability. Various load profiles were programmed for each system to note the effect on average power with different peak load magnitudes and duration. Power dissipation in each major component of the three systens was determined from the computer printouts, and various other system parameters of interest were tabulated.

A. SOLAR ARRAY PERFORMANCE

The Solar Array Synthesis Computer Program, developed for NASA-GSFC by RCA-AED under Contract No. NAS 5-10158, was programmed with the solar cell I-V curves shown in Figure 33, temperature-time profile of Figure 32, series-parallel solar cell layouts for the 94-cell and 102-cell solar arrays in Figures 34 and 35 and the solar array degradation factors and temperature coefficients listed in Table II-2 in Appendix II. The degradation factors listed in the table have been thoroughly discussed and documented for both the Nimbus B and Nimbus D Solar Array Critical Design Reviews, and will not be further discussed in this report.

The output of the Solar Array Synthesis program is a listing of the various requested solar array I-V curves, as they would appear with no blocking diode or slip-ring losses. (The voltage drop in these components plus associated connectors and spacecraft harnessing has been measured to be about 1.8 volts.)

Figures II-10 through II-12 in Appendix II show the 94 series cell (NB) F-3 and Bifold solar array I-V curves at beginning of life, one year and two years in orbit. Each figure shows curves at temperatures of -60, +30° and +60°C, spanning the expected orbital temperature range. Figures II-13 through II-15 in Appendix II show similar I-V curves for the 102-series-cell (PPFT and STS) F-3 and Bifold solar arrays. No inter-cell interconnection open circuit failures are anticipated during the two year mission with the expanded silver mesh connector design. Furthermore, the cell paralleling achieved with the silver mesh connections in each module circuit makes it highly unlikely than a randon thermal cycling increased series resistance effect on a cell would be observed at the array level I-V curve.

B. SYSTEM LOAD POWER CAPABILITY

An evaluation of the maximum orbit-average regulated bus load power that the NB, PPFT and STS system configurations can supply as a function of time in orbit, as influenced by the various time-dependent system degradations, was made, utilizing the energy balance computer program developed during this study. (A description of the computer program is presented in Appendix I.)

A significant input to the computer program is the estimated system power losses. In addition to the constant power transfer efficiency factors assumed for the tracker units (nominally 90% for the series tracker unit and 92% for the parallel charger/tracker units) the value of system loss shown in Figure II-16 and II-17, Appendix II, for the F-3 and Bifold systems, respectively, was applied. The F-3 system losses were measured during flight acceptance testing of the Nimbus B power system, and include PWM regulator inefficiency, redundant circuits, telemetry, protection circuitry and auxiliary regulator losses and the shunt loss at regulated voltage in the eight battery charge controllers. This total value of system loss is assumed to be applicable to the PPFT and STS systems also. In addition, the STS system incurs an estimated 6 watt loss at night and 15 watt loss during satellites daytime in the series tracker unit, at regulated voltage. System losses for the bifold systems, Figure II-17, were estimated by multiplying both the load power values and the system loss power values from Figure II-16 by a factor of two.

The method employed to evaluate the maximum energy balance load was to program various load profiles, as shown in Figure 39, until the desired battery C/D ratio was achieved. Changes in the load profile involved varying the orbit-constant value of regulated bus power from run to run. In every case, an additional peak load of 400 watts, having a duration of five minutes, was superimposed on the profile near the end of satellite day.

Figure 40 presents the values of maximum load power achieved for each F-3 array system during the two year mission, for nominal case system design factors. Figure 41 shows the equivalent load capability of the nominal case bifold array systems. The curves are constructed from points obtained for 0, 3, 6, 12 and 24 months in orbit.

Note in all cases that the PPFT system shows a considerable load power advantage over the NB and STS systems. The NB and STS systems have comparable load power capability throughout the mission, except close to the beginning of life, where the series tracker shows about a five-percent gain over the NB system.

Figure 42 presents the load power capability of the three systems under worst-case conditions, and Figure 43 shows the effect on load power of best-case system conditions. The various system design factors that produce the nominal, best-case and worst-case system operating conditions are tabulated in Table II-2

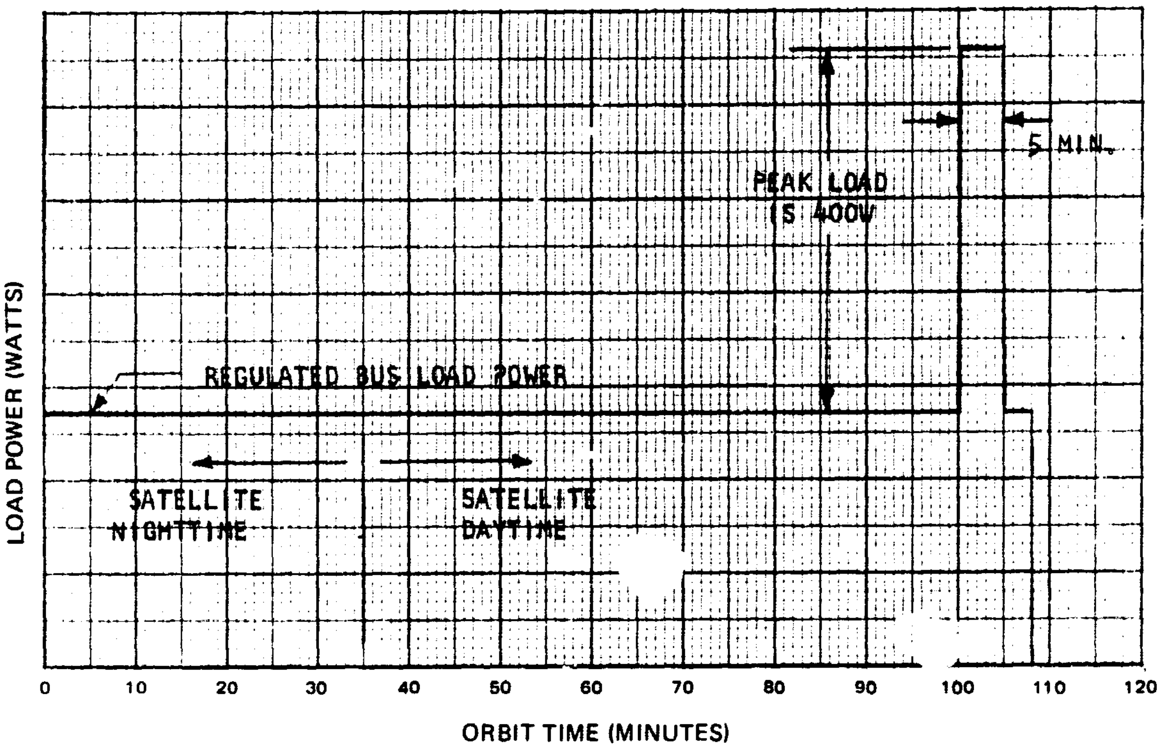

Figure 39. Load Profile Used For Maximum Load Capability Analysis

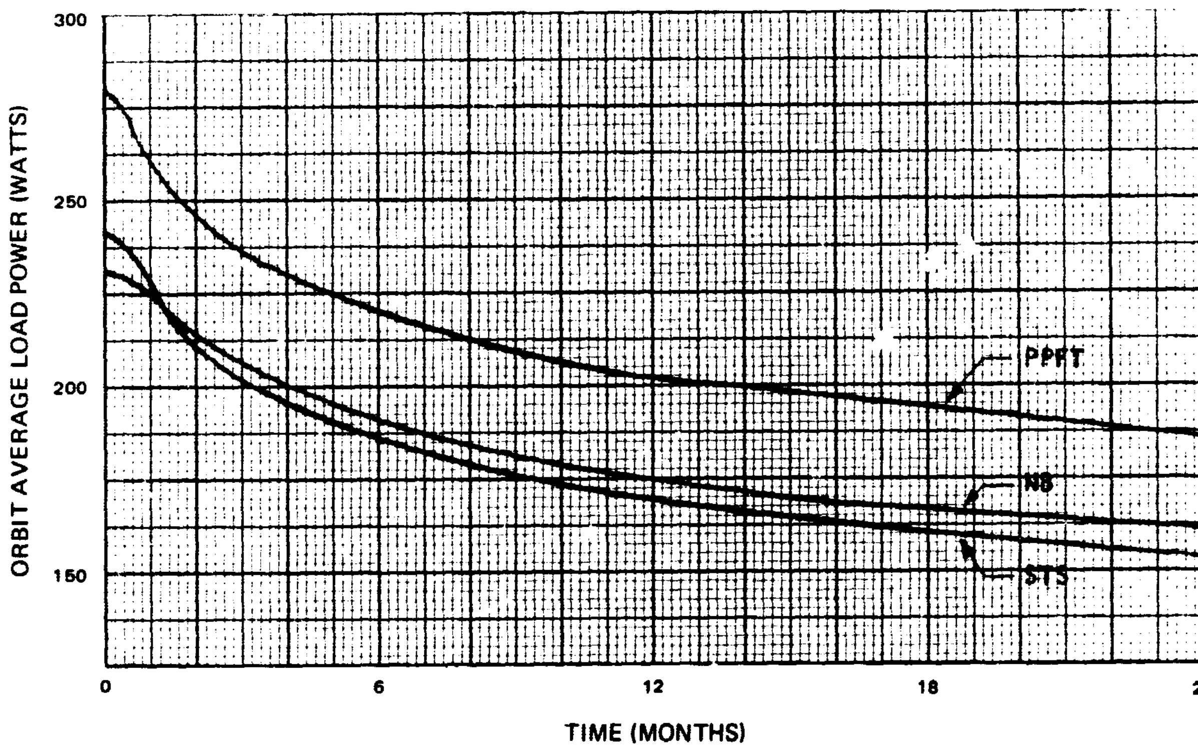

Figure 40. Load Power Vs Time, Nominal Case, F-3 Array Systems

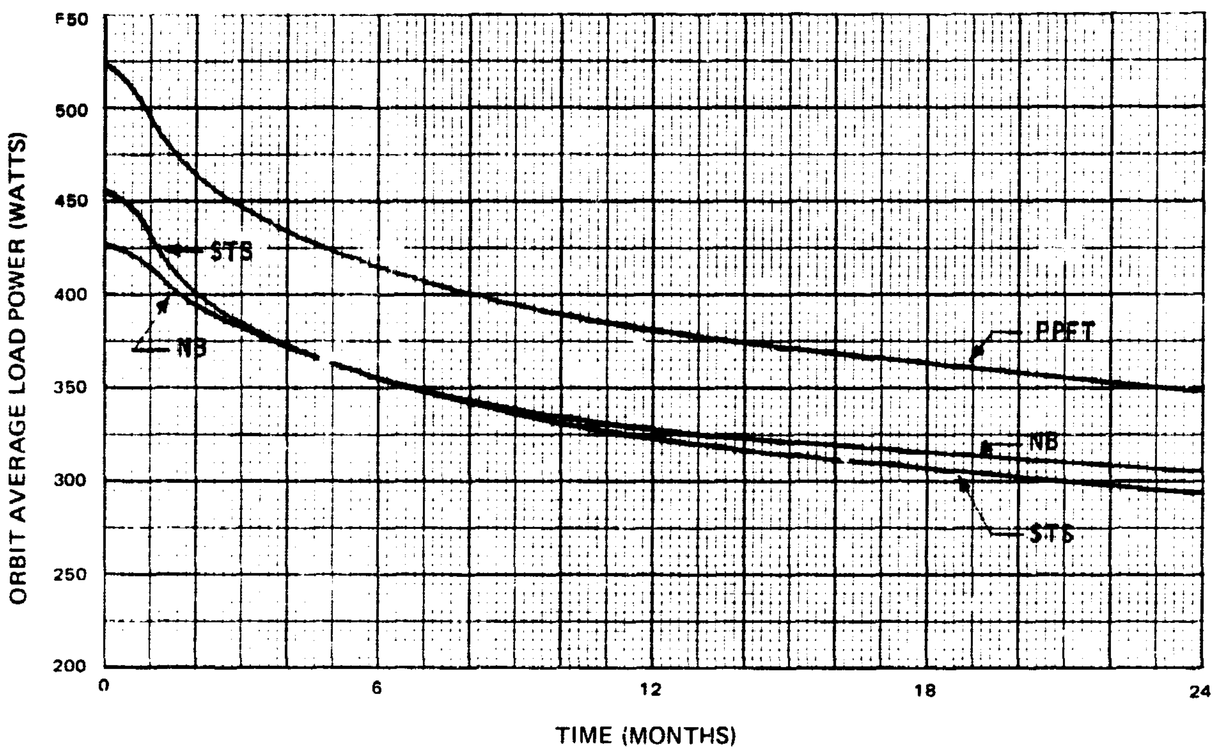

Figure 41. Load Power Vs Time, Nominal Case, Bifold Array Systems

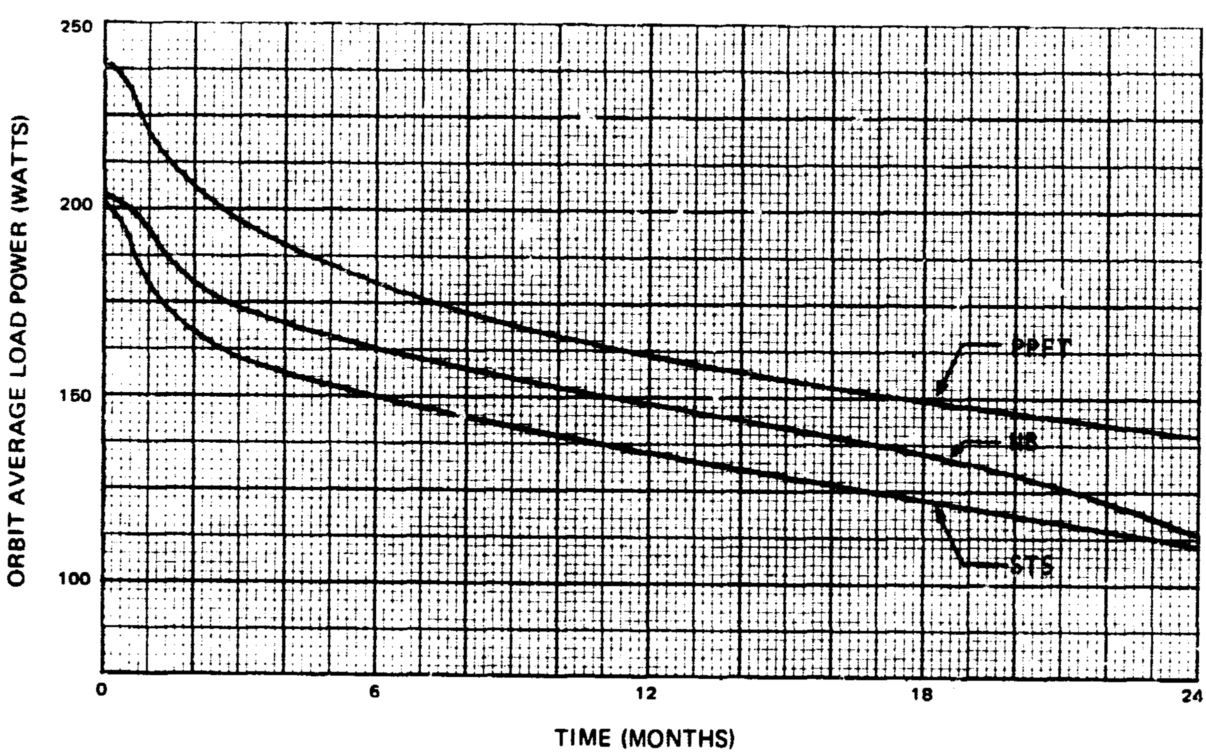

Figure 42. Load Power Vs Time, Worst Case, F-? Array Systems

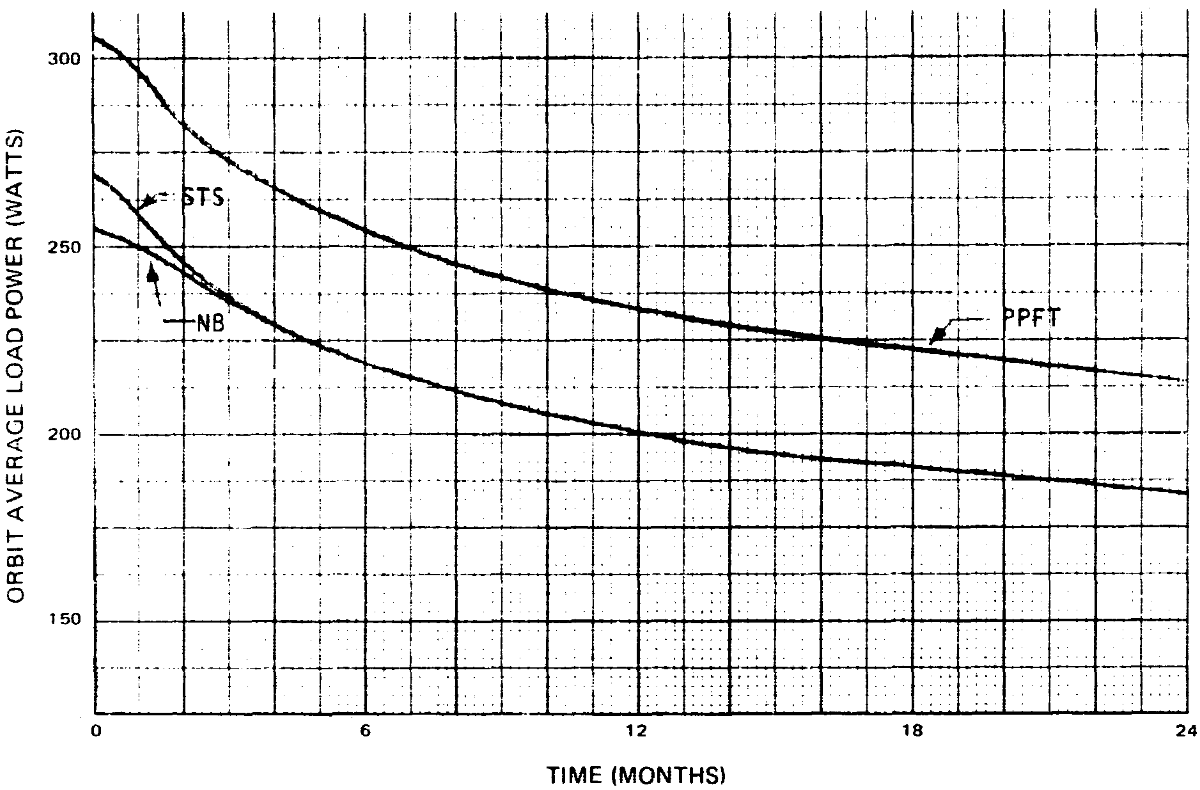

Figure 43. Load Power Vs Time, Best Case, F-3 Array Systems

in Appendix II. Note that it is highly unlikely that the simultaneous occurrence of factors needed to produce the best and worst cases will be realized. The plotted load curves for these cases, however, show an upper and lower limit on the tolerance attached to estimating the performance of the different system configurations.

C. EFFECT OF VARIOUS PEAK LOADS

Since it is uncertain at this time what the actual orbital load profile for a particular advanced Nimbus mission will be, several variations of the 5 minute 400 watt peak load were programmed into the computer. The table below shows the maximum energy balance orbit average constant load with the 400W, 5 minute load near end of day; two 400 watt, 5 minute loads (one at night, one near end of day) and a single 1000 watt, 5 minute peak load occurring near end of day.

	One 400W Peak	Two 400W Peaks	One 1000W Peak
NB	231W	211W	195W
PPFT	278W	259W	244W
STS	241W	222W	205W

The above loads apply to the nominal case, beginning of life F-3 array systems, and resulted in the d red 25°C battery C/D ratio of 1.11 being achieved. All of the above peak lo ulted in battery discharge during the duration of the load.

D. COMPONENT POWER DISSIPATION

The orbit average power dissipation in the modules of each power system is of particular interest because of the limitations of the sensory ring compartments in their ability to radiate sufficient heat energy into space to provide a spacecraft equipment temperature compatible with long-life, efficient operation of the various spacecraft subsystems and experiments.

Minute-by-minute printouts of power system voltages and currents during a simulated computer-program orbit permitted a detailed evaluation of the power dissipated in each module. As was expected, the maximum dissipations occurred at beginning-of-life when the solar array input energy is the greatest. However, various bus loading conditions were necessary to determine the maximum and minimum, as well as nominal, dissipation in each module. For example, the greatest dissipation in the PPFT sotrage module occurred at system worst case conditions, when the 35°C battery temperature required the greatest amount of recharge to maintain energy balance, while in the STS system maximum storage module dissipation occurred with a 50W bus load and a best case array, producing 9.5 watts dissipation in each battery due to a significant amount of charge energy during voltage-limited over-charge operation.

TableVI summarizes the orbit average maximum, minimum and typical value of module power dissipation for each system, and the loading conditions which produced the power dissipation. In the case of the NB system, the storage module power includes the battery, shunt loss, charge controller and shunt dissipator. The STS storage module contains the same components except no shunt dissipator is used in this system.

It is seen from the table that control modules dissipate between 24 and 34 watts, orbit average. This magnitude of dissipation was encountered with the flight Nimbus B system during testing, and did not impose a critical problem, as the adjacent bays would, by design, incorporate equipment with relatively little orbit average power dissipation. The storage modules in the NB system are subjected to an extremely high value of power dissipation during a 50W load orbit condition. This is primarily due to the shunt dissipator pass transistor mounted in each storage module. These high values of dissipation were predicted for the flight Nimbus B; it was planned to employ the ground-commanded Auxiliary Loads to relieve this potential problem during the special orbits with a very small load demand.

TABLE VI. SUMMARY OF COMPONENT POWER DISSIPATION

System	Load	Orbit-Average Power Dissipation (Watts)					
		C/M	Batt	S/M	TCM I	TCM II	STU
PPFT	278 W NC	34 typ	7 typ	3.5 typ	5.5	12.2 typ	
	50 W BC	24.4 min	3.6 min	1.8 min	5.5	3.6 min	
	306 W BC	37 max			5.5	12.8	
	240 W WC		14 max	7 max	5.5	14.8 max	
NB	231 W NC	30.4 typ	2.2 typ	5 typ			
	50 W BC	24.4 min	7	24.3			
	203 W WC	28	2.9	6.3			
	254 W BC	32.3 max	2 min	4.7 min			
	50 W BC except $T_B = 35°C$		14.3 max	30.1 max			
STS	241 W NC	30.9 typ	2.3 typ	5.2			53.5 typ
	50 W BC	24.4 min	7	9.5			30 min
	268 W BC	33.2 max	2.1 min	4.9 min			56.7 max
	50 W BC except $T_B = 35°C$		15.5 max	18.4 max			

NC = nominal case, BC = best case, WC = worst case system design factors

The power dissipation in the series tracker unit can exceed 56 watts, orbit average. This value is considered greatly excessive, even for a 4/4 module, and would probably preclude use of this system in the described configuration. It would be possible to utilize two MPT power switches, one in each of two series tracker modules, and design circuitry to force current sharing between them. However, since no load power advantage is realizable with this system in a Nimbus application, the additional complexity of the current sharing circuitry and its redundancy, as well as the requirement for up to 7 full bays, should preclude use of the series tracker configuration in the Nimbus mission.

E. SUMMARY OF SYSTEM OPERATING PARAMETERS

Table VII presents a summary of the various system voltages and currents and battery parameters for the three system configurations under maximum loading conditions at beginning of life and at two years in orbit. The parameter values in all cases were obtained directly from the energy balance computer program printout.

TABLE VII. SUMMARY OF SYSTEM OPERATING PARAMETERS

		Nominal Case		Worst Case		Best Case	
		BOL	2 Yrs	BOL	2 Yrs	BOL	2 Yrs
PPFT System	Load Power (Watts)	279	186	240	140	306	214
	Batt Depth of Dischg (%)	17.0	12.5	23.0	15.2	18.6	14.2
	V unreg minimum (Volts)	29.8	27.4	29.0	26.5	29.9	27.8
	Pwr Diss in Each Batt (W)	7.0	7.3	13.9	14.0	6.4	7.2
	SA Peak Pwr (Watts)	806	613	742	534	877	689
	I_B Chg Highest (Amps/Batt)	4.3	3.4	6.0	4.6	4.7	3.8
NB System	Load Power (Watts)	231	162	203	114	254	184
	Batt Depth of Dischg (%)	14.9	11.8	15.8	10.2	16.3	13.0
	V unreg minimum (Volts)	28.7	26.5	28.0	26.2	28.8	26.9
	Pwr Diss in Each Batt (W)	2.2	2.6	2.5	3.2	2.0	2.3
	SA Peak Pwr (Watts)	802	611	744	536	872	685
	I_B Chg Highest (Amps/Batt)	0.77	0.66	0.83	0.79	0.80	0.76
STS System	Load Power (Watts)	241	154	201	111	268	183
	Batt Depth of Dischg (%)	15.8	11.6	15.7	10.3	17.5	13.2
	V unreg minimum (Volts)	28.6	26.5	28.0	26.2	28.8	26.8
	Pwr Diss in Each Batt (W)	1.5	2.4	3.9	3.7	2.2	2.4
	SA Peak Pwr (Watts)	806	615	742	534	877	689
	I_B Chg Highest (Amps/Batt)	1.5	1.2	1.7	1.2	1.7	1.3

PRECEDING PAGE BLANK NOT FILMED.

SECTION IV

CONCLUSIONS AND RECOMMENDATIONS

The extensive power systems analytic effort that has been expended by both GSFC and RCA, the detailed post-launch analysis of the highly successful Nimbus II satellite, considerable Nimbus power supply component and subsystem test experience and advanced techniques development programs sponsored by NASA have all contributed to what is believed to be a practical, minimum-development-time, and cost-effective approach to meeting the increased power requirements of a more demanding future Nimbus mission.

This study has evaluated power system configurations having a load capability range of 200 to 500 watts, orbit average, at beginning of life. As much as 350 watts can be obtained for the entire two-year mission with the parallel part-time/full-time tracker (PPFT) system configuration, under nominal operating conditions. The higher power systems would utilize the bifold solar array already developed on the Nimbus project.

A separate peak load converter/regulator is suggested for all systems, since the steady-state load power of all systems produce about 30 watts of dissipation in the regulator bay, and any significant peak load (200 watts or more) would exceed the 20-ampere capability of the flight-qualified regulator. A very severe limitation was found to exist with the series tracker configuration; an orbit average power dissipation of greater than 50 watts would exist in the series tracker unit. This excessive dissipation plus the conclusion that no load power advantage exists with this system configuration, should preclude the use of the series tracker in a Nimbus application.

A distinct load power increase over the Nimbus B system can be realized with the parallel tracker configuration (PPFT), requiring only the same spacecraft "real estate" as the NB system and eliminating the possible excessive power dissipation condition that could be encountered in the NB Storage Modules when the shunt dissipator is activated.

It is recommended that the circuit functions not yet developed for the PPFT system (battery ampere-hour counter and solar array power sensor) be breadboarded, and an engineering model of this system configuration fabricated in order to uncover and solve any possible interface or packaging problems. In the event that a greater load capability is required for a Nimbus mission, the PPFT system appears to be the configuration best adapted to this need.

PRECEDING PAGE BLANK NOT FILMED.

BIBLIOGRAPHY

1. MacKenzie, C. M.; Greenblatt, R. C.; Cherdak, A. S.; "Nimbus Power Systems (1960-1969)", presented at the Aerospace Electronic Systems Convention, October, 1966, Washington, D. C.

2. Bolton, C. F. and Nekrasov, P. S.; "Analysis of the Advanced Nimbus Power System", July 1967, NASA-GSFC Document No. X-716-67-350.

3. Bolton, C. F. and Nekrasov, P. S.; "Multiple Operating Points in Photovoltaic Power Systems", May 1968, NASA-GSFC Document No. X-716-68-178.

4. Advanced Voltage Regulator Research and Development Program, Final Report, 6 March 1963 through 1 August 1964, Contract NAS-5-3248, Prepared for NASA-GSFC by RCA Astro-Electronics Division.

5. Advanced Voltage Regulator Techniques as Applied to Maximum Power Point Tracking Systems for the Nimbus Meteorological Satellite, Contract NAS 5-3248, Final Report issued 10 October 1967, RCA Document No. AED R-3221.

6. Nimbus-B Solar-Conversion Power Supply Subsystem Quarterly Technical Report No. 1 through 7 dated January 1966 to August 1967. Prepared by RCA Astro-Electronics Division for NASA-GSFC under Contract NAS 5-9668.

APPENDIX I

NIMBUS ENERGY BALANCE COMPUTER PROGRAM

A. INTRODUCTION

The purpose of this section is to present an engineering-oriented discussion of the Nimbus Energy Balance Computer Program. A description of the program, its capabilities and limitation, how the program performs the energy balance calculations and how to set up and use the program are the specific items presented herein.

This program was developed for NASA-GSFC by RCA-AED under Contract No. NAS 5-11549, "Study of Power Supply Configurations", as a basic tool for analyzing the orbital performance of three general types of power subsystem configurations being considered in this Study for possible future Nimbus missions.

Originally prepared in FORTRAN II version(1) to accommodate an energy balance analysis of the Nimbus B power subsystem, the program has been extensively modified to include an analytic capability for a Series Maximum Power Tracker and a Parallel Maximum Power Tracker subsystem. Conversion of the program to FORTRAN IV allows program operation on the RCA Spectra 70 and the IBM 360 computers.

B. GENERAL

The purpose of the Nimbus Energy Balance Computer Program is to simulate the operation of various power subsystems as the spacecraft passes through a complete orbital cycle. The simulation is accomplished by combining the known electrical characteristics of the solar array, battery, source control devices, load power conditioning devices, charge controller, system power losses and spacecraft load profiles. A running tally of the various power system operating parameters is provided throughout the simulated orbit; these parameters are printed out at equal user-specified time increments during the orbit.

---

(1) "Energy Balance Computer Program for the Nimbus B Solar Conversion Power Supply Subsystem", RCA Technical Report No. NB-SP-PO-137, dated July 21, 1967. Prepared under Contract No. NAS 5-9668.

Figure I-1 presents a block diagram of the computer model of three power system configurations: the Nimbus B (NB), Parallel Maximum Power Tracker (PMPT) and Series Maximum Power Tracker (SMPT) configurations. By supplying a particular "System Key" input data card, the program user specifies which system configuration he wishes to simulate, and the computer "switches" shown in Figure I-1 are positioned appropriately. All input data and computer instructions are supplied by the program user in a "data deck" consisting of 50 NCODE cards defining various power system parameters, 30 STINT tables containing solar cell, battery, temperature and load profile information, and up to 25 Panel Description Cards defining the solar array configuration to be simulated.

The following paragraphs describe the characteristics of each of the components comprising the computer model of the three types of power subsystems.

1. Solar Array and Isolation Diode

The solar array may contain from one to twenty-five solar cell panels connected electrically in parallel. Each panel may have its own number of series and parallel cells, its own solar incidence angle (which must remain constant throughout an orbit) and its own temperature-vs-time profile. All panels use the same solar cell as the basic building block, and pass current through the isolation diode ADIODE. The value of ADIODE includes the diode and slipring losses (typically, 1.8 volts). Total solar array output current, IA, is the sum of the individual panel currents at the solar array operating voltage VA.

The array I-V curve values are determined by the computer multiplying the solar cell I-V points by the number of series cells for voltage, and by the number of parallel cells for current on each panel. The charge-particle-degraded solar cell I-V curve is supplied by the user as an input table of I-V pairs along the curve. Temperature coefficients and voltage and current degradation factors are also supplied as an input by the user; subroutine STASH manipulates the tabulated cell I-V curve to account for the various design factors and temperature effects.

2. Series MPT Unit and Solar Array Bus

If the program user has elected to simulate the SMPT system, the switches in Figure I-1 are placed in the SMPT position by the computer and the Series MPT Unit is connected in series with the output of the solar array. The component transfers solar array power (VA-ADIODE) × IA to the series tracker unit output with an efficiency, PTEFF, specified by the user. The power tracker output, PTO, is then defined by the relationship PTO = (VA-ADIODE) × IA × PTEFF watts. PTEFF retains a constant value during an orbit, and a minimum drop of 1.0 volt is maintained across the series tracker unit at all times. The series tracker unit output voltage is designated VTO.

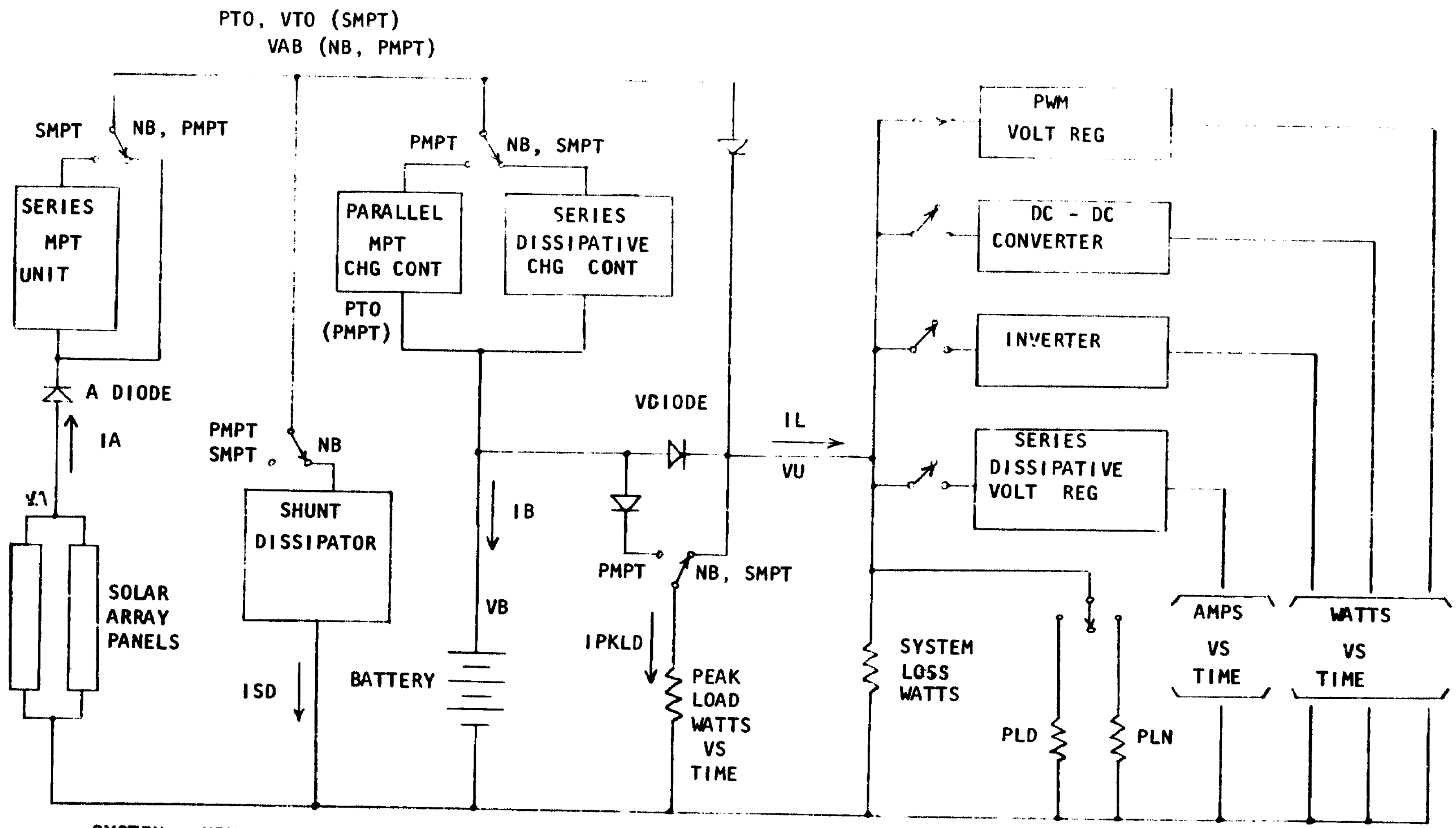

SYSTEM KEY
NB = NIMBUS B
PMPT = PARALLEL MAXIMUM POWER TRACKER
SMPT = SERIES MAXIMUM POWER TRACKER

Figure I-1. Computer Model of Three Power System Configurations

When either a NB or PMPT system is to be simulated, the switches in Figure I-1 are automatically positioned accordingly; the series tracker unit is shorted out, and the voltage on the solar array bus VAB is defined as VAB = VA - ADIODE.

3. Shunt Dissipator

The shunt dissipator is employed in the NB system only, and is represented by the equivalent circuit shown in Figure I-2.

Whenever the solar array bus voltage (VAB) exceeds the shunt dissipator threshold voltage (TVSR), shunt dissipator current (ISD) will exist, as determined by the effective shunt dissipator resistance (ERSR). The values of TVSR and ERSR are specified by the user on input NCODE cards.

4. Charge Controller

The NB and SMPT systems use the same charge controller model, shown in Figure I-3.

When the voltage drop across the charge controller (VCRR) exceeds the dead zone voltage (DZCRR), battery charge current (IB) will increase linearly to the point where the maximum permissible charge current (IBMAX) occurs at the charge controller knee voltage (VKCRR); further increases in VCRR will maintain a constant IB value. If the value of battery charge voltage reaches the maximum permissible value (VBMAX), the computer will reduce the charge current to a value such that VBMAX is not exceeded, just as in actual voltage-temperature limiting circuit operation (tapered charge operation).

Values of DZCRR, VKCRR, IBMAX and VBMAX are specified by the user.

When a PMPT system is being simulated, the series dissipative charge controller previously described is connected and replaced by the parallel maximum power tracker unit, which transfers power from the solar array bus to the tracker output with a user-specified efficiency PTEFF. The tracker output power, PTO, is normally used to charge the battery, but can also deliver power to the peak load and/or the main load regulator if necessary.

The parallel tracker unit also contains the current-limiting (IBMAX) and voltage-limiting (VBMAX) circuits which control battery charge current just as in the other two system configurations. In addition, the parallel tracker unit continuously compares the total amp-minutes into the battery with the total amp-minutes taken out of the battery during the orbit being simulated. When the ratio

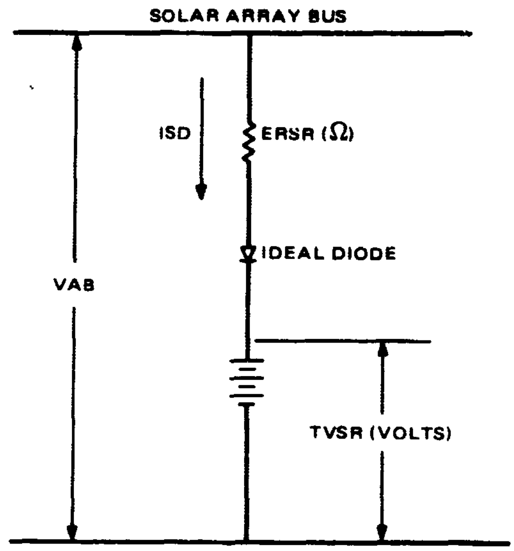

Figure I-2. Shunt Dissipator Equivalent Circuit

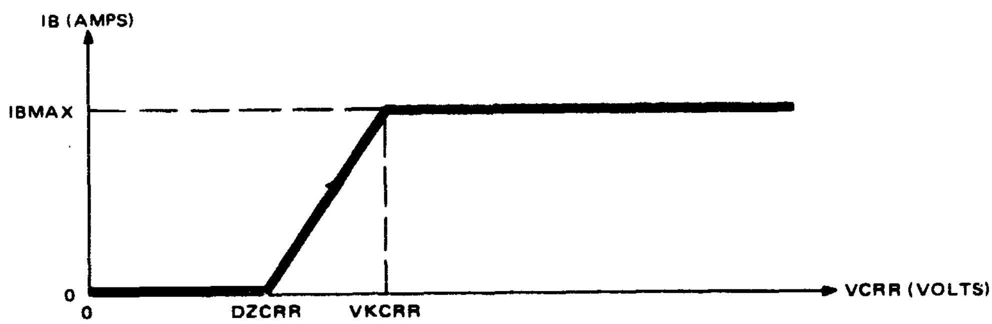

Figure I-3. Computer Model of Charge Controller of these parameters reaches the value specified by the program user as the C/D ratio (CTOD), battery charge current is automatically reduced to a nominally low (0.6A) value. This simulates the actual operation of an ampere-hour counter charge control method.

5. Battery

The computer model assumes that all batteries connected in parallel in the power system have the same electrical characteristics. They can therefore be lumped together into one equivalent battery having the combined capacities, the sum of the maximum charge currents and the same voltage as the individual batteries.

The voltage of the computer model of the battery depends upon its state of charge and the value of current going into or out of the barrery. The full capacity of the battery BAMMAX (Battery Amp-Minutes MAXimum) is defined by the user as an input and the state of charge SOC is calculated by the computer to be the amp-minutes in the battery at any given time (ACCUM), divided by BAMMAX. Storage cell data is read into the computer from an input data table which tabulates cell voltages as a function of SOC and charge or discharge current, IB. The computer multiplies the cell voltage by the number of series-connected cells in the battery (FUDGE) to obtain the battery voltage VB at a given SOC and a given value of IB. One battery is assumed in the computer system, having the combined capacity of all the storage modules, and charging or discharging at the total value of current. An example of how storage cell data is tabulated for computer input is presented later in this Appendix.

Values of BAMMAX and FUDGE are specified by the user as an input to define the system storage capacity and the number of cells in the battery. (NOTE: the variable NBAT is also used in the program to signify the number of series-connected cells in the battery.)

6. Discharge Diode, Unregulated Bus and Peak Load

In all three system configurations, the battery discharges through an isolation diode in the battery discharge path between the battery and the unregulated bus. The voltage drop across this diode is called VDIODE, and is user-specified. Current exists through this diode only during battery discharge, providing a definition for unregulated bus voltage VU during satellite nighttime: VU = VB - VDIODE.

Note that VU can be much greater than VB during solar array illumination, since the battery discharge diode is then normally reverse-biased. At all times, the spacecraft load demand (except for peak load) is determined by computer to be IL amperes demand at the unregulated bus voltage VU.

The peak load is a user-supplied input data table which defines peak load power as a function of time during an orbit. The table is prepared in the same format for all three systems, and in fact can define any type of unregulated bus power profile from a minimum duration of one minute up to an entire orbit duration load. As seen in Figure I-1, the peak load in the NB and SMPT systems is supplied from the unregulated bus. The battery will discharge if the solar array bus cannot supply enough power at VU to satisfy IL and the peak load current IPKLD.

When the PMPT system is selected, the peak load is supplied from a peak load bus which is isolated from the unregulated bus by the battery discharge diode VDIODE. This permits the solar array to operate at its maximum-power voltage at all times; the peak load current is supplied by the parallel tracker unit up to the limit of IBMAX—any additional current requirement is supplied by battery discharge to the peak load bus. The value VDIODE is applied to the voltage drop across the diode between the battery and peak load bus in the PMPT system.

7. Load Power Conditioning Devices

Figure I-1 shows four types of power conditioning devices which derive unregulated DC power from the unregulated bus and supply the spacecraft loads with the desired type of voltage. Any or all of the four devices may be used with any of the three systems—the user defines which STINT table location (explained in a later section of this report) contains the load vs time profile of a device which is to be employed in the system. The characteristics of each load power conditioning device are described below.

a. PWM Voltage Regulator

This device, which supplies all the -24.5 volt regulated loads on the Nimbus spacecraft, is a down-converting, switching regulator that basically transfers power at a relatively constant percentage efficiency. The input current can be less than the output current in this relatively efficient device. PWM regulator losses (transfer efficiency losses) are included along with other system losses in a separate stored table, as a function of regulated load power. The load profile for this device is tabulated as spacecraft load watts versus time; calculation of losses is automatically made.

b. DC-DC Converter

This device supplies regulated DC power at an output voltage which can be higher than the input (regulated) voltage. The load profile is prepared as regulated output power versus time; losses are calculated as a power transfer inefficiency with a user-supplied value of converter efficiency EFFCNV. The computer does not need the value of output voltage for its calculations; the user must define the appropriate constant value of EFFCNV for the particular device he is simulating.

c. Inverter

This device supplies an A-C output voltage to the load profile which is tabulated as required watts versus time. A constant percentage power transfer efficiency EFFINV is supplied by the user as an input. Values of output voltage, frequency or power factor are not required by the computer; the user must supply an appropriate efficiency EFFINV for the particular inverter he is simulating.

d. Series Dissipative Voltage Regulator

This device supplies current at a constant regulated DC voltage which is less than the input voltage, similar to the PWM regulator. However, in the dissipative device, the input current is assumed to be equal to the output current. The product of this current times the voltage drop across the regulator is the power lost in supplying the loads with this device. The load profile for the series dissipative regulator is tabulated as amperes demand (at regulated voltage) versus time.

8. System Power Losses and Fixed Losses

The system loss watts shown in the block diagram of Figure I-1 are values of watts, stored in a table in the computer, that represent the measured PWM voltage regulator losses, telemetry and standby circuitry losses, solar array bus-to-unregulated bus diode losses and regulated power required by the eight charge controllers in the Nimbus B flight power subsystem. These are collectively called system power losses and are strongly dependent on both the unregulated bus voltage and the total spacecraft load demand on the power subsystem. Figure I-4 presents the measured system power losses as a function of regulated bus output power for conditions of satellite nighttime (battery discharge, low unregulated voltage), solar array illumination (middle-range unregulated voltage) and shunt dissipator ON (highest unregulated voltage).

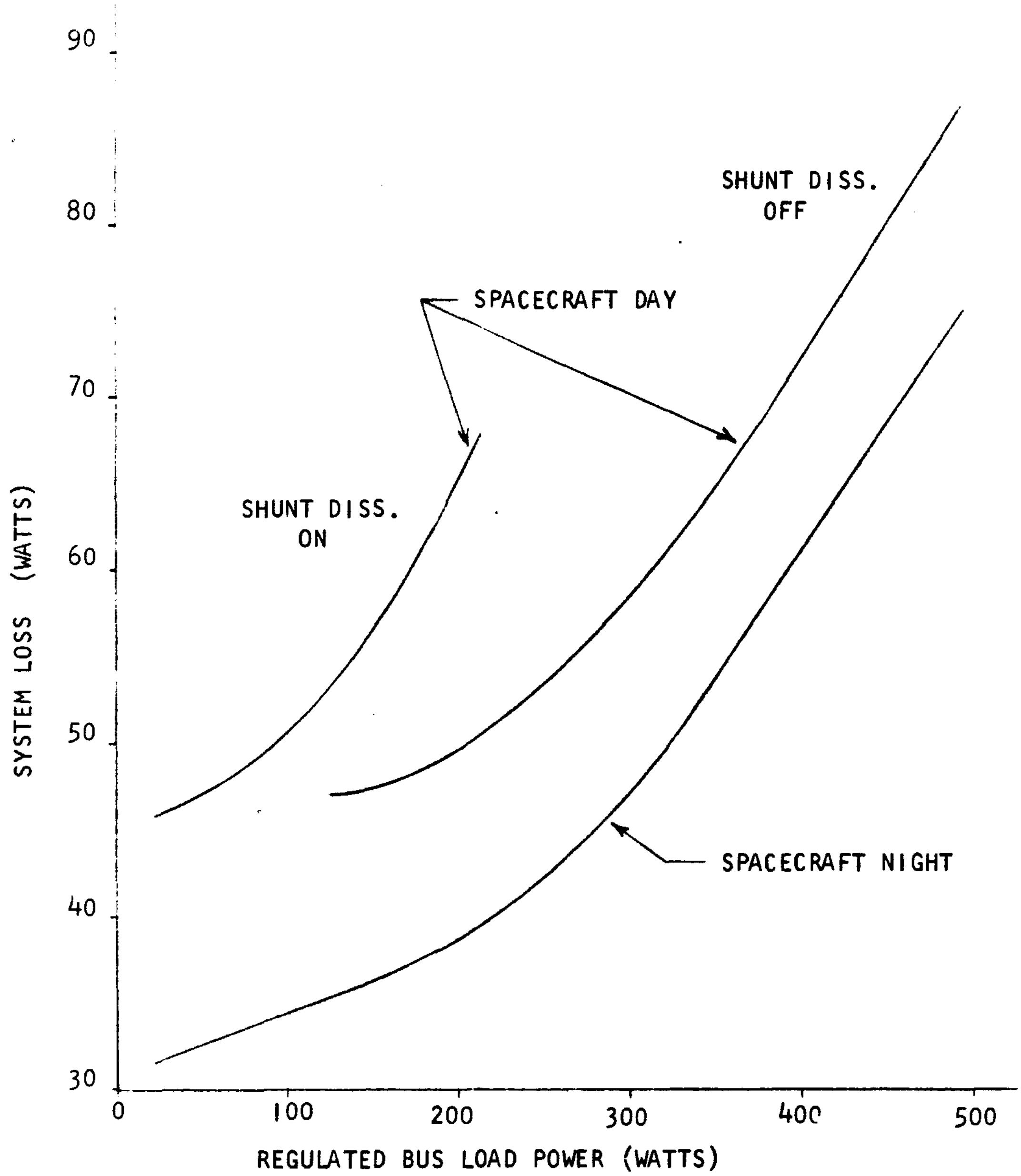

Figure I-4. System Power Loss versus Regulated Bus Load Power

When a PWM regulator is specified, the total value of system loss is obtained from the table which contains the Figure I-4 data. If a PWM regulator is not used in a system, the losses are calculated as described in 7 b, c and d, and in addition the system loss (watts) at 0 watts PWM load is obtained to account for such losses as are caused by telemetry, standby circuitry, etc.

Figure I-1 also shows a computer "switch" which can be positioned to place a "power loss, night" PLN, or "power loss, day" PLD load on the unregulated bus. The user can specify this constant value of power loss in addition to all other loads and losses by supplying the value of watts for daytime and/or nighttime system operation on an input data card. An example of the use of PLD is a 15-watt fixed loss in the series tracker unit of the SMPT system. This fixed loss is in addition to the loss caused by the power transfer efficiency of the series tracker unit, PTEFF.

C. PROGRAM DESCRIPTION

This section presents a functional description of the program subroutines, a detailed description of how to prepare the program input data, and a summary of the information printed out at the conclusion of a run.

1. Program Routines

Because of the numerous power system components and functions that must be considered when simulating orbital performance, the energy balance program is divided into a main routine, called MAIN, and the following subroutines: STASH, STINT, DRAIN, AMPS and PRINT. All five subrountines are used when simulating either the NB, PMPT or SMPT system configurations and perform identical functions for all systems.

Figure I-5 presents a basic block diagram of the energy balance program and summarizes the important functions of each subroutine. The following paragraphs provide a description of the main program and its subroutines.

a. MAIN

The purpose of MAIN is to load input data, initialize power system parameters, select the proper set of energy balance calculations for a particular system, perform a clock function during the orbit, call on the five subroutines for data as required and maintain and update values of the system parameters throughout the orbit. MAIN employs iterative processes to determine the various

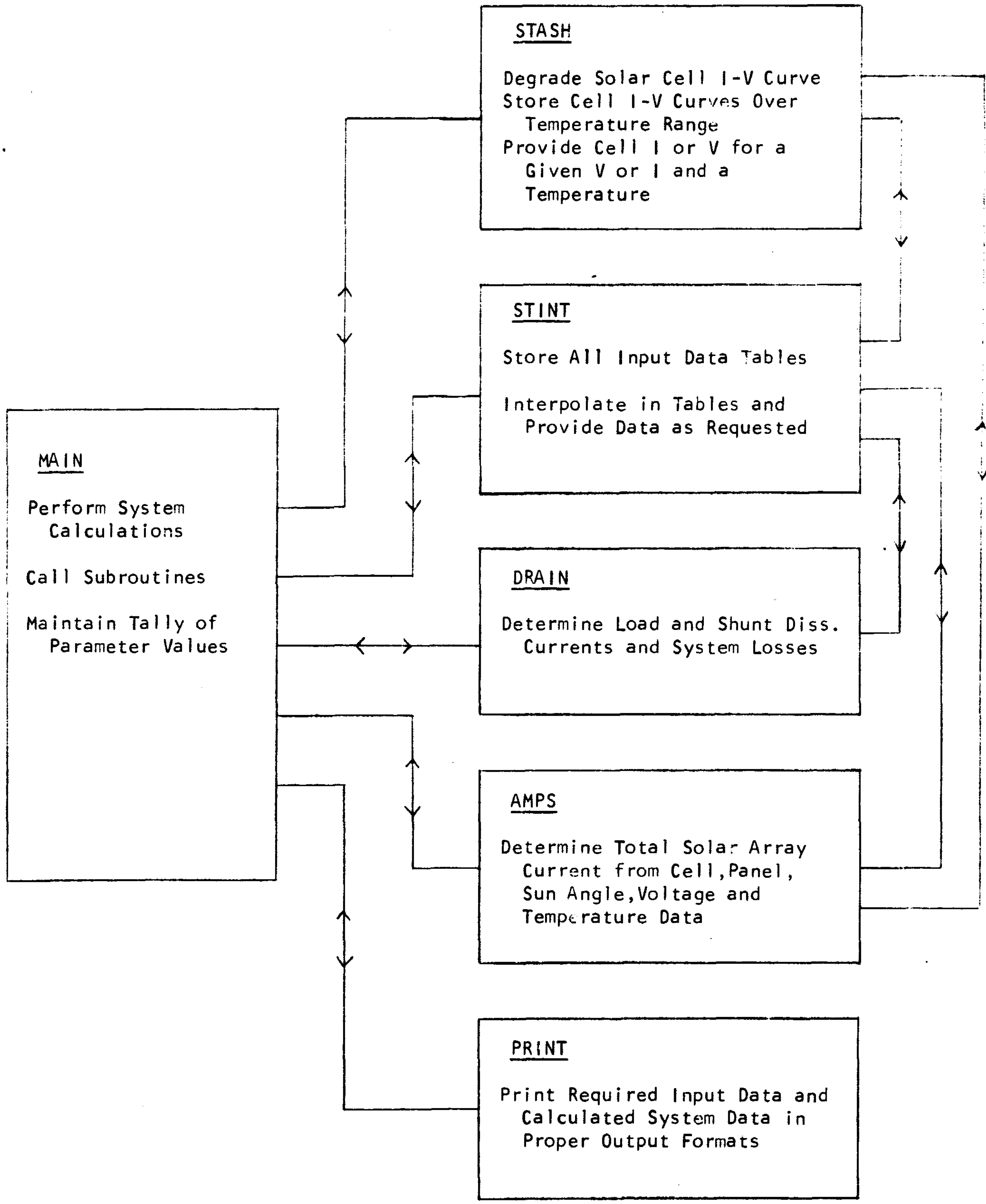

Figure I-5. Subroutine Functions In Energy Balance Program system voltages and solve for the various branch currents in the power system such that the Ohm and Kirchoff criteria are satisfied to within an arbitrarily small error. In addition to the various system voltages and currents, MAIN keeps track of battery relative state of charge (SOC), depth of discharge (DOD), accumulated ampere-minutes (ACCUM), net power dissipation in the battery on an orbit-average basis, ampere-minute C/D ratio achieved during the orbit, solar array maximum power and power at the actual operating voltage, and solar array temperature. MAIN also ensures that the maximum values of battery charge current and battery voltage are not exceeded.

b. STASH

The purpose of this subroutine is to receive a single I-V curve for a charged-particle-degraded solar cell at the temperature TNOT. Also to degrade it for various effects on current, voltage and curve shape, and expand it into a family of curves for different temperatures. STASH prepares tables of current-voltage pairs at each of fifteen temperatures, along with current and voltage at maximum power, open circuit voltage, and short-circuit current. These curves are held for ready reference when solar cell information is called for by MAIN, and sent to PRINT to appear in the output at the completion of a run.

c. STINT

Subroutine STINT is used many times throughout the program to obtain information from the input data tables. The name stands for Standard Table INTerpolation; it is an adoption of the INT routine which is a part of the IBM SHARE library.

The purpose of this routine is to store in tables, then supply on command, the values of variables which are functions of one, two or three arguments. A package of STINT tables consists of a stack of individual table card decks each beginning with a descriptive header card. In the loading mode, STINT will load such cards until it finds a blank card instead of a header. It will then exit back to the control point. The first use of the STINT routine, which is called for by MAIN, is to load all the input data tables. Subsequently, STINT is called from MAIN and from the subroutines to interpolate in the stored tables and provide the requested data values.

d. DRAIN

Subroutine DRAIN obtains the value of load power or current from the load profile table for each of the power conditioning devices specified by the user, adds to it the resulting inefficiencies and either PLD or PLN, and computes the total load current IL at the operating voltage VU. DRAIN also compares the operating voltage with the shunt dissipator threshold voltage TVSR and calculates the current ISD if TVSR has been exceeded.

e. AMPS

Subroutine AMPS determines the total solar array current available at the solar array output voltage VA, accounting for the series-parallel arrangements, sun angles, panel temperatures and blocking diodes associated with up to 25 solar-cell panels.

f. PRINT

Subroutine PRINT receives the user-specified input data and various calculated system parameters from MAIN and writes the output tape, preparing the data in the proper formats and column headings.

2. Input Data

The assembly of the complete program as it is submitted to the computer is shown in Figure I-6. This assembly basically consists of two parts—a program deck and a data deck. The program deck, which can be used in either Fortran IV or binary form, is always used and is placed first in the assembly. It contains the MAIN routine and the five subroutines used in the program (DRAIN, PRINT, STASH, STINT, AMPS) and does not require any card change from run to run to perform its function.

The data deck contains all the numerical information the program requires for computation and defines the user-selected options for each run. Consequently, the data deck must be prepared specifically for each run, or series of chained runs, to be made. Cards and tables in the data deck must be positioned in the order shown in the program assembly in Figure I-6. The input data deck description and format are presented below in the proper assembly sequence.

Date Card

Col. 1-2 Number of month

Col. 3-4 Number of day

Col. 5-6 Number of year

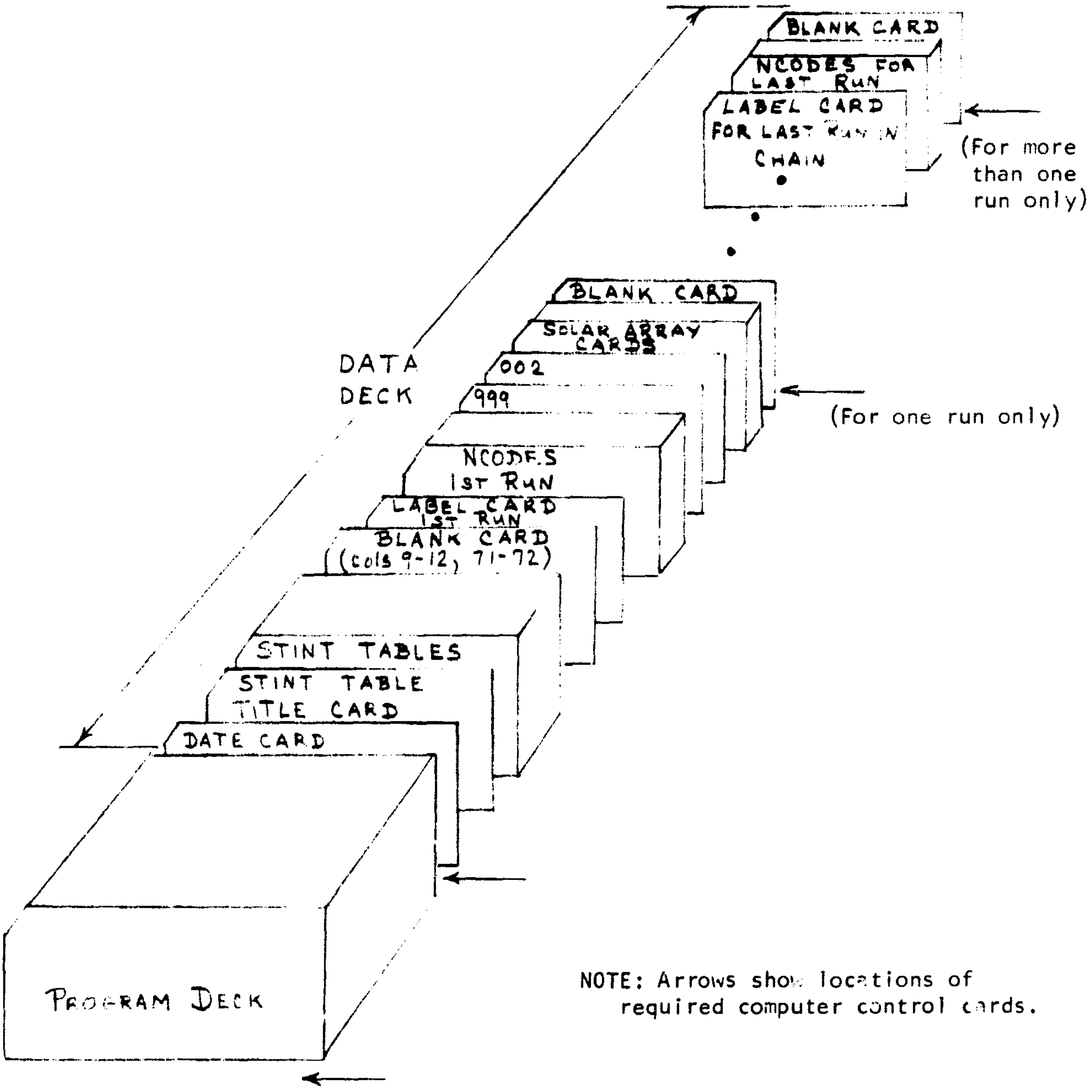

Figure I-6. Assembly of Complete Energy Balance Program and Input Data

STINT Table Title Card

Col. 1 Blank

Col. 2-72 Any alpha-numeric information

STINT Tables

The STINT tables are stacked one behind the other in the data deck in ascending numerical order. Table I-1 lists the tables present in the data deck in the order shown.

TABLE I-1. TABLES IN THE DATA DECK

Table No.	Contents	
1	2.0 amp series regulator load	
2	System power loss data	
3	ETA vs Bat. Temp. Nimbus-B	
4	Relative solar cell current vs incidence angle	
5	11.4 CRL I-V Curve Unglassed 28 Deg. C AMO	
6	3 Mos I-V Curve, Flux is 7.9 Exp 13	
7	6 Mos I-V Curve, Flux is 1.58 Exp 14	
8	Yr I-V Curve, PHI = 3.16 Exp 14, T = 28 Deg.	
9	2 Yr I-V Curve, PHI = 6.32 Exp 14, T = 28 Deg.	
10	400 Watt PKLD Table	
11	NB SA Temp. vs Time Profile, 612 NM	
12	25 Deg. C, BOL	
13	25 Deg. C, 1 Yr. Life	
14	25 Deg. C, 2 Yr. Life	
15	35 Deg. C, BOL	Storage Cell Data
16	35 Deg. C, 1 Yr. Life	
17	35 Deg. C, 2 Yr. Life	
18	PWM Reg Load 150W No XMTR	
19	PWM Reg Load 160W No XMTR	
20	PWM Reg Load 170W No XMTR	
21	PWM Reg Load 180W No XMTR	
22	PWM Reg Load 190W No XMTR	
23	PWM Reg Load 200W No XMTR	
24	PWM Reg Load 210W No XMTR	
25	PWM Reg Load 220W No XMTR	
26	PWM Reg Load 230W No XMTR	
27	PWM Reg Load 240W No XMTR	
28	PWM Reg Load 250W No XMTR	
29	PWM Reg Load 260W No XMTR	
30	PWM Reg Load 270W No XMTR	

The maximum number of STINT tables that the program can presently accommodate is thirty.

The first card of each STINT table is a header card, which must be prepared in the following format:

Cols. 1-8 :	Any alpha-numeric characters can be used for a date.
Cols. 9-12:	Table number. Cannot be zero. Fixed point and right-justified.
Cols. 13-14:	Number of $argument_1$ values. Cannot be zero. Fixed point and right-justified.
Cols. 15-16:	Number of $argument_2$ values. Cannot be zero, is 1 for a function of one argument. Fixed point and right-justified.
Cols. 17-19:	Not used.
Cols. 20-70:	Any alpha-numeric characters desired. Usually used for table title.
Cols. 71-72:	00

After the header card, each card in the table uses 10 fields of 7 columns each for the argument values and the function values. The first card contains the first nine $argument_1$ values in fields 2 through 10. In the following cards, field 1 contains an $argument_2$ value, and fields 2 through 10 contain corresponding function values. After all the $argument_2$ values have been spanned, the whole series of $argument_1$ cards followed by $argument_2$ cards can repeat until all the function values are used. If there is an $argument_3$ value for the table, it goes into field 1 of the $argument_1$ card. Columns 71 and 72 on each card must contain a sequence number, starting with 01 for the first card. Figure I-7 shows a typical STINT table coding sheet for a single argument (solar cell current as a function of voltage) STINT table. Figure I-8 shows a typical two-argument STINT table format.

After the last STINT table in the data deck, there is a card labeled END OF STINT TABLES, starting in Col. 21. Cols. 9-12 and 71-72 must be left blank on this card.

Run Label Card

Following the END OF STINT TABLES card is a card containing any desired alpha-numeric information in Cols. 2-72, which usually describes the first run to be made.

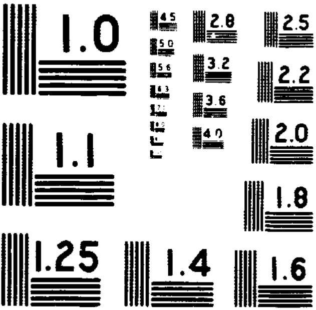
1.0
4.5
5.0
5.6
6.3
2.8
3.2
3.6
4.0
2.5
2.2
2.0
1.1
1.8
1.25
1.4
1.6

HEADER CARD

COLS 1-8 07-30-67 (TBL. DATE) COLS 9-12 0005 (TBL. NO.) COLS 13-14 27 (L1) COLS 15-16 01 (L2) COLS 71-72 00 (SN) COLS 73-77 ____ (TBL. NAME) COLS 78-80 ____ (PDN)

→ COL. 20: NB I-V CURVE, BOL, 30 DEG.C, AMO

FIELD 1 INTEGER • EXP	FIELD 2 • INTEGER • EXP.	FIELD 3 • INTEGER • EXP.	FIELD 4 • INTEGER • EXP.	FIELD 5 • INTEGER • EXP.	FIELD 6 • INTEGER • EXP.	FIELD 7 • INTEGER • EXP.	FIELD 8 • INTEGER • EXP.	FIELD 9 • INTEGER • EXP.	FIELD 10 • INTEGER • EXP.	SEQ. NO.	PROGRAM DECK NO.
1 2 3 4 5 6 7	8 9 10 11 12 13 14	15 16 17 18 19 20 21	22 23 24 25 26 27 28	29 30 31 32 33 34 35	36 37 38 39 40 41 42	43 44 45 46 47 48 49	50 51 52 53 54 55 56	57 58 59 60 61 62 63	64 65 66 67 68 69 70	71 72	78 79 80
VOLTS →	0.0	0.225	0.275	0.295	0.315	0.335	0.350	0.365	0.38[illegible]	01	
CURRENT →	0.1257	0.1245	0.1241	0.124	0.1237	0.1231	0.1229	0.1222	0.121[illegible]	0[illegible]	
	0.390	0.400	0.410	0.420	0.430	0.440	0.450	0.460	0.470	0[illegible]	
	0.1204	0.1194	0.1180	0.1167	0.1149	0.1129	0.1101	0.1066	0.10[illegible]	04	
	0.480	0.490	0.500	0.510	0.520	0.551	0.577	0.603	1.0	0[illegible]	
	0.0974	0.0917	0.0850	0.0765	0.0655	0.020	0.0	-0.030	-0.030	[illegible]	

Figure I-7. Format for a Typical Single-Argument Stint Table and Header Card

HEADER CARD

COLS.1-8 10-24-68 (TBL. DATE) COLS.9-12 0015 (TBL. NO.) COLS.13-14 09 (L1) COLS.15-16 [illegible] (L2) COLS.71-72 00 (SN)

→COL.20: STORAGE CELL VOLTS VS AMPS VS SOC
35 DEG.C,BOL

FIELD 1 INTEGER • EXP	FIELD 2 • INTEGER • EXP	FIELD 3 • INTEGER • EXP	FIELD 4 • INTEGER • EXP	FIELD 5 • INTEGER • EXP	FIELD 6 • INTEGER • EXP	FIELD 7 • INTEGER • EXP	FIELD 8 • INTEGER • EXP	FIELD 9 • INTEGER • EXP	FIELD 10 • INTEGER • EXP	SEQ NO.	PROGRAM DECK NO.
2 3 4 5 6 7	8 9 10 11 12 13 14	15 16 17 18 19 20 21	22 23 24 25 26 27 28	29 30 31 32 33 34 35	36 37 38 39 40 41 42	43 44 45 46 47 48 49	50 51 52 53 54 55 56	57 58 59 60 61 62 63	64 65 66 67 68 69 70	71 72	78 79 80
SOC →	0.10	0.80	0.8[illegible]	0.55	0.90	0.95	1.0	1.05	1.80		
100.0	1.1	1.2[illegible]	1.21[illegible]	1.220	[illegible]	1.259	1.3[illegible]	1.330	1.[illegible]		
16.[illegible]	1.1	1.217	1.218	1.22[illegible]	1.2[illegible]	1.[illegible]	1.33[illegible]	[illegible]	[illegible]	[illegible]	
8.0	1.13	1.235	1.22[illegible]	1.239	1.[illegible]	1.28[illegible]	1.360	1.36[illegible]	[illegible]	[illegible]	
0.001	1.13	1.235	1.239	1.239	1.2[illegible]	[illegible]	1.360	1.36[illegible]		[illegible]	
.0	1.15	1.237	[illegible]	[illegible]	1.2[illegible]	1.30	1.361	1.361	1.361	[illegible]	
.001	1.18	1.238	1.25[illegible]	1.2[illegible]	1.300	1.315	1.362	1.362	[illegible]	[illegible]	
.800	1.2	1.240	1.270	1.283	1.3[illegible]	1.345	1.364	1.364	1.2[illegible]	[illegible]	
.0	1.21	1.245	1.283	1.309	1.34[illegible]	1.373	1.40	1.425	1.425	[illegible]	
.0	1.215	1.250	1.306	1.329	1.3[illegible]	1.40[illegible]	1.4[illegible]	1.450	1.450	[illegible]	
8.0	1.22	1.255	1.325	1.350	1.35[illegible]	1.420	1.455	1.480	1.[illegible]	[illegible]	
0.0	1.22	1.255	1.325	1.350	1.3[illegible]	1.420	1.455	1.4[illegible]	1.[illegible]	[illegible]	
CURRENT											

Figure I-8. Format for a Typical Two-Argument Stint Table and Header Card

NCODE

Following the Run Label Card are the 50 NCODE cards. The card number, or NCODE, is right-justified against Col. 3. The numerical value of the NCODE variable is left-justified against Col. 5 and must have a decimal point. Table 1 shows the NCODE names, the NCODE numbers, the NCODE values and a brief description of each NCODE for a sample computer run. Only the NCODE (item) number and its numerical value are punched on the NCODE cards; the other data in Table 1 is for information only. All 50 of the NCODES are initially loaded into memory, thus a single run or the first of a series of chained runs must contain all the NCODES in the data deck. Most of the NCODE descriptions in Table I-2 are self-explanatory, but a few are described below:

a. C/D RATIO (NCODE 8) (typical value is 1.11). This NCODE is needed only when simulating operation of an ampere-hour controlled PMPT System, and reduces battery charge current to 0.6 amps when the prescribed C/D ratio has been achieved.

b. NPKLD (NCODE 20) (the value is a table location in STINT). This NCODE defines the table number which contains the peak load power profile. This is a separate load taken from the unregulated bus.

c. SYSTEM KEY (NCODE 25). This NCODE tells the computer to simulate a series max power tracker (-1.0), a Nimbus-B system (0.0), or a parallel max power tracker (1.0). If this card is omitted from the data deck, the Nimbus B system will be simulated. This NCODE is called PMPT in the MAIN program coding.

d. NEND (NCODE 27). This NCODE, when set to 1.0, tells the computer this is the last run. When chaining runs this NCODE must be set to 0.0 and then set to 1.0 in the last run.

e. NDGRAD (NCODE 31). This NCODE must be set to 1.0 in the first run. This causes the machine to automatically degrade the solar cell and expand it for temperature as specified by the degradation and temperature parameters in the NCODES. When chaining additional runs, if the degradations are not changed, NDGRAD should be set to 0.0. By setting NDGRAD to 0.0 needless repetitive computations in the solar cell subroutine (STASH) are eliminated.

f. PTEFF (NCODE 47) (typical value 92.0). This NCODE defines the power transfer efficiency, in percent, of the two types of max power trackers. It can be omitted when simulating Nimbus B operation.

TABLE I-2. NCODE NAMES, NUMBERS, TYPICAL VALUES AND DESCRIPTION

WRITE ITEM DESCRIPTIONS ACROSS	ITEM NO.	VARIABLE	RUN COMMENTS OR VARIABLE DESCRIPTION
TN	1	35.0	NIGHT TIME (MINUTES)
TO	2	108.0	ORBIT TIME (MINUTES)
ΔT	3	1.0	DELTA TIME (MINUTES) BETWEEN CALCULATIONS
VBMAX	4	33.5	MAXIMUM BATTERY VOLTAGE (VOLTS)
IBMAX	5	8.8	MAXIMUM BATTERY CURRENT (AMPS)
DZCRR	6	0.95	DEAD ZONE IN CHARGE RATE REGULATOR (VOLTS)
VKCRR	7	1.4	KNEE VOLTAGE, CHARGE RATE REGULATOR (VOLTS)
CTOD	8	1.11	CHARGE TO DISCHARGE RATIO
TVSR	9	38.0	TRIGGER VOLTAGE, SHUNT REGULATOR (VOLTS)
ERSR	10	0.012	EQUIVALENT RESISTANCE OF SHUNT REG. (OHMS)
PLN	11	0.0	CONSTANT NIGHT LOAD (WATTS)
PLD	12	0.0	CONSTANT DAY LOAD (WATTS)
VDIODE	13	0.5	BATTERY DIODE DROP (VOLTS)
BAMMAX	14	2160.0	BATTERY MAX. AMP. MINUTE CAPACITY (A-M)
ETA	15	0.0	PANEL NORMAL TO SUN VECTOR ANGLE
NSLT	16	2	NO. OF SYSTEM POWER LOSS TABLE
NBMINT	17	12	NO. OF BATTERY TABLE, MIN. TEMP.
NBMAXT	18	12	NO. OF BATTERY TABLE, MAX. TEMP.
NCELLT	19	5	NO. OF TABLE WITH SOLAR CELL DATA
NPKLD	20	10	NO. OF TABLE WITH PEAK LOAD POWER PROFILE
NPWM	21	25	NO. OF TABLE WITH PWM REGULATOR LOAD
NINV	22	29	NO. OF INVERTER LOAD TABLE
NCNV	23	30	NO. OF CONVERTER LOAD TABLE
NSER	24	1	NO. OF SERIES REGULATOR LOAD TABLE

TABLE I-2. NCODE NAMES, NUMBERS, TYPICAL VALUES AND DESCRIPTION (Continued)

NO.	WRITE ITEM DESCRIPTIONS ACROSS	ITEM NO.	VARIABLE		RUN COMMENTS OR VARIABLE DESCRIPTION
	SYSTEM KEY	25	0.0		SYSTEM KEY (-1.0=SNPT, 0.0=NB, 1.0=PMPT)
	NPRINT	26	2.0		INCREMENT BETWEEN CALC. WHICH OUTPUT IS PRINTED
	NEND	27	1.0		END OF RUNS KEY (1.0 OR 0.0)
	EFFINV	28	85.0		POWER TRANSFER EFF. OF THE INVERTER (%)
	EFFCNV	29	90.0		POWER TRANSFER EFF. OF THE CONVERTER (%)
	NBTEMP	30	3		NO. OF TABLE WITH BATTERY TEMP.
	NDGRAD	31	1		AUTOMATIC DEGRADATION OF ARRAY
	SIGISC	32	0.00007		AMP./DEG.C. TEMP. DEGRADATION OF CELL CURVE
	SIGVOC	33	0.0022		VOLTS/DEG.C. TEMP. DEGRADATION OF CELL CURVE
	DI1	34	95.0		CURRENT DEGRADATION (%)
	DI2	35	96.5		CURRENT DEGRADATION (%)
	DI3	36	97.0		CURRENT DEGRADATION (%)
	DI4	37	100.0		CURRENT DEGRADATION (%)
	DV1	38	99.0		VOLTAGE DEGRADATION (%)
	DV2	39	100.0		VOLTAGE DEGRADATION (%)
	AVPMO	40	0.47		MAX. PWR. POINT VOLTAGE (UNDEGRADED CELL) (VOLTS)
	AIPMO	41	0.1289		MAX. PWR. POINT CURRENT (UNDEGRADED CELL) (AMPS)
	AVOCO	42	0.59		OPEN CIRCUIT VOLTAGE OF UNDEGRADED CELL (VOLTS)
	THETA	43	100.0		VOLTAGE MEASUREMENT TOLERANCE (%)
	TNOT	44	28.0		CELL DATA TEST TEMP (DEG. C)
	NO. OF CELLS/BATT	45	23		NUMBER OF CELLS PER BATTERY
	ADIODE	46	1.8		ARRAY DIODE DROP
	PTEFF	47	92.0		POWER TRANSFER EFF. PARALLEL TRACKER UNIT (%)
	DELTT	48	10.0		Δ TEMP. BETWEEN STEPS IN STASH ROUTINE

TABLE I-2. NCODE NAMES, NUMBERS, TYPICAL VALUES AND DESCRIPTION (Continued)

NO.	WRITE ITEM DESCRIPTIONS ACROSS	ITEM NO.	VARIABLE		RUN COMMENTS OR VARIABLE DESCRIPTION
	ADDT	49	32.0		A TEMP. BETWEEN TNOT AND MAX. TEMP. OF INTEREST
	DENFAC	50	0.065		0.065 FOR 1 OHM-CM, 0.0 FOR 10 OHM-CM

Array Signal Card

Immediately following NCODE 50 card must be a card containing 999 in columns 1-3. This card tells the computer that solar array information is to follow.

NPANEL Card

Following the Array Signal Card is the NPANEL card, which contains the number (NPANEL) of solar panels in the array (maximum number of panels is 25). This number must appear right-justified in columns 1-3; no decimal point is required.

Panel Description Cards

Following the NPANEL card is a panel description card for each solar panel in the array, up to a maximum of 25 panels. The number of these cards must agree with the value of NPANEL. Each card contains four fields of ten columns each, in floating point format (requires decimal point).

Columns	Variable	Typical Value
1-10	No. of Series Solar Cells per String	94.0
11-20	No. of Parallel Strings per Panel	36 0
21-30	Solar Incidence Angle (degrees)	0.0
31-40	Panel Temperature vs Time Table Location in STINT	11.0

Following the Panel Description Cards is a blank card. This tells the computer to stop reading in data and to start computing. If it is desired to chain an additional run, a new Run Label Card and only those NCODES and Panel Description Cards that contain changed or new information should be placed after the blank card. In addition, NCODE 27 must be set to 0.0 for all except the last run, when it must have a value of 1.0. As many runs as are desired can be chained in this manner, ensuring that each new run starts with a Run Label Card and ends with a blank card. Refer again to Figure I-6 for the proper sequence of card positions for chained runs.

As indicated in Figure I-6, computer control cards are required in front of the Program Deck, in front of the Date Card, and behind the last blank card at the end of the Data Deck. The particular control cards needed vary from computer to computer, and are sometimes different for identical machines at two separate facilities.

3. Output Data

The information that the computer equipment prints out after an energy balance run consists of the following items.

a. STINT Table Summary

The STINT table number, the date on the STINT table header card and the title of the tabulated data as it appears on the header card are listed for each table stored in STINT.

b. Input Data Page

Run number and date
Run comments (as specified on input card)
Listing of NCODE numbers, names and values
Solar Array description: panel number, number of series solar cells, number of parallel solar cell strings, solar illumination incidence angle and number of STINT table which contains the array temperature-time profile.

c. Subroutine STASH Printout

Values of temperature for which the degraded solar cell I-V curve has been prepared are listed in a row across the page.

Values of degraded solar-cell maximum-power voltage and current, open-circuit voltage and short-circuit current appear in columns under each temperature.

Values of every other calculated current and voltage pair comprising the I-V curve and stored in the computer memory, are listed in columns under each temperature.

d. Power Subsystem Data

The names of the calculated power system parameters are listed in a row across the top of the page: orbit time at which the calculation was made (TIME), number of ampere-minutes in the battery (ACCUM), relative state of charge of the battery (STATE), output voltage of the series tracker unit in the SMPT system (VTO), unregulated bus voltage during satellite night or solar array bus voltage during satellite day VU (Night), VAB (DAY), solar array current (1A), solar array power at the operating point (PA), solar array maximum power (PMAX), battery voltage (VB), battery current (1B), load current including system losses (IL), shunt dissipator current (ISD), peak load current (IPKLD), and solar array temperature (TEMP).

e. Battery Data Summary

The depth of discharge, in percent, of capacity at beginning of run, the ampere-minute C/D ratio actually achieved during the run, the charge energy into the battery during the run in watt-minutes, the discharge energy out of the battery during the run in watt-minutes, and the orbit-average power dissipated in the battery during the run in watts.

If several runs are made at one time, the output data for each run is printed out in the same format as for the first run, except that only changed values of NCODES are printed out on the input data page, and subroutine STASH printout will not appear if the same solar cell I-V curve and degradation factors as in the previous run are used.

D. ENERGY BALANCE CALCULATIONS

At the start of an energy balance computer run, the values of the NCODES and other internally-used system parameters are initialized. The data deck is then read in: STINT table data is stored in the computer memory, the NCODES for the new run are read in, updating the initialized values, and the solar array configuration, sun angles and temperature profile are defined from the panel description cards. This preliminary effort is done by MAIN, from the beginning of the routine through instruction 105.

1. Solar Cell Data

After the initialization described above, subroutine STASH obtains the user-supplied solar cell I-V curve from STINT and degrades the curve with the current, voltage and series resistance factors specified in the NCODES. This degraded I-V curve is then corrected for temperature effects and finally 15 I-V curves are stored in memory at 15 different temperature values, over the temperature range (TNOT + ADDT) to (TNOT + ADDT -15 × DELTT), as specified by the NCODES. STASH will interpolate between the 15 stored I-V curves when called upon by MAIN or subroutine AMPS for particular solar cell data.

A more detailed discussion of how the solar cell I-V curve is manipulated can be found in Ref. (2).

2. Spacecraft Nighttime Calculations

Energy balance calculations for spacecraft nighttime are made in MAIN, from instructions 106 through 3005. Since all three system configurations (NB, PMPT and SMPT) operate in the same manner during solar array eclipse periods, the same set of instructions in the computer is used for all three systems during the nighttime duration, TN.

Initialized parameters for the nighttime caluclations are: orbit time (T) = 0, ampere-minutes out of battery (TOTOUT) = 0, energy out of battery (EOUT) = 0, battery state of charge (SOC) = 1.0, and ampere-minutes presently in battery (ACCUM) is set equal to the value of BAMMAX. The orbit time counter in the computer now begins to advance at the specified time increment DELTAT. The nighttime portion of the orbit (TN minutes duration) comes first, with the following computations being made at each DELTAT time increment.

Step 1. Increment T = T + DELTAT. If new T is greater than TN, nighttime calculations are completed; if not, continue with Step 2.

Step 2. Battery cell discharge voltage VDDCH is looked up at SOC and at a discharge current IB = 0.001 ampere.

Step 3. Unregulated bus voltage VA and battery voltage VB is calculated: VA = VBDCH × FUDGE - VDIODE and VB = VBDCH × FUDGE.

Step 4. The total regulated bus load watts, PWM, at time T are looked up in the STINT table by subroutine DRAIN, peak load watts PKLD are obtained from STINT and total load current ILT and peak load current IPKLD are determined: ILT = (PWM + SL)/VA and IPKLD = PKLD/VA, where SL is system loss watts. (Note that DRAIN will compute ILT from converter, inverter and series dissipative regulator loads also, if these are specified).

Step 5. Battery table reentered at SOC and at IB = -ILT-IPKLD to obtain VBDCH at new discharge current; new VA is calculated from new VBDCH.

---

(2) Harmon, H. and Rasmussen, R., "Temperature, Illumination Intensity and Degradation Factor Effects on Solar Cell Output Characteristics", presented at the IEEE Aerospace and Electronic Systems Conference, Seattle, Wash., July, 1966.

Step 6. New value of ILT and IPKLD determined with new VA.

Step 7. Compare new ILT and IPKLD with IB from Step 5. If difference is less than 10 mA, go to Step 8; if not, go to Step 5.

Step 8. Ampere-minutes out of battery during time period DELTAT is computed: AMPMIN = IB × DELTAT.

Step 9. Compute ampere-minutes remaining in battery: ACCUM = ACCUM + AMPMIN.

Step 10. Compute new state of charge: SOC = ACCUM/BAMMAX.

Step 11. Increment amp-minutes removed from battery: TOTOUT = TOTOUT + AMPMIN.

Step 12. Increment energy removed from battery: EOUT = EOUT + (AMPMIN) × (VB).

Step 13. Compere T with TN. If they are the same, calculate depth of discharge: DEPTH = (1.0 - SOC) × 100, and return to Step 1; if T and TN have different values, go to Step 1.

When, in Step 1, T is greater than TN, the spacecraft has emerged into sunlight, the solar array is illuminated, and a much more complicated set of computations must be made at each time increment.

3. Spacecraft Daytime Calculations

Energy balance calculations for spacecraft daytime (solar array is illuminated and orbit time T is greater than TN) are made in MAIN, with a different set of computer instructions used for each of the three system configurations.

Before the daytime calculations are begun, the value of equivalent charge controller resistance is calculated: RCRR = (VKCRR-DZCRR)/IBMAX. Instructions 130 through 806 are common to all three systems and are executed at each time increment during the daytime before the energy balance computations are started; the solar array maximum power PMAX at the orbit time T is calculated. The values of total ampere-minutes into the battery TOTIN and total energy into the battery EIN are set to 0.0 before the daytime computation begins.

a. Nimbus B (NB) Daytime Energy Balance Calculations

The NB system uses the 900 series of instructions in MAIN for daytime energy balance calculations.

Step 1. Increment time T = T + DELTAT. If T > TO, run is complete; if not, continue to Step 2.

Step 2. Storage cell voltage VBO is looked up at SOC and IB = 0.0. Battery voltage is defined as VB = VBO × FUDGE and solar array bus voltage is initially defined as VAB = VB.

Step 3. Load current and peakload current ILT and IPKLD are determined as in the nighttime calculations. Subroutine AMPS is entered with VAB and the resulting solar array current IA is obtained. The value of battery current is now checked: IB = IA-ILT-IPKLD.

Step 4. If IB from Step 3 is negative, cell discharge voltage VBDCH at IB and SOC is looked up. VB and VAB are defined as in Step 2; IA, ILT and IPKLD are found at the new VAB as in Step 3, and the final value of battery current is determined: IB = IA-ILT-IPKLD. Solar Array operating power is defined: PA = IA × (VAB + ADIODE). Battery parameters are updated: AMPMIN = IB × DELTAT

ACCUM = ACCUM + AMPMIN

SOC = ACCUM/BAMMAX

EOUT = EOUT + AMPMIN × VB

TOTOUT = TOTOUT + AMPMIN

Return to Step 1 to begin calculations at the next time increment in the orbit.

Step 5. If IB from Step 3 is positive, IB is set equal to IBMAX, cell voltage VBM is found at SOC and IBMAX, battery voltage is set to VB = VBM × FUDGE and solar array bus voltage is set to VAB = VB + DZCRR + IB × RCRR. Subroutine DRAIN is called to get ILT at VAB, IPKLD is again calculated from IPKLD = PKLD/(VAB-VDIODE), and subroutine AMPS yields the value of IA at VAB. Battery current is redefined as IB = IA - ILT - IPKLD. IB is compared with IBMAX:

(a) If IB > IBMAX, a voltage increment is defined: DELTAV = 0.1. Solar array bus voltage is set to VAB = TVSR + DELTAV. A new IA is obtained from AMPS at VAB, and new values of ILT and IPKLD are found. Battery current is then checked: IB = IA - ILT - IPKLD (note that ILT now contains some value of shunt dissipator current, ISD = ILT - IL). If IB is still greater than IBMAX, DELTAV = DELTAV/2.0

and VAB = VAB + DELTAV (VAB is now equal to TVSR + 0.1 + 0.05). System currents are again evaluated, and a new DELTAV is added to VAB in order to further increase ISD and reduce IB if IB still exceeds IBMAX. A maximum of 10 iterations is allowed in this manner to zero—in on the values of system currents.

(b) If IB < IBMAX, solar array bus voltage is set to VAB = VBO × FUDGE + DZCRR. ILT, IPKLD and IA are found at this value of VAB, and then IB is determined as IB = IA - ILT- IPKLD. Cell voltage VB is found at SOC and this value of IB, and VAB is now VAB = VB × FUDGE + DZCRR + IB × RCRR. Load currents and IA are found at the new VAB and a new battery current is defined: IBN = IA - ILT- IPKLD. If IBN is within 10 mA of IB, the error is deemed small enough; if IBN is not within 10 mA of IB, IB is set equal to IBN, a new cell voltage is looked up, a new set of load currents are found and the next value for IBN is arrived at. Eventually the small error criterion is met, and the next check is made as in Step 6 below.

Step 6. Finally, when a permissible value of IB is found, the resulting battery voltage VB is compared with the maximum battery voltage VBMAX, which is user-specified in an NCODE. If the calculated value of VB exceeds VBMAX, the computer moves the system operating voltage out along the solar array I-V curve just as in Step 5 a, obtaining less input power from the array, and consequently less charge current until finally both the currents and voltages are compatible with acceptable small errors and maximum limits.

Step 7. Battery parameters are updated:

AMPMIN = IB × DELTAT

ACCUM = ACCUM + AMPMIN

EIN = EIN + AMPMIN × VB

SOC = ACCUM/BAMMAX

TOTIN = TOTIN + AMPMIN

Solar array operating power is defined: PA = IA × (VAB + ADIODE), and shunt dissipator current (if any) is defined:

ISD = ILT - IL (actually DRAIN computes ISD as (VAB-TVSR)/ERSR). All system parameters are sent to subroutine PRINT. Orbit time is again incremented in Step 1: if T < TO, Step 2, etc., are repeated. If T > TO, go to Step 8.

Step 8. C/D ratio is calculated: RATIO = TOTIN/TOTOUT. Orbit average power dissipated in the battery is calculated: PD = (EIN + EOUT)/TO. The energy balance run for the NB system is now complete.

b. Parallel Maximum Power Tracker (PMPT) Daytime Energy Balance Calculations

The PMPT system uses the 600 series of instructions in MAIN for daytime energy balance calculations. Another parameter is also used with this system and is computed at each time increment: RATIO = TOTIN/TOTOUT. TVSR is set to 1000 volts to avoid unintentional use of a shunt dissipator in this system, which can operate at a solar array bus voltage up to 80 volts or greater. Refer to Figure I-1 for the PMPT system block diagram.

Step 1. Unregulated bus voltage is defined as the previously-calculated solar array maximum-power voltage minus the array diode drop, VU = AVMPSA-ADIODE, and solar array current is set equal to the current found earlier at the maximum power point, IA = IAM. Total load current ILT is found by DRAIN, and this value is compared with the array current.

Step 2. If (IA - ILT) from Step 1 is negative, battery discharge power is needed to support the load. Cell discharge voltage VBD is looked up by STINT at SOC and at IB = -1.0 ampere. Unregulated bus voltage is calculated VU = VBD × FUDGE - VDIODE. Solar array current IA is found at VU, as well as ILT and IPKLD. Total value of battery discharge is calculated: IB = IA - ILT- IPKLD, solar array operating power is determined, PA = (VU + ADIODE) × IA, and the battery parameters are updated just as in Step 4 of the NB daytime calculations, except RATIO is also calculated. Orbit time is incremented and Step 1 above is repeated.

Step 3. If (IA - ILT) from Step 1 is positive, the value of RATIO is compared with the user-specified CTOD; if RATIO is greater, the battery has reached a full state of charge and a limit value of charge current is set: ILIM = 0.6A. If RATIO is less than CTOD, ILIM = IBMAX.

Step 4. The parallel tracker unit output power is calculated: PTO = VU × (IA - ILT) × PTEFF. Battery voltage at SOC and 0.0 amps is calculated and an initial value of charge current is found: IB = (PTO/VB) - PKLD/(VB-VDIODE). Note that this value of IB will be high since a low VB (open-circuit voltage) was assumed.

Step 5. If IB from Step 4 is negative (this can occur only if a high peak load exists), a cell discharge voltage VBD at SOC and IB = -1.0A is looked up, a battery voltage defined as VB = VBD × FUDGE, and a final value of battery discharge current is determined: IB = PTO/VB - PKLD/(VB-VDIODE). The other system parameters are defined: VA = VU, PA = (VA + ADIODE) × IA, the battery parameters are updated (SOC, AMPMIN, ACCUM, TOTOUT, EOUT and RATIO), time is incremented again and calculations in Step 1 begun again.

Step 6. If IB from Step 4 is positive, it is compared with the value of ILIM. If IB is greater than ILIM, battery voltage VB is found at SOC and at IB = ILIM and IB is redefined: IB = PTO/VB - PKLD/(VB-VDIODE). If IB is still greater than ILIM, a new operating voltage is specified: VU = VU + 0.1. IA is found by AMPS at the new VU, DRAIN supplies the new value of ILT and Step 3 is repeated. Eventually, the increasing value of VU will reduce the available IB below ILIM. Battery voltage is found at the new value of IB, and now another value of IB is obtained from VB: IB = PTO/VB - PKLD/(VB-VDIODE). This value of IB is now compared with ILIM: if IB is greater, VU is again incremented, further reducing IB. If IB is less than ILIM, the last value of VB is compared with VBMAX.

Step 7. If VB is greater than the maximum permissible VBMAX, VU is incremented just as it was when IB was too great. Charge current is further reduced at the higher operating voltage and eventually the VBMAX limit will not be exceeded. At this time the battery parameters (AMPMIN, RATIO, EIN, TOTIN, ACCUM and SOC) are updated, array operating power is calculated and the values of all system parameters sent to PRINT and orbit time is again incremented.

Step 8. If orbit time T is less than or equal to TO, Step 1 is repeated; if time T is greater than orbit duration TO, the actual C/D ratio achieved is calculated: RATIO = TOTIN/TOTOUT, battery power dissipated as heat is calculated: PD = (EIN + EOUT)/TO and the energy balance run is complete.

An additional feature of the PMPT coding instructions is that when a final system operating point has been determined from energy balance considerations, a check is made to see if the unregulated bus voltage VU is at least one volt greater than the battery voltage, during system charge. This check is necessary since an operating point is assumed at the maximum-power voltage, which conceivable could be even less than battery voltage for an unusual combination of high array temperature, low battery temperature and a severe solar array voltage degradation. If VU is too low, the computer will increment VU = VU + 0.1 until a satisfactory operating point is reached, and an error message will be printed out at the completion of the run.

c. Series Maximum Power Tracker (SMPT) Daytime Energy Balance Calculations

The SMPT system uses the 700 series of instructions in MAIN for daytime energy balance calculations. As seen in the system block diagram of Figure I-1, the operation of the SMPT system is identical to that of the NB system after the series tracker unit has processed the solar array power.

Step 1. Tracker output power is calculated as PTO = IA × VAB × PTEFF, with operation assumed at the array maximum power point (IA = IAM and VAB = AVMPSA - ADIODE). Battery open-circuit voltage is found, ILT is calculated by DRAIN, and a first value of IB is found:

IB = PTO/VB - PKLD/(VB - VDIODE) - ILT.

Step 2. If IB is negative, battery voltage is found at IB = -1.0A and at SOC, DRAIN supplies a new ILT at the lower VB, and a refined value of IB is calculated as in Step 1. Battery parameters are updated, and calculation at the next time increment is begun in Step 1 after the values of system parameters have been sent to PRINT.

Step 3. If IB from Step 1 is positive, IB is set to equal IBMAX, VB is found at this IB and tracker output voltage is initially defined as VTO = VB + VKCRR. ILT is found at VTO by DRAIN, and a value of IB is determined:

IB = PTO/VTO - ILT - PKLD/(VTO-VDIODE).

Step 4. If IB from Step 3 is greater than IBMAX, system operating voltage on the array is incremented VAB = VAB + 0.1, a new IA is obtained from AMPS, and Step 1 is executed again. Eventually IB will be less than IBMAX.

Step 5. If IB from Step 3 is less than IBMAX, or after Step 4 when IB is less than IBMAX, a maximum of 10 iterations is started to find the proper value of IB: charge controller resistance is calculated as RCRR = (VKCRR - DZCRR)/IBMAX and tracker output voltage is initially set at VTO = VBO + DZCRR, where VBO is battery open-circuit voltage. ILT is found by DRAIN at VTO, and a value of IB is calculated: IB = PTO/VTO - ILT - PKLD/(VTO-VDIODE). STINT is called to find VB at the value of IB, and then VTO is redefined: VTO = VB + DZCRR + IB × RCRR. ILT is found at the new VTO and then a new value if IB is found:

IBN = PTO/VTO - ILT - PKLD/(VTO-VDIODE).

Step 6. If the value of IBN is within 10 mA of the previous IB, the error is deemed small enough; if not, IB is set equal to IBN and the steps in 5 are repeated, up to a maximum of 10 times, each time replacing IB with IBN and allowing the operating point to be determined with very little error.

Step 7. After IB from Step 6 has been determined, the resulting battery voltage VB is compared with VBMAX. If VB is greater than the user-specified VBMAX, the array voltage is incremented VAB = VAB + 0.1, as in Step 4, until the available power at the higher VAB produces a low enough value of IB such that VBMAX is not exceeded.

Step 8. System operating voltage is checked, just as with the PMPT system, to ensure that VAB is greater than VB by at least 1.0 volt. When this criterion is satisfied, battery parameters (SOC, AMPMIN, TOTIN, EIN, ACCUM) are updated, solar array power is calculated: PA = IA × (VAB + ADIODE), and Step 1 is repeated for the next time increment. If T > TO, RATIO and PD are calculated as with the other two systems, and the energy balance run is completed.

APPENDIX II

SYSTEM AND COMPONENT DATA

TABLES AND FIGURES

TABLE II-1. PARAMETERS USED IN ENERGY BALANCE EQUATIONS

Symbol	Definition	Value
C/D	Ampere-minute charge to discharge ratio	1.11
E_A	F-3 solar array output energy (W-Min)	40,000 (F-3)
		73,600 (Bifold)
E_D+SR	SA blocking diodes and slip rings energy (W-min)	1,750
e_c	Power transfer efficiency of DC-DC converter	0.85
e_{DR}	Power transfer efficiency of PWM discharge voltage regulator	0.9
e_R	Power transfer efficiency of PWM voltage regulator	0.9
e_T	Power transfer efficiency of max power tracker	0.9
I_A	Daytime average solar array current (Amps)	13.5 (NB)
P_A	Solar array output power at operating point (W)	400 W F-3
P_M	Solar array output power at max power point (W)	500 W 50°C
P_L	Orbit average steady-state load power (W)	
P_{SL}	Orbit average shunt loss power (W)	23 W (F-3)
		30 W (Bifold)
ΔP	Power supplied to peak load (W)	400 W
TD	Orbit daytime duration (minutes)	73
TN	Orbit nighttime duration (minutes)	35
TP	Peak load duration, one per orbit (minutes)	5
V_{BC}	Average battery charge voltage (Volts)	32.9
V_{BD}	Average battery discharge voltage (Volts)	30.0
V_{BM}	Maximum battery charge voltage (Volts)	34.0
V_{CC}	Charge controller voltage drop (Volts)	1.4
V_R	Regulated bus voltage (Volts)	24.5

TABLE II-2. PPFT SYSTEM DESIGN FACTORS FOR COMPUTER (1 of 3)

	Nominal Case			Worst Case				Best Case	
Months in Orbit	0	3, 6	12,24	0	3, 6	12	24	0, 3, 6	12, 24
Batt Temp (°C)	25			35				15	
No. of Batts	3			2				3	
No. of Cells/Batt	24			24				24	
Sys Storage Cap. (A-H)	36			24				36	
Required C/D Ratio	1.11			1.19				1.06	
Batt Volt. Limit (V)	35.0			34.5				35.4	
Chg Current Limit (A)	18.0 (Total)			12.0 (Total)				18.0 (Total)	
Chg Cont Dead Zone (V)	—			—				—	
Chg Cont Knee Volt. (V)	—			—				—	
Shunt Diss Turn-On (V)	—			—				—	
Constant Loss Day (W)	—			—				—	
Nite (W)	—			—				—	
Solar Cell dI/dT (μA/°C)	70	70	140	70	70	140	140	70	140
dV/dT (mV/°C)	-2.2	-2.2	-2.4	-2.2	-2.2	-2.4	-2.4	-2.2	-2.4
Glassing Loss (%)	95.0			95.0				95.0	
Solar Intensity (%)	100.0			96.5				103.5	
Prediction Error (%)	100.0			96.0				104.0	
UV & Cycling Loss (%)	100.0	97.0	97.0	100.0	95.0	95.0	92.0	100.0	
Series Res Effect (%)	99.0			99.0				99.0	
Voc Error (%)	100.0			99.0				101.0	
Tracker Unit Eff (%)	92.0			90.0				92.0	
SA Series Cells	102			102				102	
Parallel Cells	102			102				102	
Dischg Diode Loss (V)	0.5			0.5				0.5	
Array Diode & SR Loss (V)	1.8			1.8				1.8	

Note: Blank Space Indicates No Change in Parameter Value

TABLE II-2. STS SYSTEM DESIGN FACTORS FOR COMPUTER (2 of 3)

	Nominal Case			Worst Case				Best Case	
Months in Orbit	0	3, 6	12,24	0	3, 6	12	24	0, 3, 6	12, 24
Batt Temp (°C)	25			35				15	
No. of Batts	8			7				8	
No. of Cells/Batt	23			23				23	
Sys Storage Cap. (A-H)	36			31.5				36	
Required C/D Ratio	1.11			1.19				1.06	
Batt Volt. Limit (V)	33.5			33.05				33.95	
Chg Current Limit (A)	18.0 (Total)			15.75 (Total)				18.0 (Total)	
Chg Cont Dead Zone (V)	0.95			0.95				0.95	
Chg Cont Knee Volt. (V)	1.70			1.70				1.70	
Shunt Diss Turn-On (V)	—			—				---	
Constant Loss Day (W)	15.0			15.0				15.0	
Nite (W)	6.0			6.0				6.0	
Solar Cell dI/dT (μA/°C)	70	70	140	70	70	140	140	70	140
dV/dT (mV/°C)	-2.2	-2.2	-2.4	-2.2	-2.2	-2.4	-2.4	-2.2	-2.4
Glassing Loss (%)	95.0			95.0				95.0	
Solar Intensity (%)	100.0			96.5				103.5	
Prediction Error (%)	100.0			96.0				104.0	
UV & Cycling Loss (%)	100.0	97.0	97.0	100.0	95.0	95.0	92.0	100.0	
Series Res Effect (%)	99.0			99.0				99.0	
Voc Error (%)	100.0			99.0				101.0	
Tracker Unit Eff (%)	90.0			88.0				90.0	
SA Series Cells	102			102				102	
Parallel Cells	102			102				102	
Dischg Diode Loss (V)	0.5			0.5				0.5	
Array Diode, SR Loss (V)	1.8			1.8				1.8	

Note: Blank Space Indicates No Change in Parameter Value

TABLE II-2. NB SYSTEM DESIGN FACTORS FOR COMPUTER (3 of 3)

Month in Orbit	Nominal Case 0	3, 6	12,24	Worst Case 0	3, 6	12	24	Best Case 0, 3, 6	12, 24
Batt Temp (°C)	25			35				15	
No. of Batts	8			7				8	
No. of Cells/Batt	23			23				23	
Sys Storage Cap. (A-H)	36.0			31.5				36.0	
Required C/D Ratio	1.11			1.19				1.06	
Batt Volt. Limit (V)	33.5			33.05				33.95	
Chg Current Limit (A)	8.8 (Total)			7.7 (Total)				8.8 (Total)	
Chg Cont Dead Zone (V)	0.95			0.95				0.95	
Chg Cont Knee Volt. (V)	1.40			1.40				1.40	
Shunt Diss. Turn-On (V)	38.0			38.0				38.0	
Shunt Diss Res (Ω)	0.012			0.012				0.	
Constant Loss Day (W)	—			—					
Nite (W)	—			—					
Solar Cell dI/dT (μA/°C)	70	70	140	70	70	140	140	70	10
dV/dT (mV/°C)	-2.2	-2.2	-2.4	-2.2	-2.2	-2.4	-2.4	-2.2	-2.4
Glassing Loss (%)	95.0			95.0				95.0	
Solar Intensity (%)	100.0			96.5				103.5	
Prediction Error (%)	100.0			96.0				104.0	
UV & Cycling Loss (%)	100.0	97.0	97.0	100.0	95.0	95.0	92.0	100.0	
Series Res Effect (%)	99.0			99.0				99.0	
Voc Error (%)	100.0			99.0				101.0	
SA Series Cells	94			94				94	
Parallel Cells	108			108				108	
Discharge Diode Loss (V)	0.5			0.5				0.5	
Array Diode, SR Loss (V)	1.8			1.8				1.8	

Note: Blank Space Indicates No Change in Parameter Value

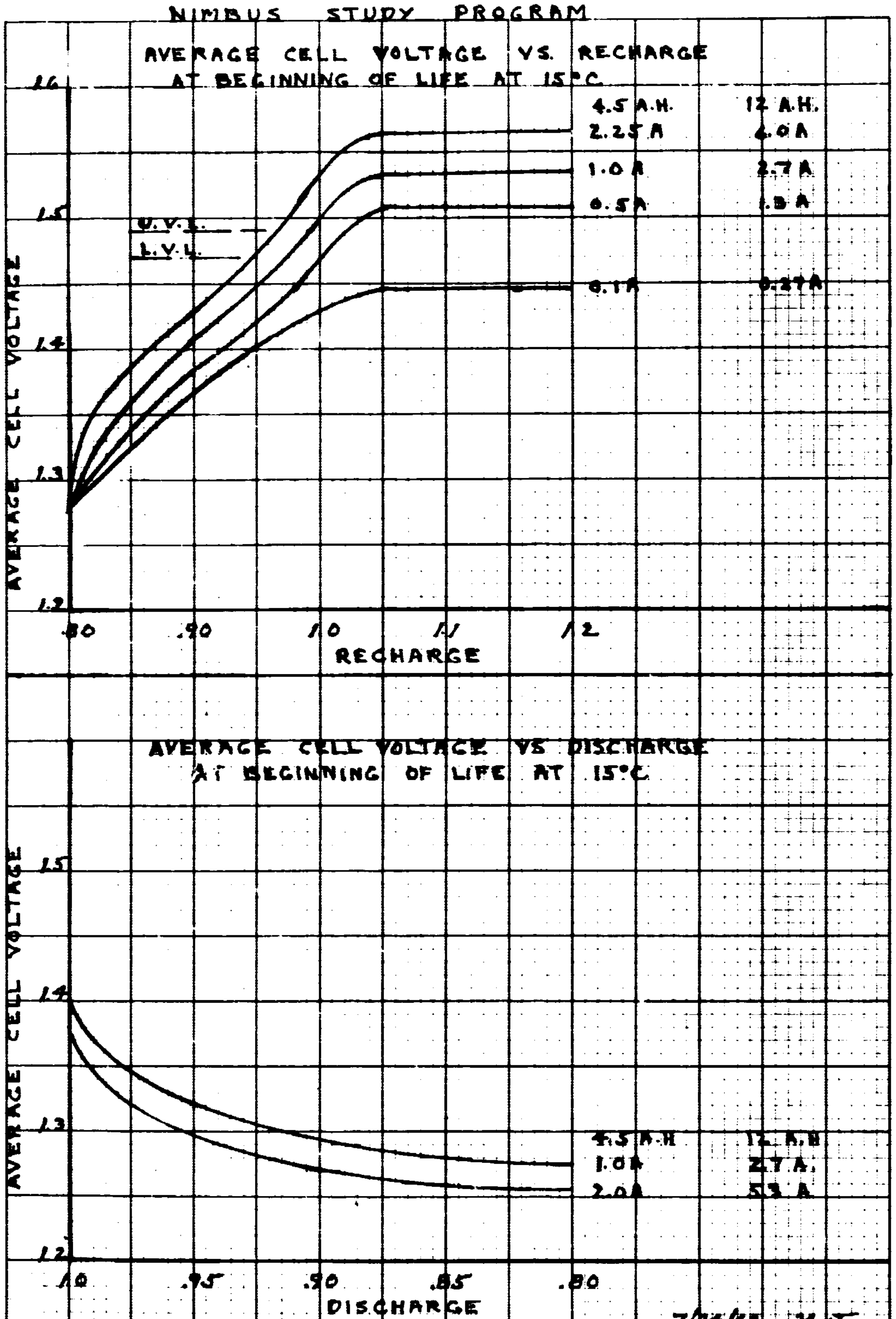

NIMBUS STUDY PROGRAM
AVERAGE CELL VOLTAGE VS. RECHARGE
AT BEGINNING OF LIFE AT 15°C
4.5 A.H.
12 A.H.
2.25 A
6.0 A
1.0 A
2.7 A
0.5 A
1.3 A
0.1 A
0.27 A
U.V.L.
L.V.L.
1.6
1.5
1.4
1.3
1.2
AVERAGE CELL VOLTAGE
.80
.90
1.0
1.1
1.2
RECHARGE
AVERAGE CELL VOLTAGE VS DISCHARGE
AT BEGINNING OF LIFE AT 15°C
1.5
1.4
1.3
1.2
AVERAGE CELL VOLTAGE
4.5 A.H
12 A.H
1.0 A
2.7 A.
2.0 A
5.3 A
1.0
.95
.90
.85
.80
DISCHARGE

Figure II-1

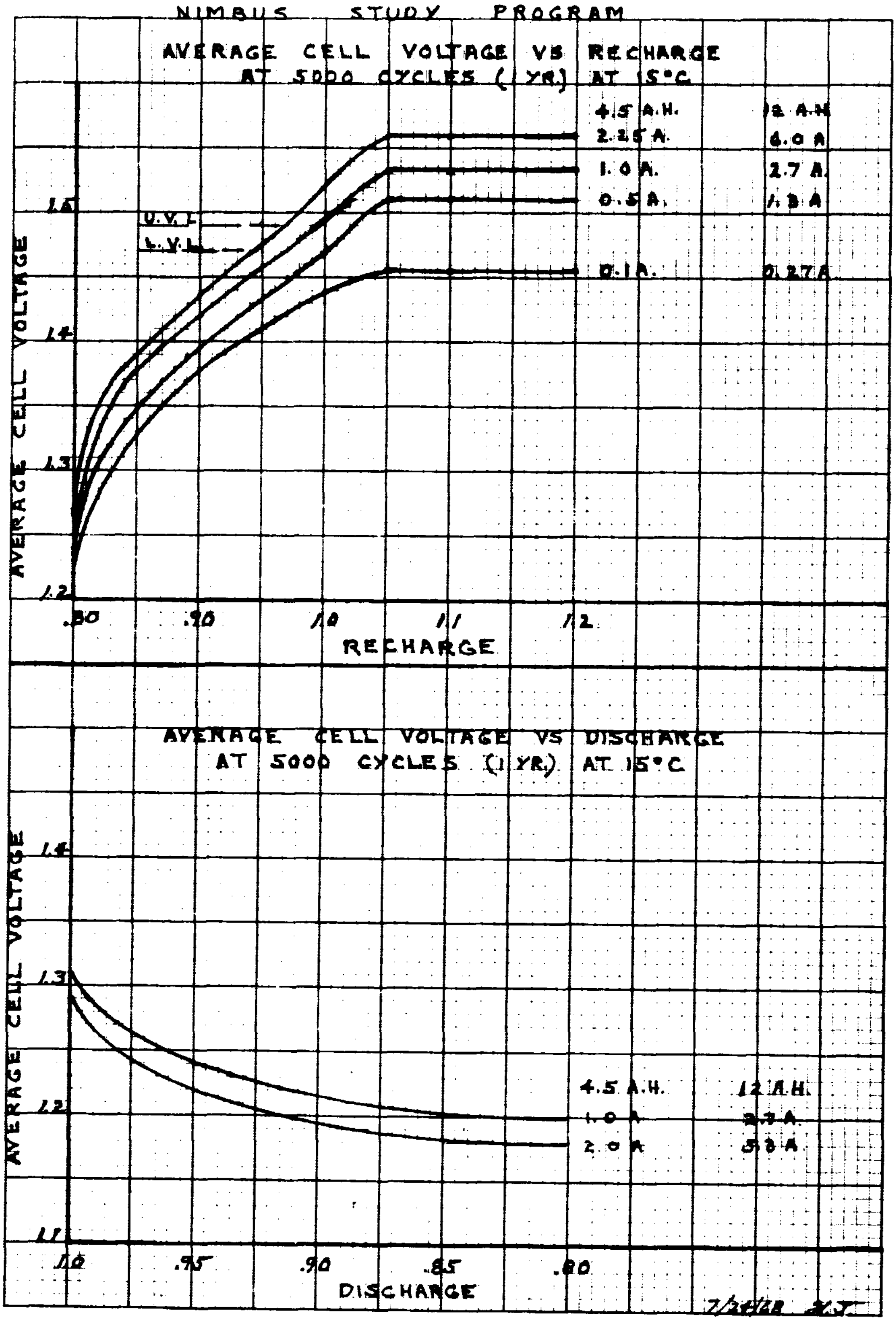
NIMBUS STUDY PROGRAM
AVERAGE CELL VOLTAGE VS RECHARGE
AT 5000 CYCLES (1 YR) AT 15°C
4.5 A.H.
12 A.H.
2.25 A.
6.0 A
1.0 A.
2.7 A.
0.5 A.
1.3 A
0.1 A.
0.27 A
U.V.L.
L.V.L.
1.5
1.4
1.3
1.2
AVERAGE CELL VOLTAGE
.80
.90
1.0
1.1
1.2
RECHARGE
AVERAGE CELL VOLTAGE VS DISCHARGE
AT 5000 CYCLES (1 YR.) AT 15°C
4.5 A.H.
12 A.H.
1.0 A
2.7 A.
2.0 A
5.3 A
1.4
1.3
1.2
1.1
AVERAGE CELL VOLTAGE
1.0
.95
.90
.85
.80
DISCHARGE

Figure II-2

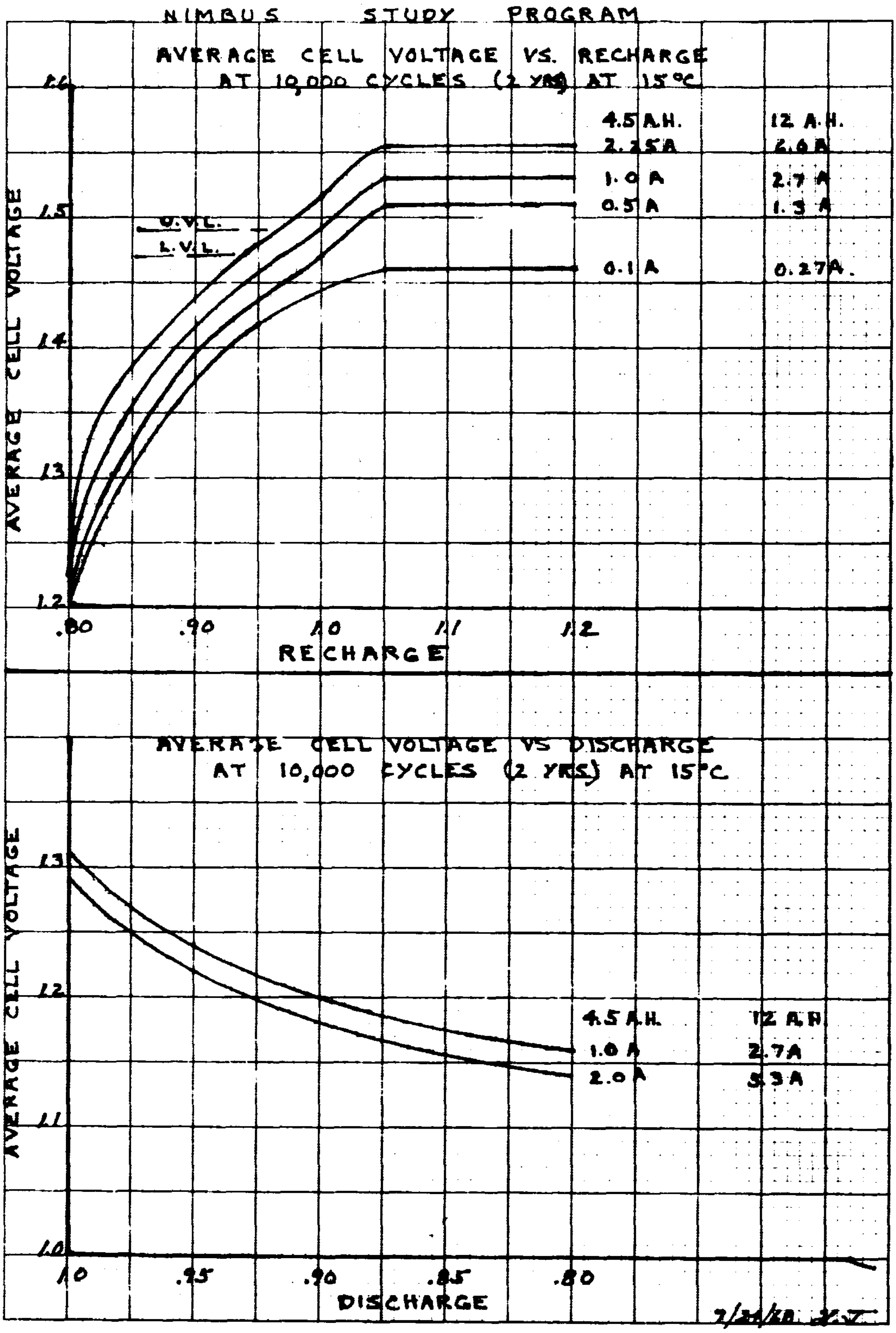
NIMBUS STUDY PROGRAM
AVERAGE CELL VOLTAGE VS. RECHARGE AT 10,000 CYCLES (2 YRS) AT 15°C
AVERAGE CELL VOLTAGE
1.6
1.5
1.4
1.3
1.2
O.V.L.
L.V.L.
4.5 A.H.
2.25 A
1.0 A
0.5 A
0.1 A
12 A.H.
2.7 A
1.3 A
0.27 A
.80
.90
1.0
1.1
1.2
RECHARGE
AVERAGE CELL VOLTAGE VS DISCHARGE AT 10,000 CYCLES (2 YRS) AT 15°C
AVERAGE CELL VOLTAGE
1.3
1.2
1.1
1.0
4.5 A.H.
1.0 A
2.0 A
12 A.H.
2.7 A
5.3 A
1.0
.95
.90
.85
.80
DISCHARGE

Figure II-3

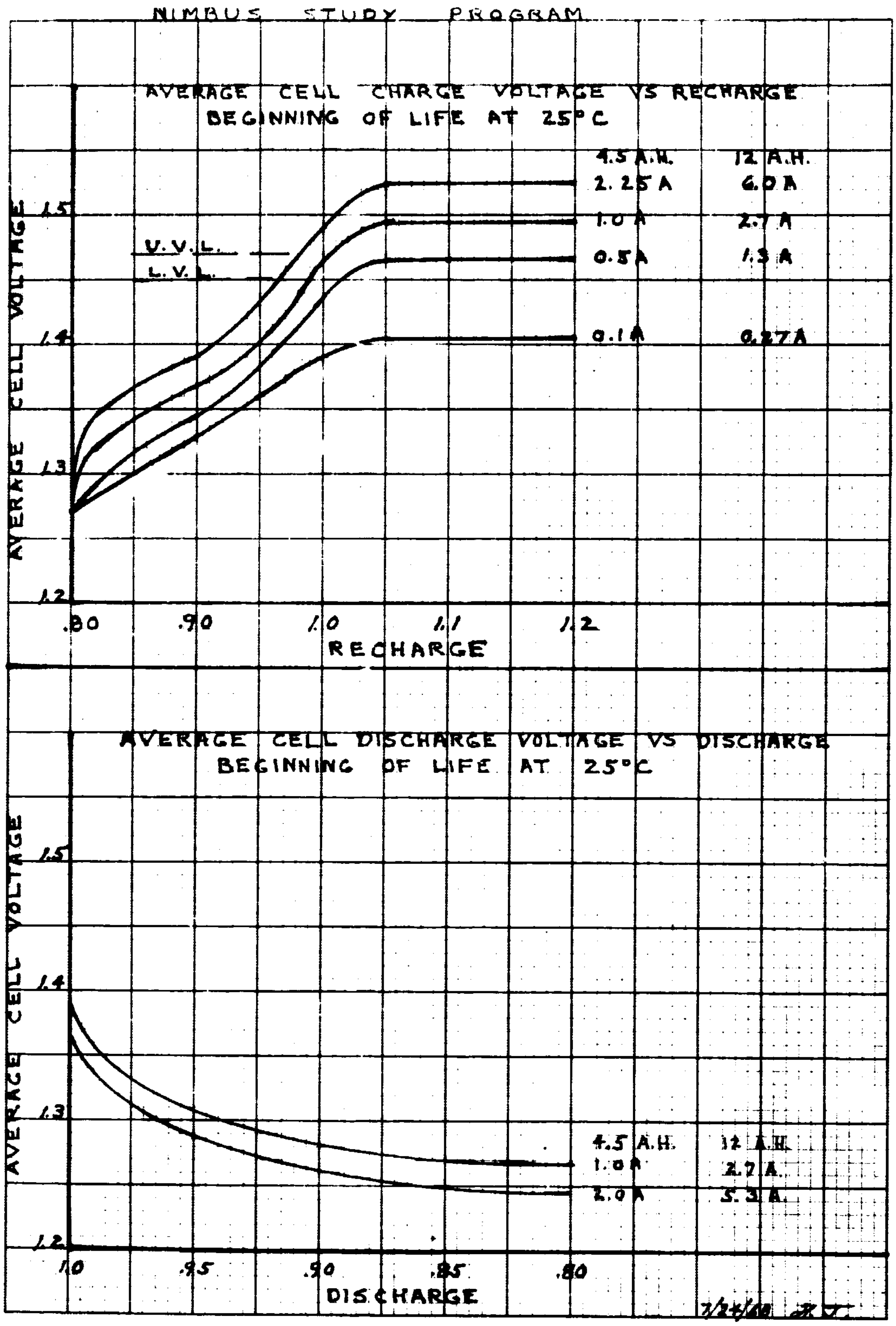
NIMBUS STUDY PROGRAM
AVERAGE CELL CHARGE VOLTAGE VS RECHARGE
BEGINNING OF LIFE AT 25°C
4.5 A.H.
12 A.H.
2.25 A
6.0 A
1.0 A
2.7 A
0.5 A
1.3 A
0.1 A
0.27 A
U.V.L.
L.V.L.
AVERAGE CELL VOLTAGE
1.5
1.4
1.3
1.2
.80
.90
1.0
1.1
1.2
RECHARGE
AVERAGE CELL DISCHARGE VOLTAGE VS DISCHARGE
BEGINNING OF LIFE AT 25°C
AVERAGE CELL VOLTAGE
1.5
1.4
1.3
1.2
4.5 A.H.
12 A.H.
1.0 A
2.7 A
2.0 A
5.3 A
1.0
.95
.90
.85
.80
DISCHARGE

Figure II-4

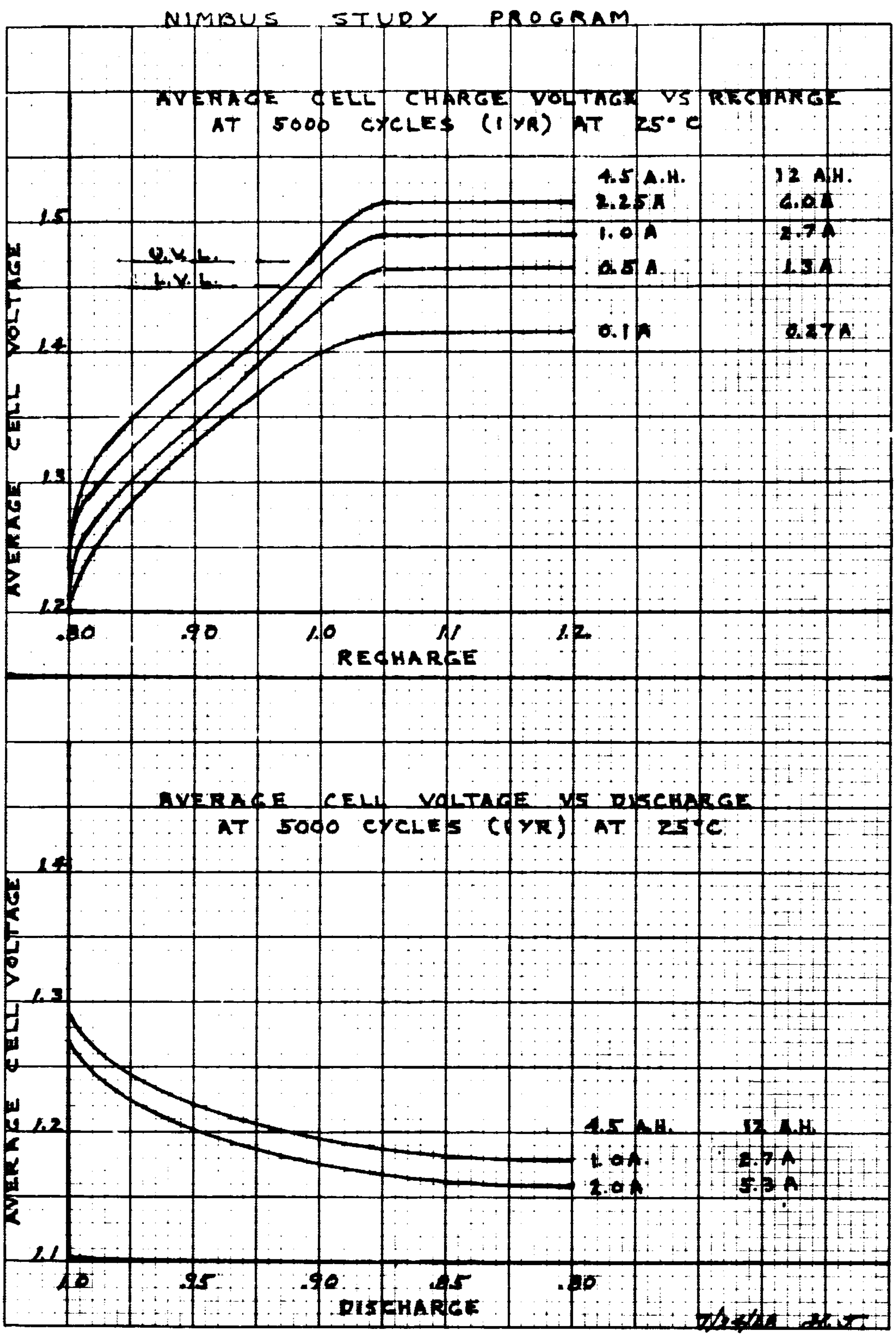
NIMBUS STUDY PROGRAM
AVERAGE CELL CHARGE VOLTAGE VS RECHARGE
AT 5000 CYCLES (1 YR) AT 25° C
4.5 A.H.
2.25 A
1.0 A
0.5 A
0.1 A
12 A.H.
6.0 A
2.7 A
1.3 A
0.27 A
U.V.L.
L.V.L.
AVERAGE CELL VOLTAGE
1.5
1.4
1.3
1.2
.80
.90
1.0
1.1
1.2
RECHARGE
AVERAGE CELL VOLTAGE VS DISCHARGE
AT 5000 CYCLES (1 YR) AT 25°C
4.5 A.H.
1.0 A
2.0 A
12 A.H.
2.7 A
5.3 A
AVERAGE CELL VOLTAGE
1.4
1.3
1.2
1.1
1.0
.95
.90
.85
.80
DISCHARGE

Figure II-5

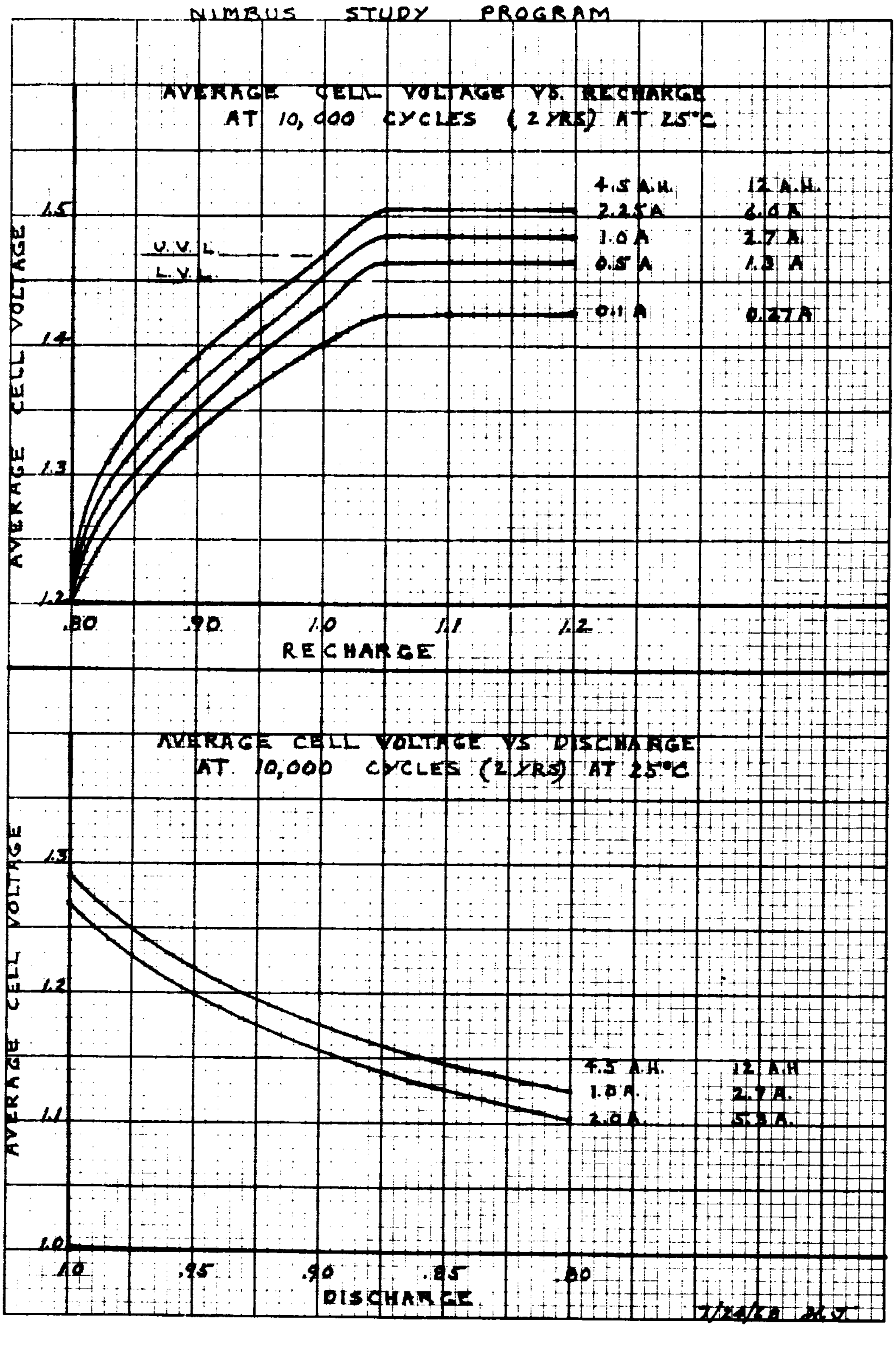
NIMBUS STUDY PROGRAM
AVERAGE CELL VOLTAGE VS. RECHARGE
AT 10,000 CYCLES (2 YRS) AT 25°C
4.5 A.H.
2.25 A
1.0 A
0.5 A
0.1 A
12 A.H.
6.0 A
2.7 A
1.3 A
0.27 A
U.V.L.
L.V.L.
AVERAGE CELL VOLTAGE
1.5
1.4
1.3
1.2
.80
.90
1.0
1.1
1.2
RECHARGE
AVERAGE CELL VOLTAGE VS DISCHARGE
AT 10,000 CYCLES (2 YRS) AT 25°C
AVERAGE CELL VOLTAGE
1.3
1.2
1.1
1.0
4.5 A.H.
1.0 A
2.0 A
12 A.H
2.7 A.
5.3 A.
1.0
.95
.90
.85
.80
DISCHARGE

Figure II-6

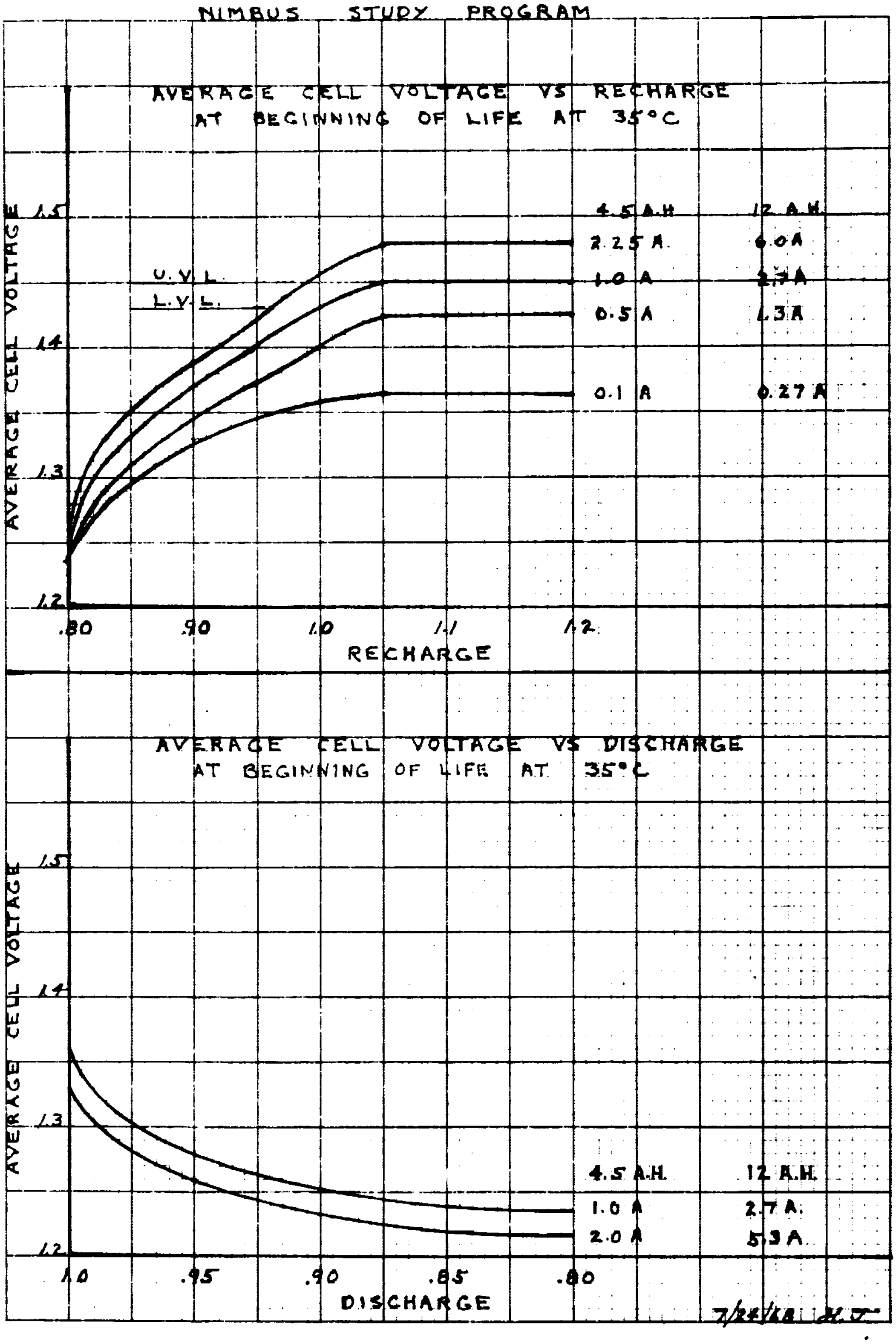
NIMBUS STUDY PROGRAM
AVERAGE CELL VOLTAGE VS RECHARGE
AT BEGINNING OF LIFE AT 35°C
4.5 A.H.
12 A.H.
2.25 A.
6.0 A
1.0 A
0.5 A
1.3 A
0.1 A
0.27 A
U.V.L.
L.V.L.
AVERAGE CELL VOLTAGE
1.5
1.4
1.3
1.2
.80
.90
1.0
1.1
1.2
RECHARGE
AVERAGE CELL VOLTAGE VS DISCHARGE
AT BEGINNING OF LIFE AT 35°C
AVERAGE CELL VOLTAGE
1.5
1.4
1.3
1.2
4.5 A.H.
12 A.H.
1.0 A
2.7 A.
2.0 A
5.3 A.
1.0
.95
.90
.85
.80
DISCHARGE

Figure II-7

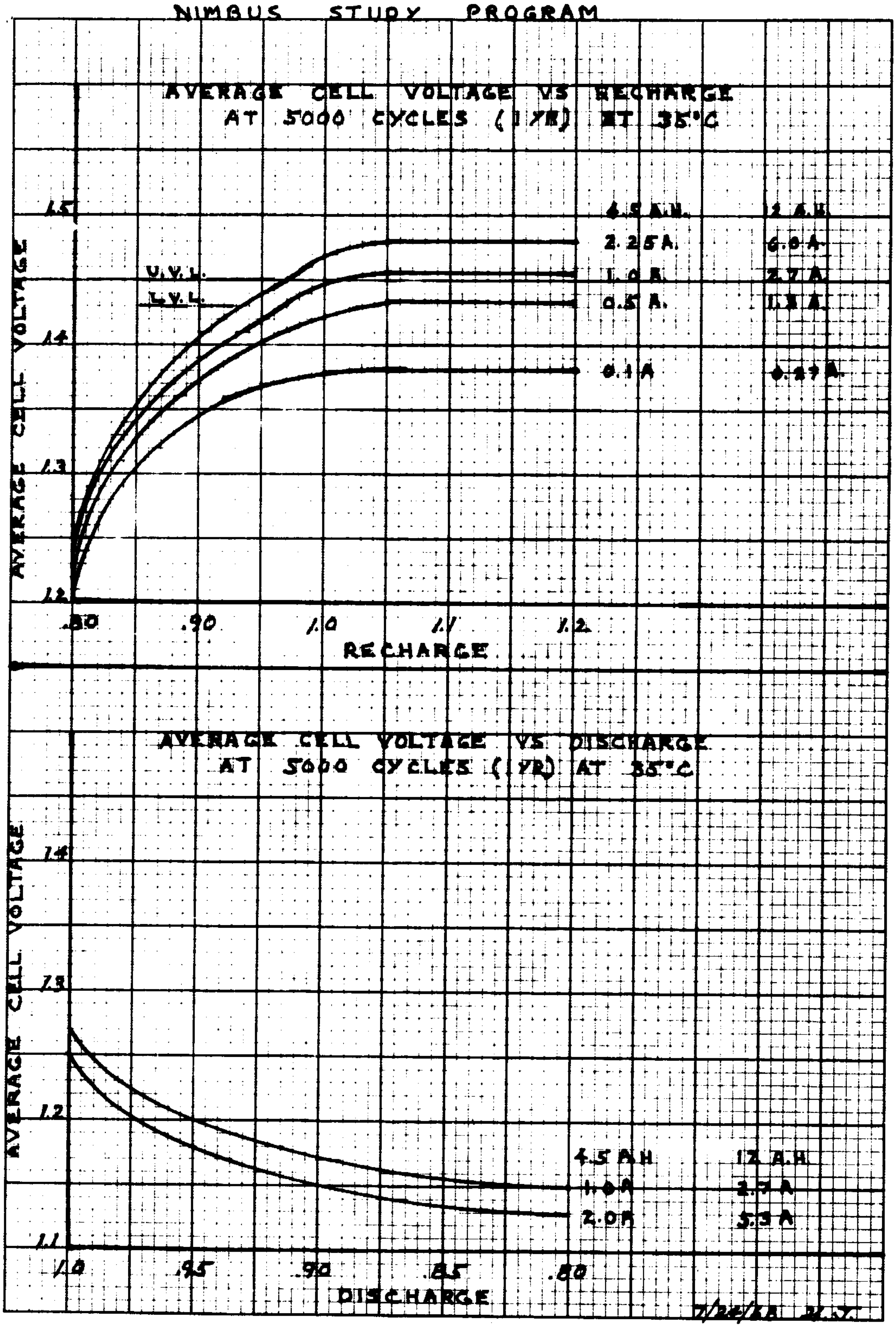
NIMBUS STUDY PROGRAM
AVERAGE CELL VOLTAGE VS RECHARGE
AT 5000 CYCLES (1 YR) AT 35°C
AVERAGE CELL VOLTAGE
RECHARGE
AVERAGE CELL VOLTAGE VS DISCHARGE
AT 5000 CYCLES (1 YR) AT 35°C
DISCHARGE

Figure II-8

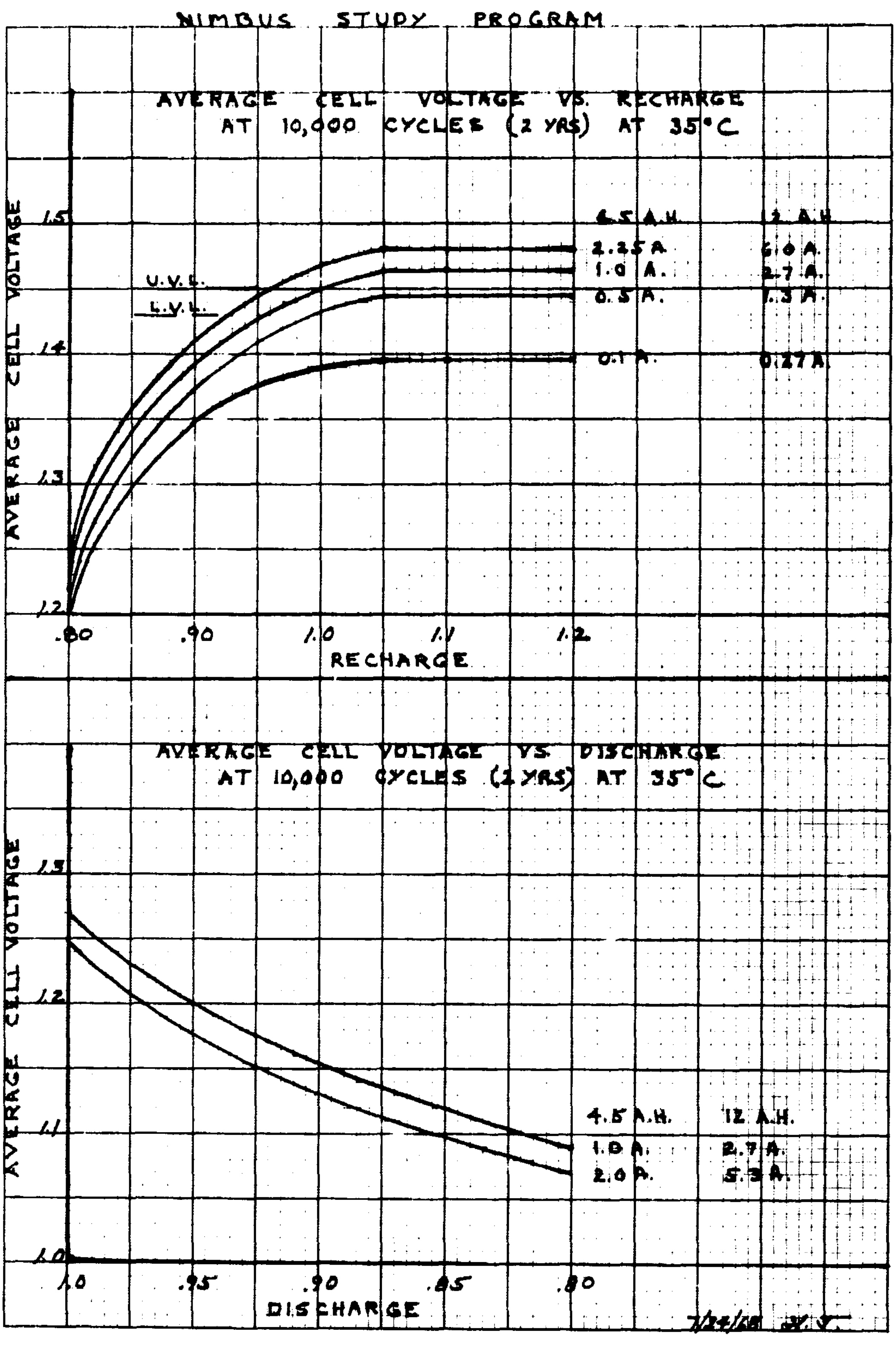
NIMBUS STUDY PROGRAM
AVERAGE CELL VOLTAGE VS. RECHARGE
AT 10,000 CYCLES (2 YRS) AT 35°C
AVERAGE CELL VOLTAGE
U.V.L.
L.V.L.
4.5 A.H.
2.25 A.
1.0 A.
0.5 A.
0.1 A.
12 A.H
6.0 A.
2.7 A.
1.3 A.
0.27 A.
RECHARGE
AVERAGE CELL VOLTAGE VS. DISCHARGE
AT 10,000 CYCLES (2 YRS) AT 35° C
AVERAGE CELL VOLTAGE
4.5 A.H.
1.0 A.
2.0 A.
12 A.H.
2.7 A.
5.3 A.
DISCHARGE

Figure II-9

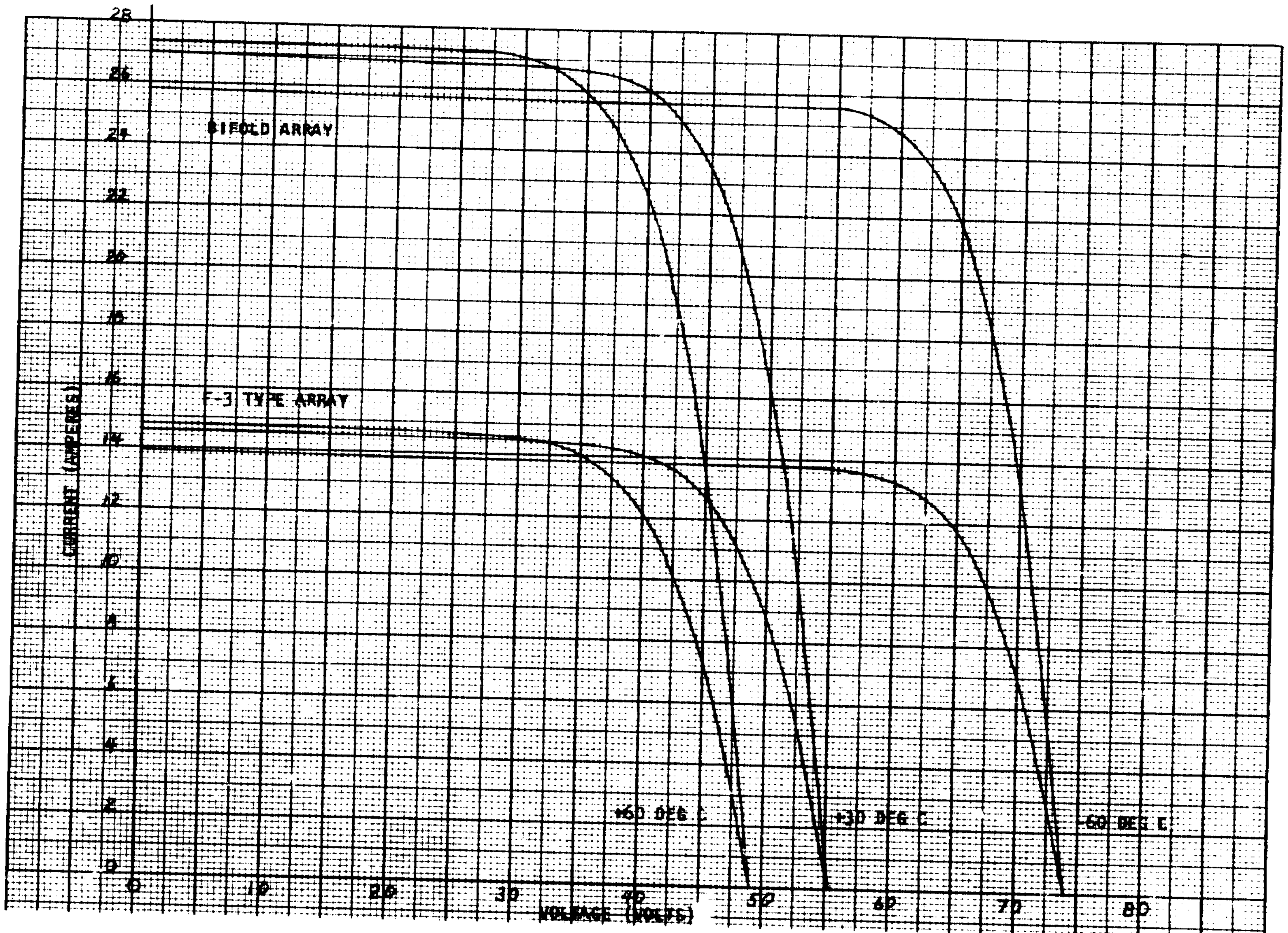

Figure II-10. 94-Cell Solar Array I-V Curves, Nominal Case, Beginning of Life

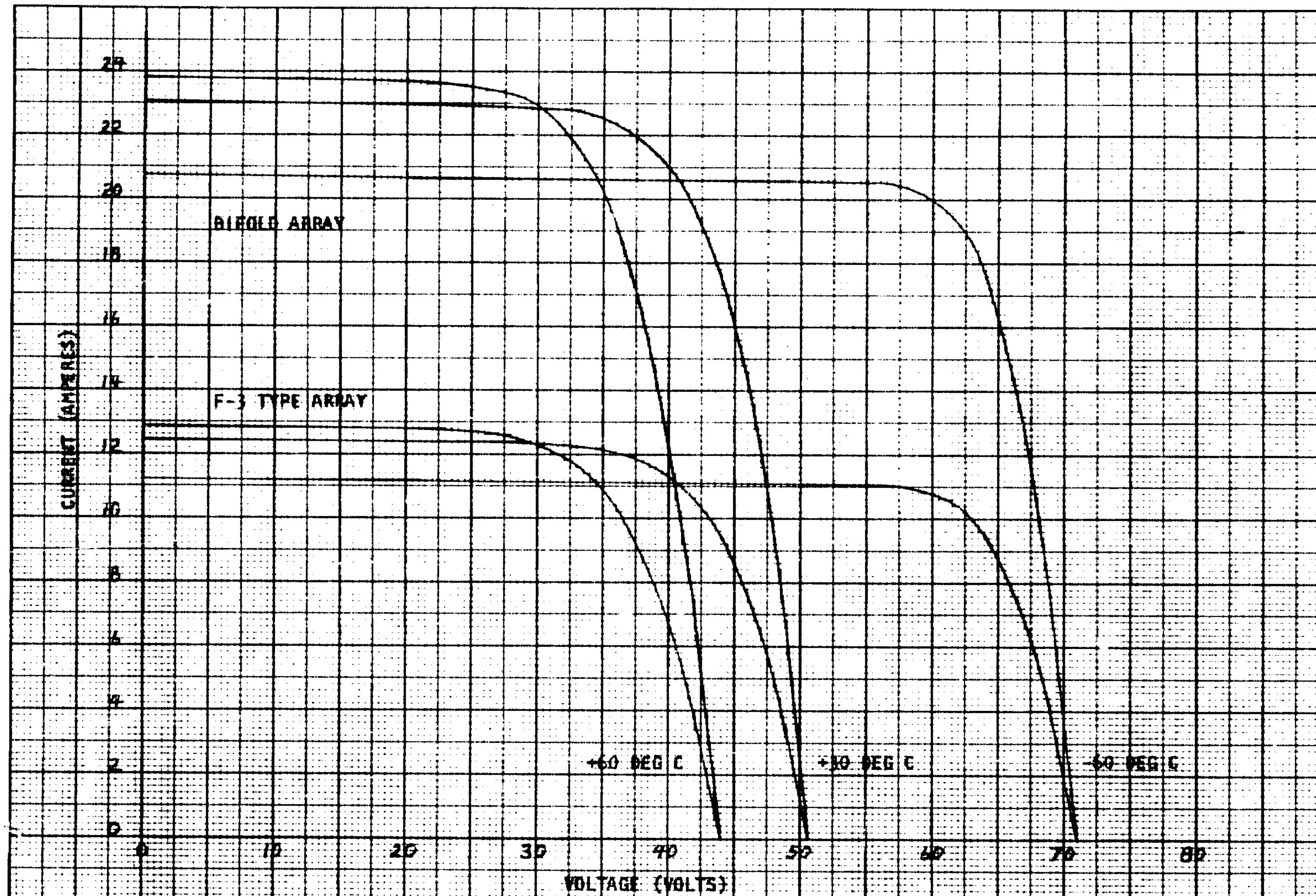

Figure II-11. 94-Cell Solar Array I-V Curves, Nominal Case, One Year In Orbit

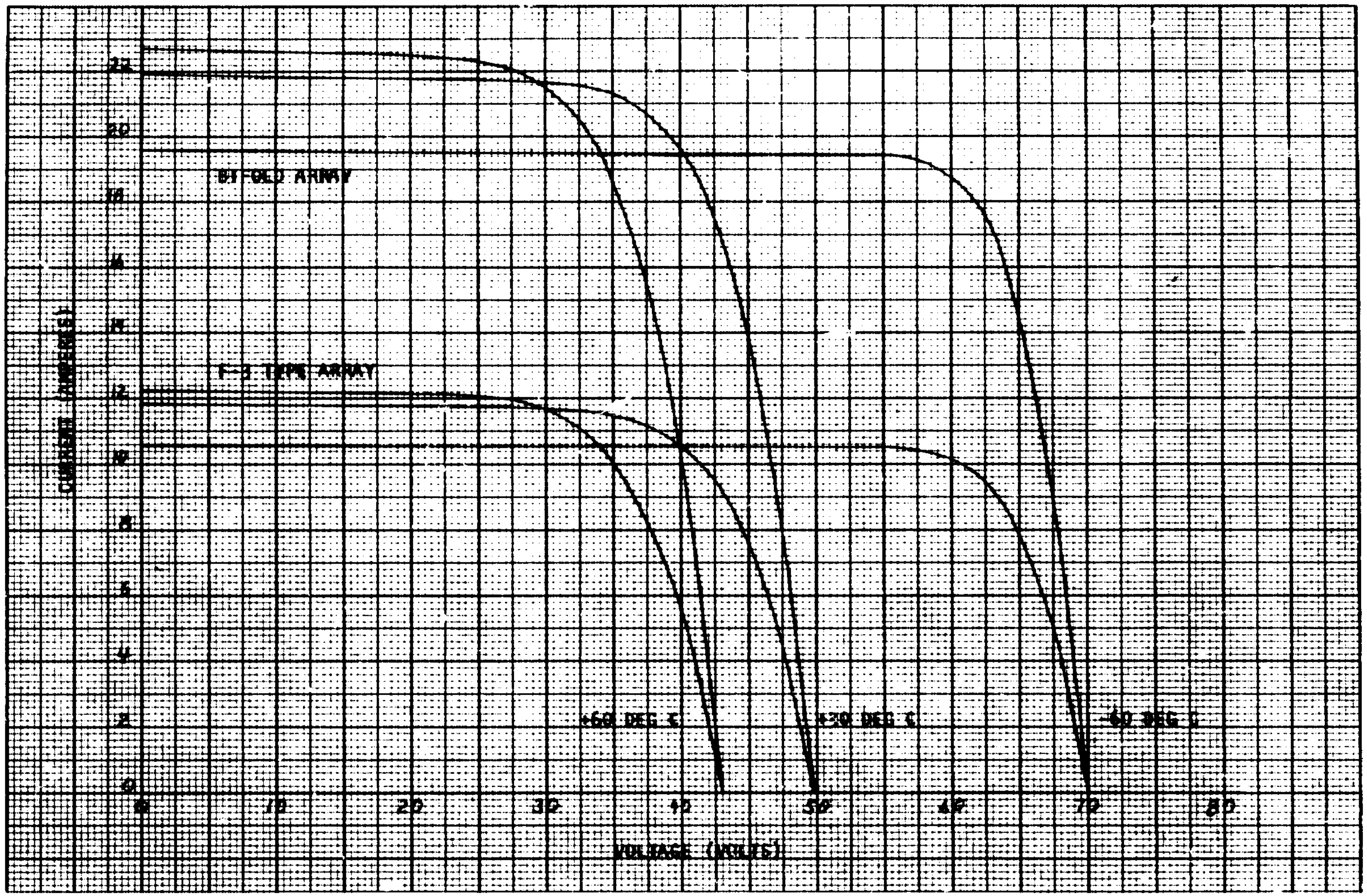

Figure II-12. 94-Cell Solar Array I-V Curves, Nominal Case, Two Years In Orbit

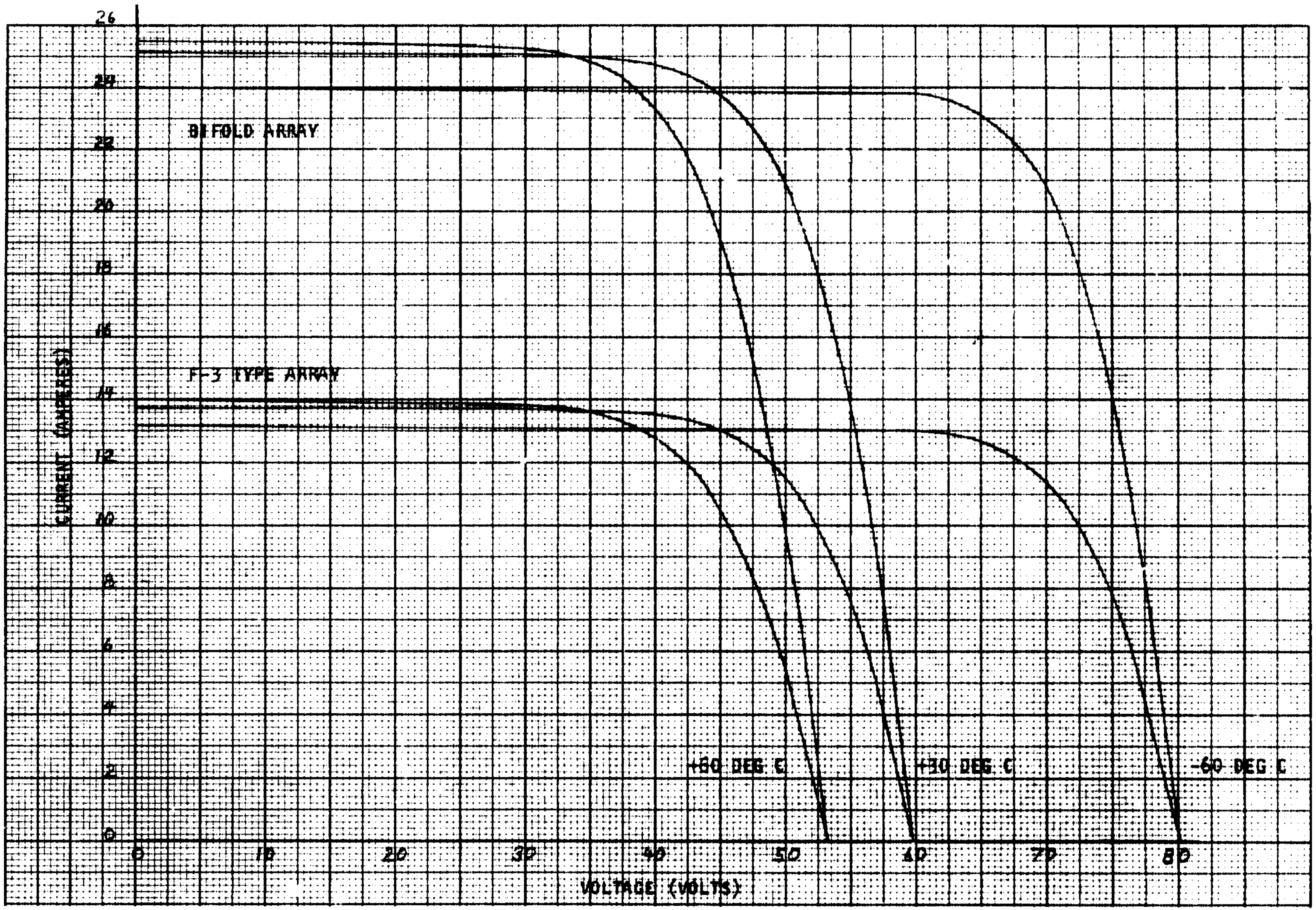

Figure II-13. 102-Cell Solar Array I-V Curves, Nominal Case, Beginning of Life

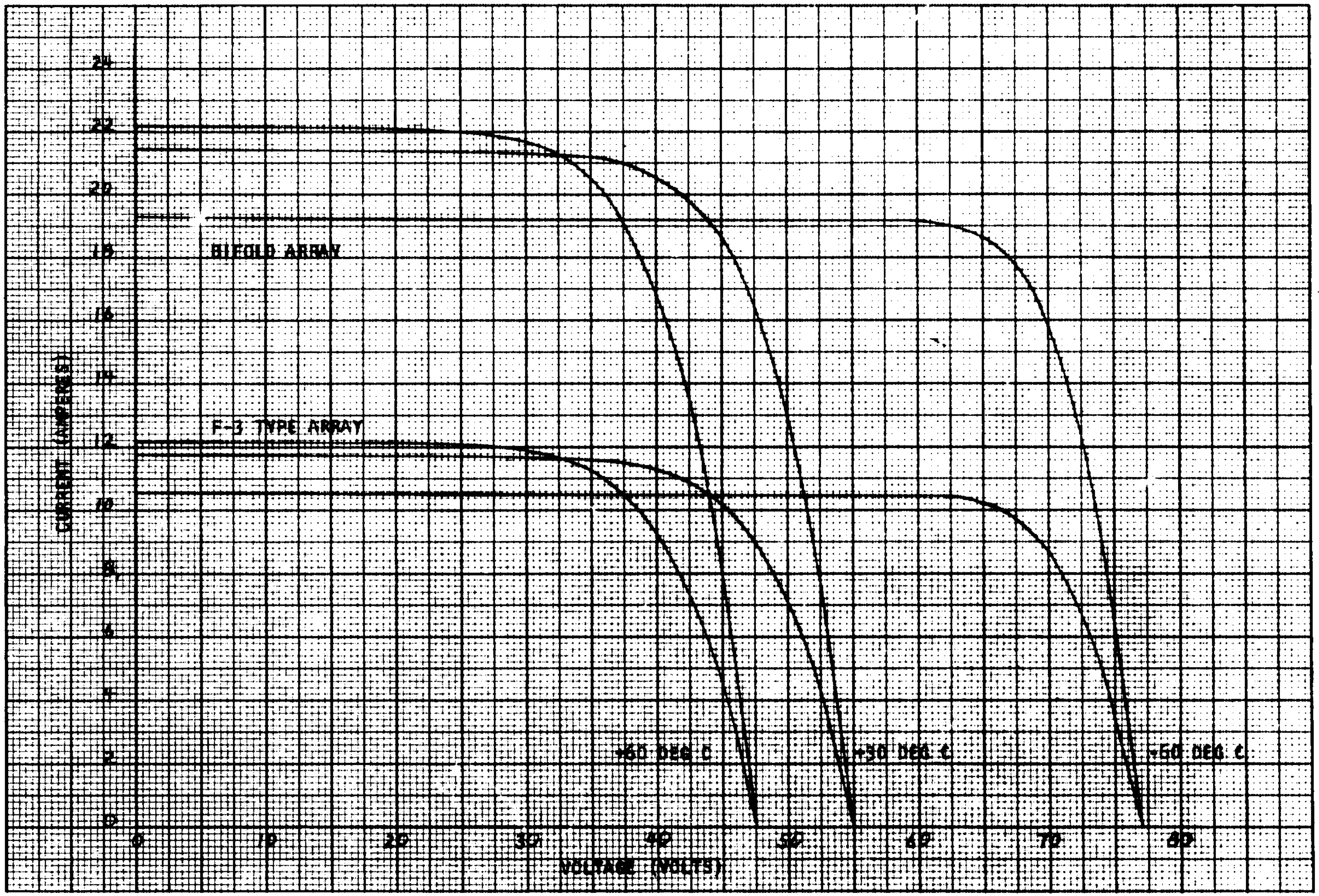

Figure II-14. 102-Cell Solar Array I-V Curves, Nominal Case, One Year In Orbit

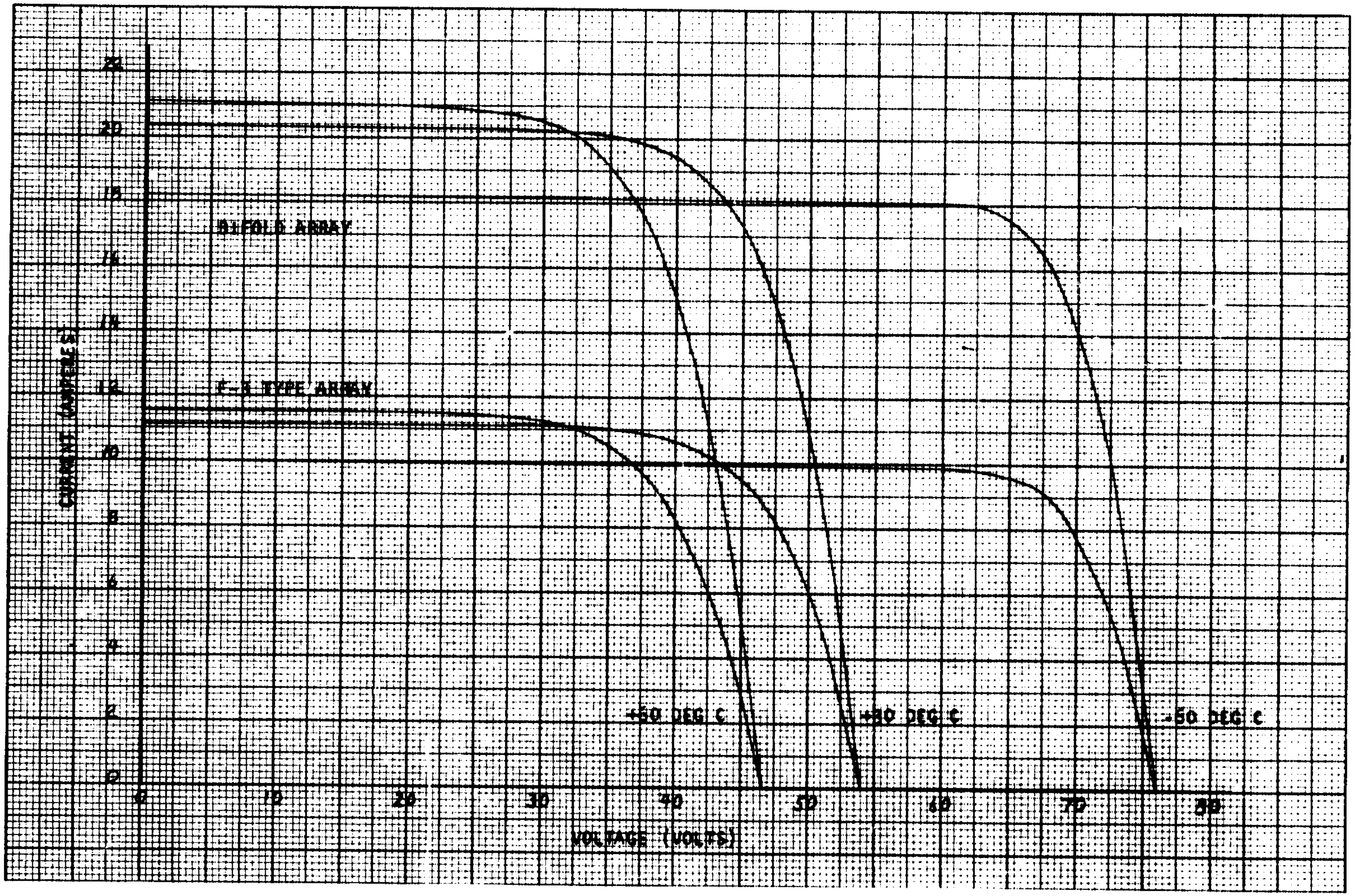

Figure II-15. 102-Cell Solar Array I-V Curves, Nominal Case, Two Years in Orbit

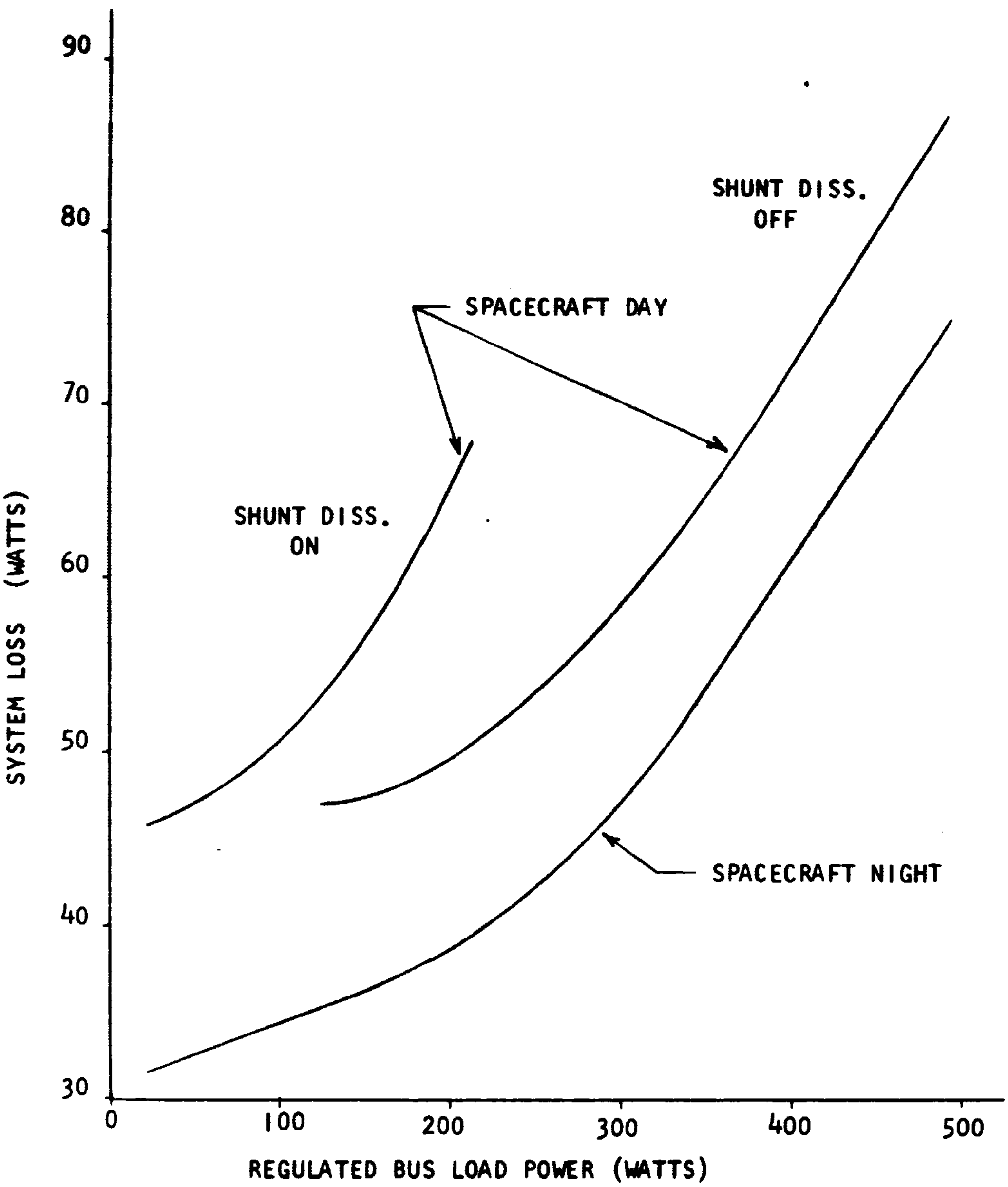

Figure II-16. F-3 System Power Loss versus Regulated Bus Load Power

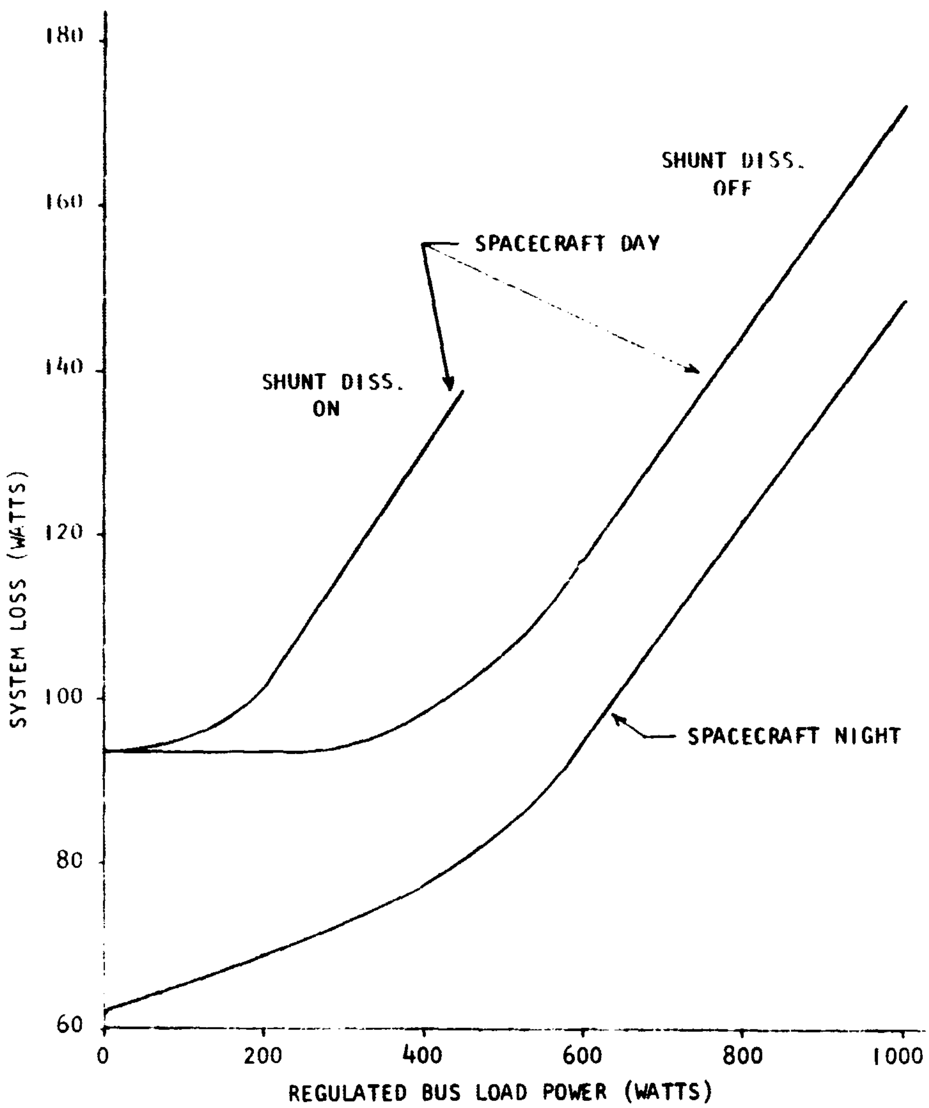

Figure II-17. Bifold System Loss versus Regulated Bus Load Power